August 2015

Climate Impact on Groundwater Flow Processes in the Cedar Creek Watershed and Cedarburg Bog

Jackson Graham
University of Wisconsin-Milwaukee

CLIMATE IMPACT ON GROUNDWATER FLOW PROCESSES IN THE CEDAR CREEK WATERSHED AND CEDARBURG BOG

by

Jackson Graham

A Thesis Submitted in

Partial Fulfillment of the

Requirements for the Degree of

Master of Science

in Geosciences

at

The University of Wisconsin-Milwaukee

August 2015

ABSTRACT

CLIMATE IMPACT ON GROUNDWATER FLOW PROCESSES IN THE CEDAR CREEK WATERSHED AND CEDARBURG BOG

by

Jackson Graham

The University of Wisconsin-Milwaukee, 2015
Under the Supervision of Professor Dr. Weon Shik Han

A local-scale groundwater-flow model of the Cedar Creek Watershed and Cedarburg Bog area was constructed to determine the effects of future changes in temperature and precipitation on water resources. The Cedar Creek Watershed is a 330 km^2 sub-basin of the Milwaukee River Watershed located about 30 km north of Milwaukee. The importance of this watershed lies in its location at the sub-continental divide separating the Mississippi River Basin from the Great Lakes Basin. The coupled steady-state and transient flow models incorporate interaction between surface water features and groundwater-surface water interactions. The 4 layer model simulates the influence of recharge on the local flow regime using recharge estimates using the Soil-Water-Balance Code (SWB) from the USGS. The model contains two geologic units, surficial glacial deposits and the Silurian dolomitic bedrock. The hydraulic conductivities and storage parameters were calibrated using the parameter estimation software, PEST, based on 192 head targets of the static groundwater level reported by well drillers over the past four

decades. Calibrated hydraulic conductivities from a 15-year average climate result in model simulations with residual mean of 0.14 m, standard deviation of 2.68 m and RMS error of 2.69 m. Results from the simulations show that the water table remains relatively stable over years of very low recharge and very high recharge, in addition to an approximate three month lag of lowering groundwater table after a summer of significant low recharge.

TABLE OF CONTENTS

LIST OF FIGURES vi

LIST OF TABLES viii

ACKNOWLEDGEMENTS ix

1. Introduction 1

2. Study Site 4

2.1 Cedar Creek Watershed 4

2.1.1. Land Cover 7

2.1.2. Population and Economic Activity 9

2.1.3. Glacial Geology 10

2.1.4. Hydrogeology 13

2.2. Cedarburg Bog 14

2.2.1. Land Use, Vegetation 14

2.2.2. Population and Economic Activity 16

2.2.3. Glacial Geology 16

2.2.4. Hydrogeology 17

3. Climate Change Prediction in Cedar Creek Watershed 18

3.1. Global Climate Change 18

3.2. Historical Climate Change in Wisconsin 19

3.2.1. Temperature and Precipitation 20

3.2.2. Evapotranspiration 24

3.3. Modeling of Future Climate Change 25

3.3.1 Temperature and Precipitation 26

3.3.2 Evapotranspiration 29

4. Groundwater Modeling 30

4.1. Watershed Scale: Cedar Creek Aquifer Model 30

4.1.1. Surface Water 35
4.1.2. Soil-Water Balance Recharge Modeling 38
4.1.3. Hydrogeologic Parameters 46
4.1.4. Boundary Conditions 50
4.1.5. Model Calibration 58
5. Results and Discussion 61
5.1 Base Case (Scenario 1): Steady-State Non-Pumping 66
5.2 Scenario 2: Steady-State Pumping 69
5.3 Scenario 3: Transient State Non-pumping 72
5.4. Sensitivity Study on Cedar Creek Watershed 78
5.4.1. Scenarios 4-9: Future Recharge Simulations 78
5.4.2. Scenario 10: Drain Package Replaces River Package 92
5.5. Groundwater Resource Management at the Cedarburg Bog 95
5.5.1. Scenario 11: Low-K layer beneath the Cedarburg Bog 102
6. Limitations 103
7. Conclusions 105
References 108

LIST OF FIGURES

Figure 1. Map of Southeastern Wisconsin 5

Figure 2. Digital elevation model (DEM) map covering the groundwater model. 6

Figure 3. Land cover in the groundwater model area. 8

Figure 4. Surficial glacial units in the Cedar Creek Watershed 12

Figure 5. The Cedarburg Bog. 15

Figure 6. Monthly averages of temperature and precipitation from the Germantown weather station 23

Figure 7. Cedar Creek aquifer model area 32

Figure 8. Bedrock Elevation of groundwater flow model 34

Figure 9. Lake Michigan stage data. 35

Figure 10. Stream discharge of Cedar Creek 37

Figure 11. Hydrologic Soil Groups 39

Figure 12. Spatial Distribution of Recharge 44

Figure 13. Stratigraphy of the MODFLOW model 47

Figure 14. Locations of the 27 High Capacity Pumping Wells 57

Figure 15. Steady-State Base Case full model water budget. 59

Figure 16. Location of 194 wells used for calibration head targets. 60

Figure 17. Monthly means of temperature and precipitation. 65

Figure 18. Steady-state groundwater table Scenario 1 68

Figure 19. Steady-state head distribution change from the pumping scenario. 70

Figure 20. Histogram showing the change in head from the steady-state base case non-pumping scenario and the pumping scenario. 71

Figure 21. Hydrographs from the transient simulation 74

Figure 22. Comparison of steady-state non-pumping model and the transient non-pumping model. 77

Figure 23. Comparison of heads from variable Lake Michigan stage simulations..... 80

Figure 24. Histograms from variable Lake Michigan stage simulations 82

Figure 25. Change in head from base case scenario when recharge is decreased 20% ... 84

Figure 26. Change in head from base case when recharge increased 20%..... 86

Figure 27. Histogram showing the frequency of head change in both the decreased and increased recharge simulations. 88

Figure 28. Steady-state water budgets from the full model area and the Cedar Creek watershed 90

Figure 29. Spatial distribution of head change from Steady-State base case scenario to DRN scenario..... 94

Figure 30. Water budget from only the Cedarburg Bog 97

Figure 31. Steady-state base case non-pumping scenario head distribution within the Cedarburg Bog (Scenario 1). 99

Figure 32. Maps showing the change in head in the Cedarburg Bog throughout 6 climate change steady-state simulations..... 101

LIST OF TABLES

Table 1. Land Cover distribution within the Cedar Creek Watershed 9

Table 2. Seasonal temperature (^{o}C) and precipitation (mm) expressed as a percent (change/mean) since 1944..... 24

Table 3. Predicted minimum and maximum changes in temperature and precipitation .. 29

Table 4. Mean output of Soil Water Balance Code across the Cedar Creek Watershed . 45

Table 5. Initial values for hydraulic conductivity 48

Table 6. Maximum pumping rates from the 27 high capacity pumping wells..... 56

Table 7. Scenarios implemented in the groundwater flow model..... 64

ACKNOWLEDGEMENTS

First and foremost I would like to thank Dr. Weon Shik Han for everything he has done for me in the past three years. I began as a raw SURF student and he primed me to be able to tackle the Master's Degree. I have not encountered anyone who is more dedicated to his students and who works so hard to ensure the success of said students. I'd also like to thank my committee members, Dr. Cherkauer and David Hart, in addition to Daniel Feinstein for their continual support and constructive criticisms. The faculty and staff of the Geosciences Department also deserve a huge thanks, especially Julianna, Chris, Lisa, Adrianna and Lynn, for all the help they have provided me. A big thank you to my colleagues Zach Watson, Ethan Guyant, and Na-Hyun Jung for all the help they have provided both in the lab and in the field putting up with hot, sweaty and buggy summers and cold and brutal trips to the bog. Finally, my parents deserve the largest thanks of all for getting me through college and providing the best backing team any son could ask for.

1. Introduction

Climate change has been a growing concern globally for the past decade because of the potential effects of climate change on resources, such as crop production and surface/ groundwater depletion. Wisconsin is a leading state in agriculture and forestry, which can both be heavily affected by changes in the future climate. Many studies have been produced detailing the past and future climate change of Wisconsin showing a statewide average increase in temperature of about 1^{o}C and increase in precipitation of 7-8 cm since 1950 [*Kucharik et al.*, 2010b; *Moran and Hopkins*, 2002; *Serbin and Kucharik*, 2009; *Veloz et al.*, 2011; *WICCI*, 2011]. The statewide projected increase in temperature of 2-5^{o}C and increase of 3-4 cm of precipitation through 2055 indicate a generally warmer and wetter climate.

These changes in climate have the potential to destroy ecological landmarks across the state and particular interest has been on the Cedarburg Bog located in Ozaukee County in southeast Wisconsin. The Cedarburg Bog is one of the largest and most diverse wetlands in Wisconsin and is home to a wide variety of flora and fauna; some found exclusively in environments similar to the Bog. The Cedarburg Bog lies within the Cedar Creek Watershed, a sub-basin of the Milwaukee River watershed, and constitutes a significant part of the water budget within the underlying aquifer. Traditionally, the hydrologic system of the Bog is thought to be dominated by groundwater but also with significant influences from precipitation and surface water features. Due to the strong groundwater component of the water budget, the Bog's waters are nearly neutral, which is typically indicative of a fen, and the neutral pH of the water is a result of the local

carbonate bedrock [*Reeve et al.*, 2001]. This aspect of the Bog is the primary driver for the diverse and unique ecological communities found within the peatland. Due to the importance of groundwater on both the plants and animals that are supported by the Bog, it is crucial to understand the role of the Bog in the surrounding aquifer.

The primary tool for determining the effects of climate change on both groundwater and surface water is groundwater flow modeling. This project utilizes *MODFLOW-2005* to simulate the groundwater flow processes around the Cedar Creek Watershed in order to determine the effect of future climate change through simulations of variable recharge and Lake Michigan stage *[Harbaugh, 2005; Niswonger et al., 2011]*. The graphical user interface for the MODFLOW code that was used is called Groundwater Vistas 6. This project focuses on the seasonal and yearly changes in recharge to the water table and its relationship to groundwater head, specifically depletion and enrichment. The past 15-year average recharge was used to determine the mean steady-state water table. Based on the steady-state model the transient simulation of the past 4 years of recharge was developed. Finally, recharge values representative of the extreme cases of climate change were implemented into the calibrated flow model in order to determine the effect of either severe decreases or increases in the precipitation around southeastern Wisconsin.

In addition to investigating the effects of climate change on the Cedarburg Bog, this study is a preliminary research effort into the effects of climate change on any Northern Wetland throughout North America and Europe. Northern peatlands and other wetlands play a crucial role in the sequestration of carbon from the atmosphere. The decaying organic matter in temperate wetlands has the ability to sequester up to 160 g-

C/(m^2·year) (grams of carbon per m^2 per year), with northern peatlands sequestering less, but still up to 50 g-C/(m^2·year) [*Mitsch et al.*, 2013; *Turunen et al.*, 2002]. This is extremely important because as wetlands disappear we not only lose the ecologic diversity but also the sequestering ability wetlands have for carbon. On the other hand, northern peatlands only release 7.5 g-C/m^2·year or less in the form of CO_2 and CH_4 [*Moore and Roulet*, 1995]. With this in mind it is critical to determine the rate of increased carbon release from wetlands as the climate changes. It is very likely the positive feedback event of a warming climate releasing greenhouse gases from wetlands will cause the climate to warm more rapidly.

Many factors play a role in groundwater quality and quantity including but not limited to climate, land-use and groundwater extraction for irrigation and drinking water [*Allen et al.*, 2004; *Auterives et al.*, 2011]. This study is designed to determine the role of climate change on water resources in the Bog and surrounding area in order to protect the diverse and unique ecology at the Bog. In addition to rare and unique flora and fauna, peatlands have significant importance on the chemistry of local groundwater and the exchange of atmospheric gases [*Wu*, 2012]. A brief literature review of historical climate change and climate change projections is presented in addition to a detailed MODFLOW model developed to assess the relationship between groundwater and recharge at the Cedarburg Bog and the Cedar Creek Watershed.

2. Study Site

2.1 Cedar Creek Watershed

The Cedar Creek Watershed is located in Southeastern Wisconsin about 30 km (20 miles) north of the City of Milwaukee (Figure 1). Cedar Creek is a relatively large tributary of the Milwaukee River, which flows 53 km (33 miles) from the source at Big Cedar Lake, southwest of West Bend and then to the outlet at the Milwaukee River southeast of Cedarburg (Figure 2). The river flows through one other lake, Little Cedar Lake, after emanating from Big Cedar Lake. The watershed itself drains large parts of Ozaukee and Washington Counties and is a sub-basin of the much larger Milwaukee River basin.

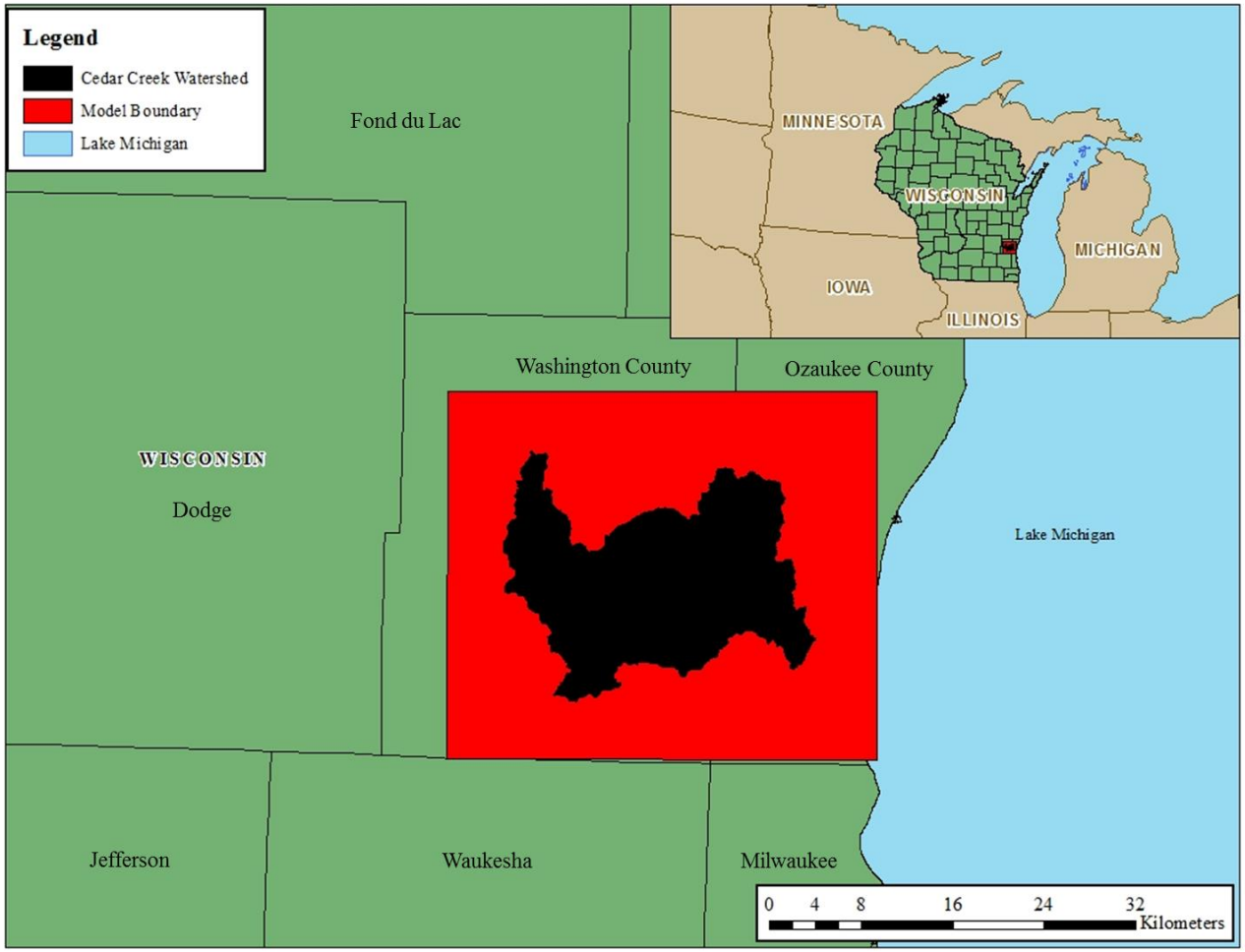

Figure 1. Map of Southeastern Wisconsin, showing the location of the groundwater model boundary (red) and the Cedar Creek Watershed (black). The City of Milwaukee is shown in gray, with a yellow star indicating the location of Downtown.

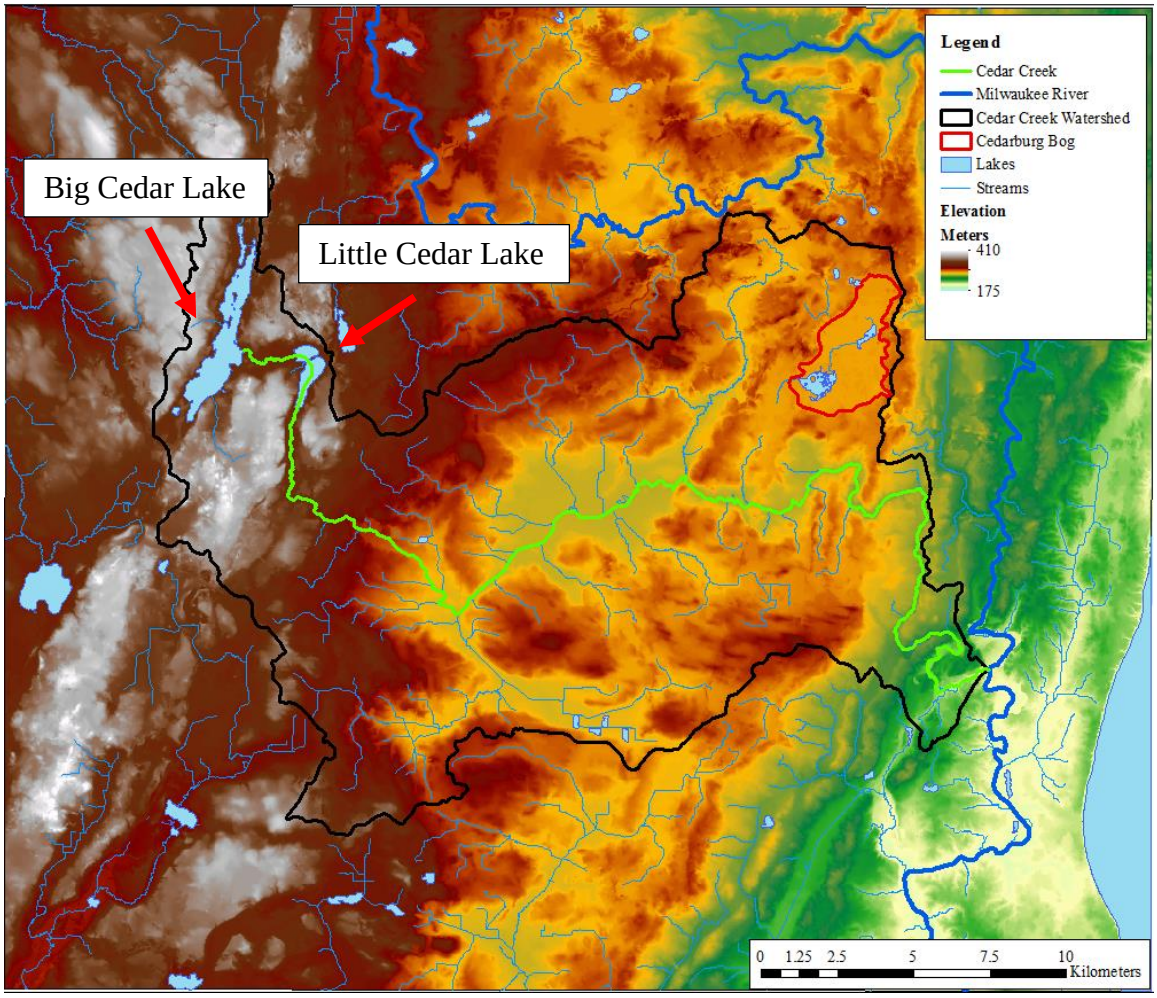

Figure 2. Digital elevation model (DEM) map covering the groundwater model. The DEM map is sourced from the National Elevation Dataset USGS (http://viewer.nationalmap.gov/viewer/). Cedar Creek watershed and Cedarburg Bog is outlined in black and red lines, respectively. Surface water features including rivers and lakes are shown in blue, but the Cedar Creek is delineated in green.

2.1.1. Land Cover

Land cover has potential to affect both quantity and quality of groundwater and surface water. Furthermore, land cover is one of the most important factors controlling recharge to the groundwater table. Spatially, Cedar Creek Watershed is dominated by agriculture (90% of the 334 km^2 watershed) (Figure 3 and Table 1). Forests and wetlands (the Cedarburg Bog and the Jackson Marsh) cover about 6% of the watershed area. Both agricultural and forested land provided the most effective pathway for groundwater recharge. The area of urban land cover is growing, coinciding with both population and municipality growth, and is less than 3% (Figure 3). This developed land allows for the least recharge as almost all precipitated water is directly diverted to surface water features as runoff, or surface discharge. Generally, the land cover labelled barren in this watershed denotes quarries of either dolomite or sand and gravel from the glacial till. Some small areas represent exposed bedrock at the land surface.

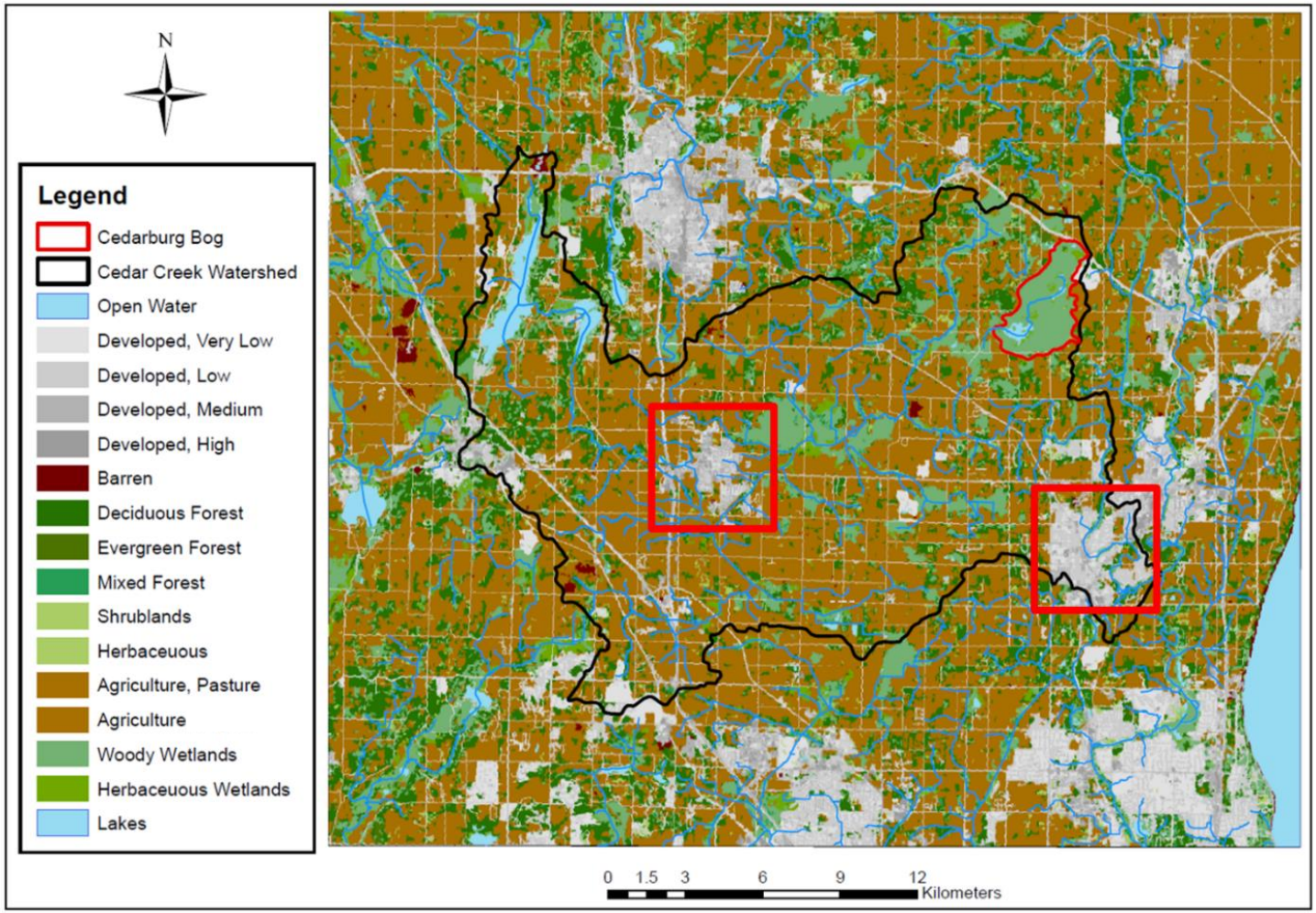

Figure 3. Land cover in the groundwater model area; data is sourced from the 2011 National Land Cover Database (NLCD). Cedarburg and Jackson are shown in the eastern and western boxes respectively.

Table 1. Land Cover distribution within the Cedar Creek Watershed

	# Cells	LC Area (m^2)	% Area
High Intensity Urban	1.87E+03	1.68E+06	0.1
Low Intensity Urban	3.51E+04	3.16E+07	2.2
Golf Course	2.57E+04	2.31E+07	1.6
Field Crops	5.82E+04	5.24E+07	3.6
Row Crops	1.37E+06	1.23E+09	85.3
Grassland	2.06E+03	1.86E+06	0.1
Coniferous Forest	7.73E+02	6.96E+05	0.0
Deciduous Forest	4.30E+04	3.87E+07	2.7
Mixed Forest	1.32E+03	1.19E+06	0.1
Open Water	7.70E+03	6.93E+06	0.5
Emergent Wetland	5.37E+03	4.83E+06	0.3
Forested Wetland	5.01E+04	4.51E+07	3.1
Barren	1.83E+03	1.64E+06	0.1
Shrubland	2.57E+03	2.31E+06	0.2

2.1.2. Population and Economic Activity

Two municipalities, Cedarburg (Ozaukee County) and Jackson (Washington County), are within the Cedar Creek watershed with the majority of the population residing in rural areas with water supply coming from private wells (Figure 3). Since 2000, the population within the two counties has increased approximately 5% with a vast majority of the population increasing in urban areas. In contrast, the rural population, population outside of municipal boundaries, has increased less than 1% since 2010 [*Crowe*, 2014]. A significant portion of the extracted groundwater in the rural areas is returned to the aquifer through septic systems located at most private residences.

2.1.3. Glacial Geology

The western portion of the watershed lies at the confluence of the Green Bay and Lake Michigan lobes of the Laurentide ice sheet. This unique location develops a series of complex and heterogeneous glacial deposits. The majority of western Washington County is covered by the Horicon member of the Holy Hill Formation, which was deposited by the Green Bay lobe as it moved southwest [*Syverson*, 1988] (Figure 4). Moving east, the New Berlin Member of the Holy Hill formation, deposited by the Lake Michigan Lobe's melt water streams, is similar to the sandy Horicon Member. Both units are dolomite rich due to the regional dolomite bedrock in this area and northward. Separating these units is an undifferentiated sediment of the Holy Hill Formation in the Kettle Moraine that is indistinguishable from either the Horicon or the New Berlin member [*Mickelson and Syverson*, 1997]. Presumably, this undifferentiated sediment was deposited by either or both of the glacial lobes in this area.

The relatively thin Waubeka Member overlying the New Berlin member covers the largest area in the model (Figure 4). The central portion of the watershed, at the border of Washington and Ozaukee Counties, is entirely covered by the thin diamicton, the Waubeka Member, deposited by the re-advance of the Lake Michigan Lobe from the Lake Michigan Basin. The easternmost unit in the watershed is the Oak Creek Formation, which was deposited during the retreat and advance of the Lake Michigan Lobe after the deposition of the Waubeka Member.

The soils and surficial geology are dominated by glacial deposits; outwash sediments such as sand and gravel, and subglacial silts and clays. This highly variable surficial aquifer creates an interesting landscape dominated by glacial land formations

such as hummocks and hollows, kettles, and moraines. The soils and sediments within the watershed have highly variable hydraulic conductivities ranging from clay (8.64×10^{-8} m/day) to well sorted gravel outwash deposits (up to 864 m/day), which leads to difficulty in determining the rate of recharge through different soils and sediments [*Bear,* 1972; *Domenico and Schwartz,* 1997; *Heath,* 1983; *Syverson,* 1988]. The thickness of the glacial sediment ranges from 210 m to 0 m (in areas where the bedrock is exposed). The thickest glacial deposits are found in glacial outwash stream beds, where melting glaciers contributed immense amounts of water which eroded the dolomitic bedrock and created deep valleys subsequently filled with outwash. Also, some areas are covered by windblown loess, which has a low hydraulic conductivity which is not mapped due to the insignificant thickness.

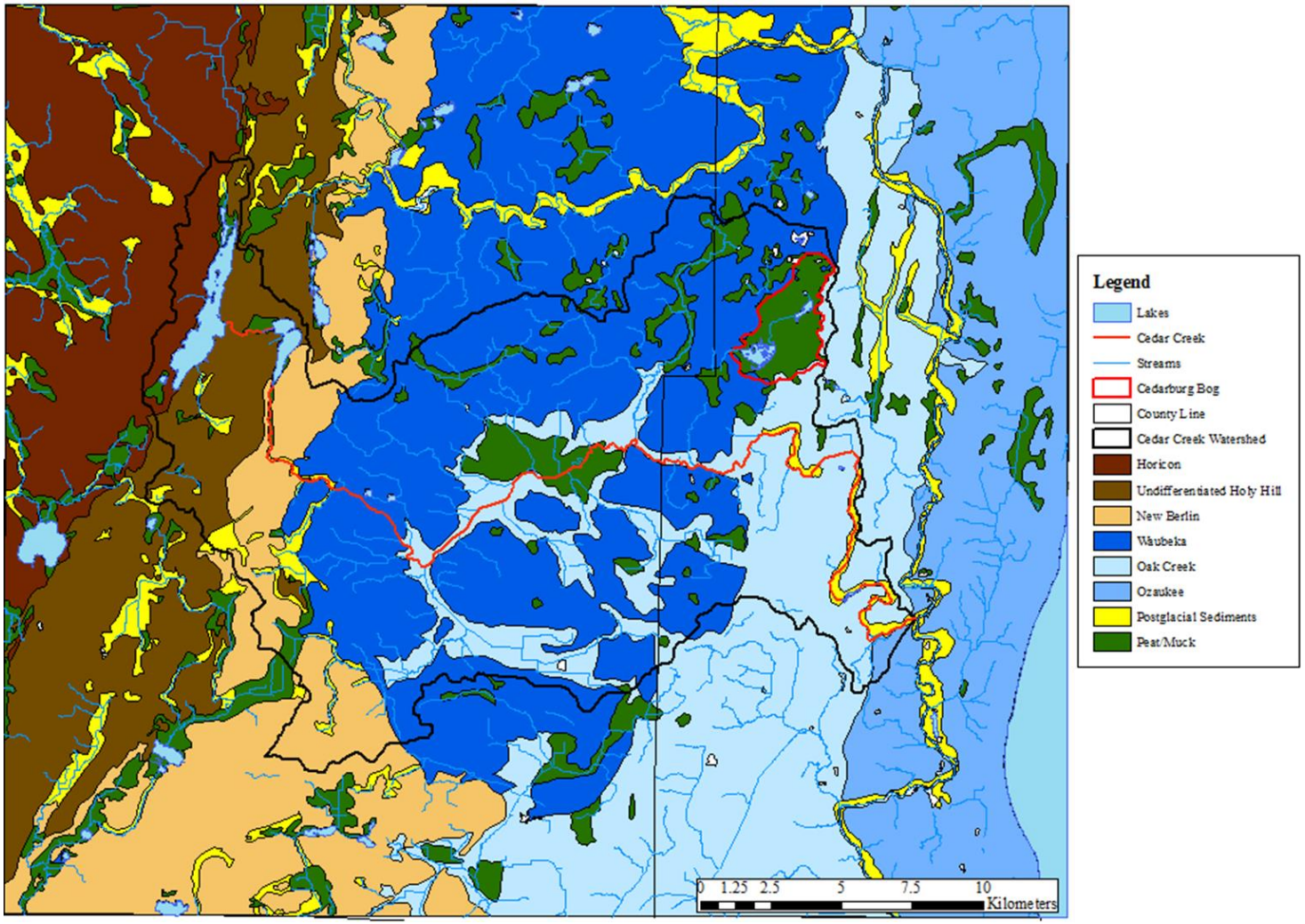

Figure 4. Surficial glacial units in the Cedar Creek Watershed

2.1.4. Hydrogeology

Both the glacial sediments and Silurian dolomite comprise the surficial aquifer from which a majority of the residents get their drinking water. Underlying the surficial glacial sediments is the Silurian Dolomite bedrock. This unit has highly variable hydraulic conductivities, similar to the glacial sediments, ranging from 8.64 $x10^{-6}$ m/day to 1 m/day [*Rovey and Cherkauer*, 1995]. The large hydraulic conductivities are found near the surface of the bedrock where the dolomite is highly fractured and weathered. The Silurian dolomite was the land surface around 21,000 years before present and was weathered and fractured due to the high stress caused by repeated glacial advances and retreats. This high hydraulic conductivity in the upper bedrock allows for generally high recharge to reach the lower parts of the shallow aquifer. Lower hydraulic conductivities are found beneath the weathered dolomite layer where hydraulic conductivity varies both horizontally and vertically.

Underlying the Silurian dolomite is an interbedded shale/dolomite aquitard known as the Maquoketa Shale, which acts as a confining unit for a deeper sandstone aquifer. Most of the high capacity municipal wells and high capacity irrigation wells in the watershed are drilled into the dolomite drawing groundwater from both the glacial sediments and bedrock, with very few wells in this watershed drilled into the deep sandstone aquifer [*Smail*, 2014].

2.2. Cedarburg Bog

The Cedarburg Bog was designated a National Natural Landmark in 1973 by the United States Department of the Interior and earlier a Wisconsin State Natural Area in 1952. The largest, nearly undisturbed bog in southeastern Wisconsin, the Cedarburg Bog has developed in a post-glacial lake basin, which supports seven wetland types and regionally rare species of flora and fauna many of which are at their southernmost limits geographically (Figure 5).

2.2.1. Land Use, Vegetation

Within the Cedarburg Bog, there are eight habitats supported; seven of them being wetland types and the eighth being upland hardwood forest, which is isolated to the several glacial islands scattered throughout the bog [*Reinartz,* 1985]. Although colloquially known as the Cedarburg Bog, contained within the natural area are seven types of wetland land cover; coniferous bog dominated by tamarack, black spruce and sphagnum moss, coniferous swamp with northern white cedar, fen, lowland hardwood swamp, marsh ringed by shrub-carr. The final wetland type is a patterned peatland also known as a "string bog", which is alternating parallel rows of high ridges "strings" with stunted tamarack and cedar trees and low areas "flarks" of sedges and mosses, approximately 2-6 meters across [*Grittinger,* 1970]. There are six lakes of varying depths and sizes within the bog; the largest two are Mud Lake, 0.60 km^2 (148 acre) with a maximum depth of 1.2 m, and Long Lake, 0.16 m (39 acre) with a maximum depth of 1.52 m [*Reinartz et al.*, 2013].

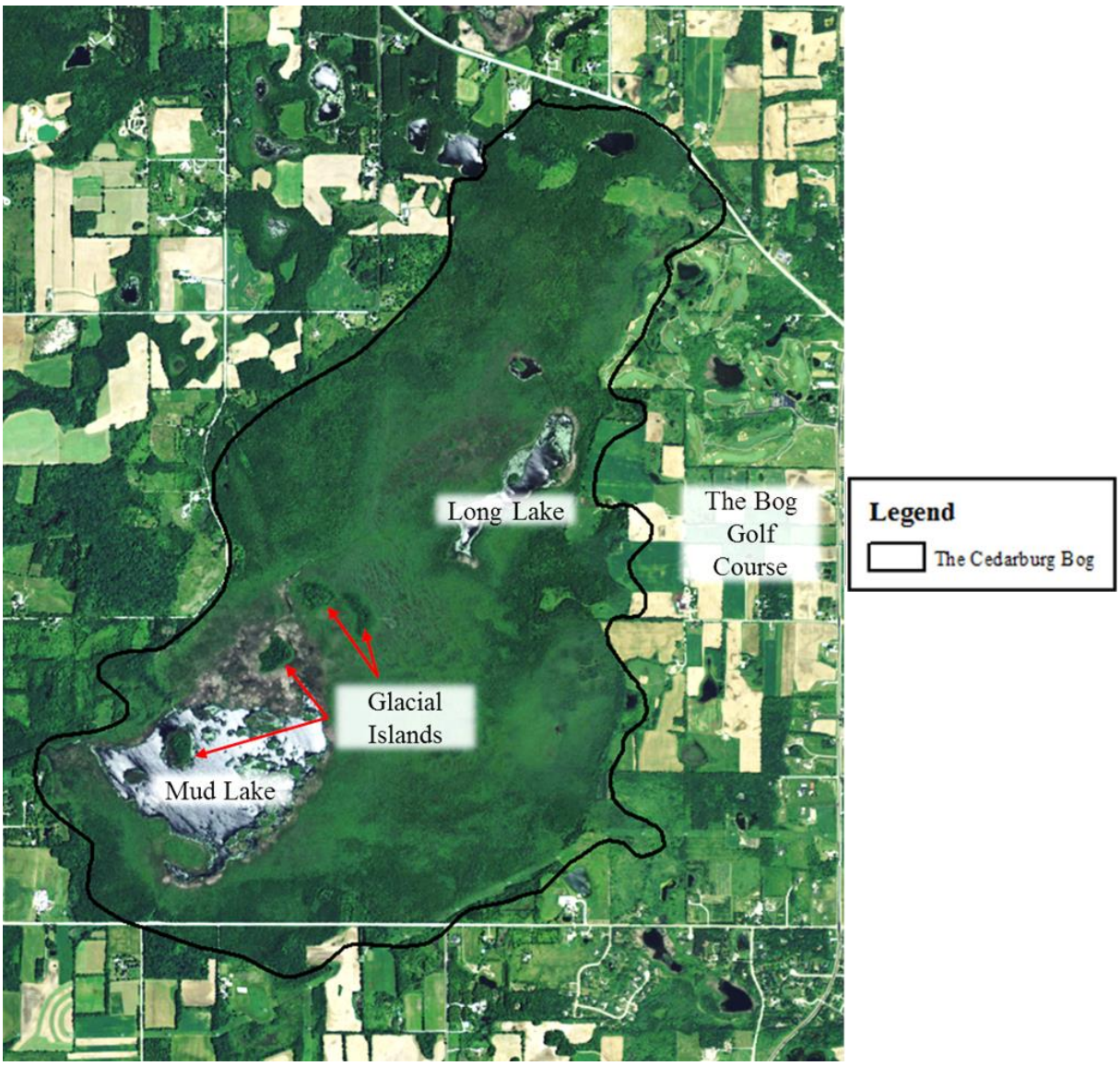

Figure 5. The Cedarburg Bog. Showing locations of the two large lakes, glacial islands and The Bog Golf Course on the eastern side of the Cedarburg Bog.

2.2.2. Population and Economic Activity

The main change in population and economy around the Cedarburg Bog over the last 50 years is the development of a few subdivisions and also a golf course in the northeast corner of the bog (Figure 5).

2.2.3. Glacial Geology

The Cedarburg Bog and surrounding landscapes are remnant of this locality's glacial history. The deposition and erosion of sediment from the Michigan Lobe of the Laurentide Ice Sheet approximately 12,000 years ago shaped the landscape and created the glacial lake basin in which the bog is situated at present day. The hummocky topography of the landscape and the presence of numerous kettles and kettle lakes give this area its landscape and subsurface characteristics. In the west and south of the bog, both drumlins and eskers are found, which are formed beneath glacial ice, and were deposited between 14,500 and 14,000 years before present [*Mickelson and Syverson*, 1997]. The eastern boundary of the bog is formed by the terminal moraine of the main glacial lobe and was deposited as the glacier retreated to the east. The area to the west of the bog is covered by glacial outwash deposits that were laid during the retreat of the glacier to the east [*Mickelson and Syverson*, 1997]. These sediments were carried by meltwater from the base of the glacier and covered the area of the bog. Within the bog itself there are glacial lakes and islands that were formed when the glaciers were retreating and left behind stagnant ice that was cover by sediment which subsequently melted leaving the hummocky topography found throughout the locality. The combined

effect of this glacial history resulted in the Cedarburg Bog being formed in a high area of topography relative to the surrounding elevation.

2.2.4. Hydrogeology

The hydrogeology of the Bog is dependent on the properties and characteristics of the peat formations. The surficial peat mat is primarily composed of living flora and plant litter in its beginning stages of decomposition. This mat ranges in depth from centimeters to half a meter [*Kuhns and Reinartz,* 2007]. Beneath are the decomposing organic matters that make up the majority of the Bog volume. The thickness of the peat deposits within the Bog ranges from centimeters near the glacial islands to over 15 m [*Kuhns and Reinartz,* 2007]. It is likely that beneath the peat lies an impermeable boundary presumably made up of low permeability clays and other lakebed sediments from the glacial lake. This layer likely limits vertical flow through the base of the bog due to the low hydraulic conductivities of fine sediments such as silt and clay which are typically found in lakebed deposits.

As previously mentioned, there are seven islands composed of glacial sediment, typically ice-contact deposits, similar to kames, scattered throughout the Bog (Figure 5). These islands provide high permeability pathways through localized areas in the Bog with a possibility of providing a buffering capacity through chemical weathering of the carbonate rich till to the Bog waters, which may partially explain the near neutral pH of the Bog waters.

3. Climate Change Prediction in Cedar Creek Watershed

3.1. Global Climate Change

Climate change prediction is crucial to the well-being of Wisconsin residents due to the vast role of agriculture in the state's economy. In addition to large quantities of crop production, Wisconsin is also a valuable resource for large swaths of forest and large quantities of freshwater features such as lakes and streams. This special combination of agricultural land and forests bordered by two enormous freshwater lakes, Michigan and Superior, gives rise to a necessity for understanding of the effects of climate change on the weather patterns, precipitation events, growing season change and rises in temperature.

Typically climate change observation and prediction has been performed at specific sites across the world, which have allowed for both national and global estimates. In 2014, the IPCC published the Fifth Assessment (AR5), which outlined the changes in historical climate as well as predicting future climate scenarios and simulations. Historically, the global mean temperatures have changed over a range of -0.53 to 2.5 ^{o}C, with a mean warming of about 0.6 to 0.7 ^{o}C since 1950 [*Kucharik et al.*, 2010b]. In addition to the warming trends, an increase in precipitation has been observed, up to 5%, with the majority of rainfall occurring in extreme events. For future climate projections, the fifth report uses Representative Concentration Pathways (RCPs) in order to project climate change based on the concentrations of the four greenhouse gases. In order from lowest to highest concentration of gases, the RCPs are RCP 2.6, 4.5, 6.0, and 8.5. The RCPs are distinguished from one another based on the total radiative forcing,

which is the difference between the energy absorbed by Earth from sunlight and the energy radiated out of the atmosphere, in Watts/m^2. RPC 2.6 reaches peak concentrations between now and 2020, while the highest emissions in RCP 8.5 will peak after the end of the 21st century. Under the conditions of RCP 2.6, a projected increase in global mean temperatures is about 1 ^oC but up to 2 ^oC, while the RCP 8.5 projects a 4 ^oC increase but could be up to a 5.5 ^oC increase [*IPCC*, 2013].

The implications of these national and global scale projections are the ability of local and regional entities to develop predictions and projections for more localized areas. Utilizing from global/national projections, the Wisconsin Initiative on Climate Change Impact and the internal Climate Working Group have downscaled and applied these to local climates [*Kucharik et al.*, 2010b]. The results presented were generated from the CMIP3 archive of daily outputs through the mid-21st century and the late 21st century, which simulations include representations of the Great Lakes and their effect on climate. Furthermore, the use of regional climate models and General Circulation Models (GCMs) have allowed for more precise and localized climate projections and predictions which were used to develop variable recharge conditions simulated in the groundwater flow model.

3.2. Historical Climate Change in Wisconsin

In order to fully comprehend future climate change locally, one must be familiar with historical climate change. Also, understanding the changes in agriculture, forestry, surface water quality and more importantly groundwater quality and quantity, which are

governed by climate factors, is extremely beneficial for management and planning for future climate change.

The Midwest Regional Climate Center analyzed the historical climate of the Midwestern states since the early 1900's and reported a 0.6 ^{o}C increase in Wisconsin, with the most warming occurring in the winter months about 1.5 ^{o}C [*MRCC*, 2015]. Also, annual precipitation has increased about 56 mm with summer mean precipitation increasing 28 mm. *Kucharik et al.* [2010a] outlined the historical climate change of Wisconsin using spatially interpolated data at 133 temperature and 176 precipitation stations across the state from 1950 to 2006. Specific to the Cedar Creek watershed, the analyses revealed an annual average minimum temperature increase of about 1 ^{o}C and annual average maximum temperature increase of 0.5 ^{o}C, with an average increase in precipitation of 100 mm annually and up to 10 fewer days with temperatures below -17.8 ^{o}C (0 ^{o}F). In addition, an important factor reviewed by *Kucharik et al.* [2010a] was the growing season length increasing by a full week.

3.2.1. Temperature and Precipitation

Due to the proximity of Wisconsin to the Great Lakes, there are highly variable precipitation and temperature patterns across the state. *Kucharik et al.* [2010a] showed warming temperatures across the north and central parts of the state in all seasons except autumn and also showed nighttime temperatures increasing more than daytime temperatures. On the other hand, the temperature change is negligible in the southeastern portion of the state, but there was a significant decrease in the number of nights below -17.78 ^{o}C (0 ^{o}F) across the state. Air temperatures range from the historic maximum of

39.4 ºC in July to a minimum of -32.3 ºC in February. On average, daily temperatures range from a high in July and August of 28 ºC to a low of -8 ºC in January.

The more important aspect of climate change for this region is precipitation. The annual average precipitation increased about 15% throughout the state with some localized areas experiencing a decrease in precipitation rates since 1950. The WICCI Climate Working Group Report called Climate Change in Wisconsin showed a statistically significant (by the Mann-Kendall trend detection test) increase in heavy precipitation events in a nearby weather station in Milwaukee, 32 km from the bog [*Kucharik et al.*, 2010a]. Southeastern Wisconsin experienced an increase in annual average precipitation of over 10 cm during the period of 1944-2014, trending towards a wetter climate.

Climate normals since 1944 for the Cedar Creek Watershed are shown in Figure 6, and seasonal temperature and precipitation change are shown in Table 2. The annual mean temperature is approximately 7.5ºC with summer temperatures often surpassing 25ºC, and the annual mean precipitation was 2.3 mm/day. These high temperatures often coincide with high precipitation rates generally at or exceeding 80 mm/month. Conversely the winter months experience the lowest temperatures, often at or below 0 ºC. The winter months also tend to experience the least precipitation throughout the year, less than 50 % of the summer precipitation.

In a review of more recent climate, the months with the highest temperature correspond to the months with the highest precipitation. From January 2000 to December 2014, June, July and August have received both the highest amounts of precipitation, over 80 mm/month and the highest temperatures, all over 25 ºC. Specifically, for the year

of 2014 June has the highest precipitation at 231.28 mm with April and May having the second and third highest precipitation rates at 135.37 and 71.21mm, respectively. The implication of this trend (high precipitation coinciding with high temperatures) on recharge is the highest amount of precipitation is falling on the hottest months of the year, which coincide with the peak of the growing season. This means that little to no recharge will reach the water table during the summer months. This trend is even more evident in the 2014 data as July, August and September have recharge rates of 0 mm/month (from SWB output) due to the high temperatures and lower precipitation rates in these months. The largest amount of recharge comes when the ground begins to thaw during March and April. These months have high precipitation rates, low evapotranspiration, due to low temperatures and inactive vegetation, and this in combination with the spring freshet result in large amounts of recharge to the water table. This is seen in 2014 as the recharge rates, generated from the Soil-Water Balance code, for March and April are the highest in the year at 31.7 and 53.34 mm/month respectively.

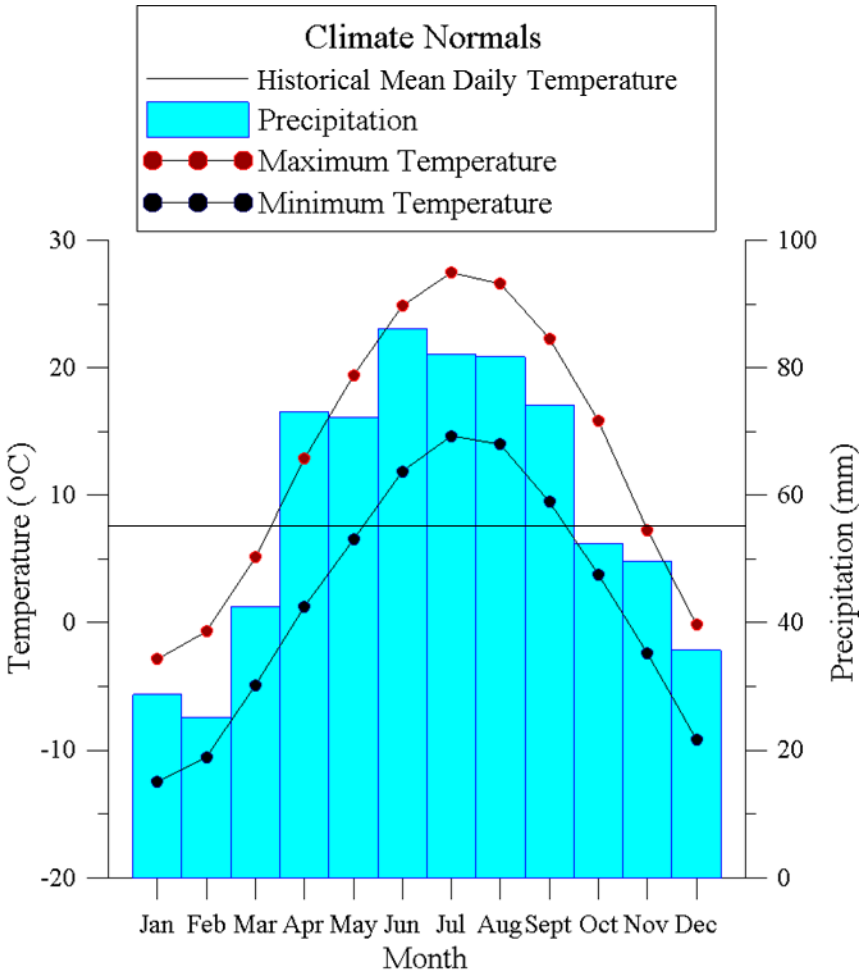

Figure 6. Monthly averages of temperature and precipitation from the Germantown weather (43.2388°, -88.1222°) station since June 1st, 1944 (http://www.ncdc.noaa.gov/cdo-web/datasets/GHCNDMS/stations/GHCND:USC00473058/detail)

Table 2. Seasonal temperature (°C) and precipitation (mm) expressed as a percent (change/mean) since 1944. These values were generated by calculating decadal mean temperature and precipitation values for each season since 1944. These means were then used to calculate the change in both temperature and precipitation seasonally for each decade i.e. 1944-1953 mean values were subtracted from 2004-2013. The subsequent values were then divided by the seasonal mean of the entire data series 1944-2014 and expressed as a percent.

	Winter	Spring	Summer	Fall
Temperature (%)	4.2	13.4	4.2	-0.2
Precipitation (%)	13.4	25.4	16.4	-18.6
Mean Temperature (°C)	-6.16	6.63	19.79	9.09
Mean Precipitation (mm/day)	1.22	2.42	3.17	2.31

3.2.2. Evapotranspiration

Evaporation of water from the surface water features, soils and leaves of plants in addition to transpiration of water directly from tissues of plants are commonly known as evapotranspiration (ET). Evapotranspiration is typically referred to as either Potential Evapotranspiration (PET) or Actual Evapotranspiration (AET) with PET being the maximum possible loss of water through evaporation and transpiration from the soil and plants. The ET has been the most difficult climate/water budget parameter to measure as it is extremely variable based on soil type, solar radiation, wind speed, plant type and more. Specifically, this difficulty arises due to the complex relationship between many meteorological parameters and surface features (soils, flora, and land cover). Additionally, vast amounts of land use were changed over the years. With a changing landscape, it will be nearly impossible to quantify the ET change over large areas of the state. However, with trends towards a warmer and wetter climate in Wisconsin, the

growing season will presumably be longer, consequentially increasing transpiration of water as well as elevating evaporation rates.

Given this premise, ET in the Cedar Creek Watershed should be greatest during the summer months when the temperature was highest (Figure 6). The growth of crops and other flora also cause an increase in ET during the growing season. The ET in the early spring and late fall was interpreted to be low, while the winter months experienced no evapotranspiration. Additionally, the largest contributors to ET are the large surface water bodies located in the watershed; Big Cedar and Little Cedar Lakes have a large amount of surface area from which evaporation can occur. The wetlands in the watershed allow for large amounts of ET as well, due to the near surface water table and high density of flora.

3.3. Modeling of Future Climate Change

Modeling of future climate is an intensive and difficult process due to the highly variable nature of climate on both a spatial and temporal scale. To achieve this, General Circulation Models (GCMs) are employed to develop a broad global prediction for future climate. In order for the GCMs to be of use to local entities, a process called statistical downscaling is employed. Statistical downscaling is a two-step process with the first step using local historical climate data in conjunction with large scale climate patterns to develop a relationship between local weather and global climate. Second, this relationship is combined with large scale future projections from the GCMs to determine the effect of large scale climate patterns up to 100 years in the future on local weather events.

Due to the highly variable content used within the climate change projections, there are multiple emission scenarios for the greenhouse gas emissions across the globe. As the greenhouse gases have been shown to be influential on climate change, the emission scenarios dictate the extent or severity of the climate change. The emission scenarios are based on multiple variables outlined as either: environmentally focused or economically focused, and globalization or regionalization. Initially reported in the Special Report on Emissions Scenarios (SRES), and subsequently used in the IPCC Third Assessment Report, Fourth Assessment Report and Fifth Assessment Report, the four families of scenarios are as follows: A1, A2, B1, and B2.

Within the groundwater flow model, the recharge maps for the future scenarios will be based on the most extreme ends of the spectrum, A2 and B1, so those results along with the median emission scenario of A1B will be discussed here. The A2 scenario is generally considered the "worst-case" scenario as it ends the 21st century with the highest atmospheric content of CH_4, and the second highest concentrations of CO_2 and N_2O, while the B1 is the "best-case" scenario with the lowest concentrations of CO_2, CH_4, and near lowest N_2O. These simulations are modeled at two separate time periods; the mid-21st century, through 2055, and the late 21st century, through 2100.

A very important thing to note about climate change projection is the uncertainty involved in every aspect of future climate projections.

3.3.1 Temperature and Precipitation

The temperature increases across the state are not sensitive to the emission scenario through the mid-21st century as all scenarios have a mean increase in

temperature of around 4.5 ^{o}C [*WICCI*, 2011]. Specifically within the Cedar Creek watershed, the annual average temperature is projected as rising up to 4 ^{o}C through 2055 and with winter temperatures rising the most (4.2 ^{o}C). All other seasons experience around a 3 ^{o}C warming compared to the climate normal shown in Figure 6. More importantly for this projection are the values from the end of the 21st century, up to 8 ^{o}C warming for the A2 and A1B scenarios and up to 5.5 ^{o}C for the B1 scenario, as these reflect the most extreme change in climate. Another aspect of climate change is the seasonal trend of days above 32.2 ^{o}C (90 ^{o}F) and below -17.8 ^{o}C (0 ^{o}F). Through the mid-21st century, the Cedar Creek Watershed will receive up to 22 more days with temperatures above 32.2 ^{o}C and 10 fewer days with temperatures below -17.8 ^{o}C. All of the projections and models indicate an increase in temperature annually but also showed many fewer extreme cold events with increasing hot periods. This is expected to affect both the snow cover, duration of frozen ground, and the average temperature of Lake Michigan which will influence the effect of warming on the Cedar Creek Watershed area.

The future climate scenarios implemented into the groundwater flow models focus on changes in recharge as the primary climate factor. As precipitation is the most influential factor in recharge, it is necessary to review the changes in precipitation leading to the variable recharge rates. The annual mean precipitation in the locality of the Cedar Creek Watershed is simulated to increase by nearly 40 mm per year (relative to today's average of 850 mm per year) with nearly equal increases in precipitation through winter, spring and fall, but no change in the summer months across all emission scenarios. With this being said, it must be noted that there is a very large range of potential changes in precipitation and GCM projections have suggested that the possibility for no change in

precipitation is high but there is a 75% chance that precipitation will rise based on probability distribution of model results [*Kucharik et al.*, 2010b].

Table 3 shows the maximum and minimum predicted changes in temperature and precipitation at the Cedar Creek watershed through the end of the 21st century. Winter temperatures are expected to increase the most, with up to a 7 ^{o}C increase but may increase only 2 ^{o}C. Spring, summer and fall show a similar trend with the upper bound to be approximately 5-6 ^{o}C increases in temperature. Another aspect that controls recharge to the groundwater table is the duration of frozen ground throughout the winter. When precipitation other than snow falls on frozen ground recharge cannot occur, and with a future warming climate it is more than likely that the duration of frozen ground will be shorter which in turn will increase recharge during the winter months. The first freeze of the winter will come later in the year and the spring freshet will come earlier than present. In addition to the shorter duration of frozen ground it is also possible that some thaws will occur during the three months that the ground is typically frozen, this will also allow for more recharge to reach the groundwater table. Precipitation values on the other hand are much more variable in future predictions. For example, winter precipitation is expected to increase up to 40% greater than current rates, with little to no chance of a decrease in winter precipitation. On the other hand, summer precipitation ranges from a decrease of 25% of current values to an increase of 20%. Spring and fall values are similar in the fact that both have predictions showing a possibility of a decrease in about 5% but also an increase up to 25%.

An important aspect to recharge is the intensity and duration of rainfall events. Soils with holding small capacity of infiltration rate will cause large amounts of rainfall

to be forced into overland flow and runoff. Therefore, precipitated water will not be recharged to the groundwater table directly but possibly redirected to surface water features or storm drains. This is most likely to occur during high intensity rain events with short duration. Currently, there is approximately one 50 mm rain event every 2 years in the State of Wisconsin [*Choi et al.*, 2013]. This number of high intensity rain events is projected to increase by about 25% through the middle of the 21st century or two to three more events per decade, indicating a trend towards a wetter climate with more precipitation falling in extreme events.

Table 3. Predicted minimum and maximum changes in temperature and precipitation through the end of the 21st century in the Cedar Creek Watershed area as a result of the down-scaled climate model (WICCI, 2011).

Season	Temperature (ºC)	Precipitation (%)
Winter	2.0 to 7.0	0 to +40
Spring	2.0 to 5.0	-5 to +25
Summer	1.0 to 5.0	-25 to +20
Fall	2.0 to 6.0	-5 to +15

3.3.2 Evapotranspiration

Due to the nature of ET, it is difficult to predict future actual evapotranspiration. Nevertheless, the estimation of potential ET (PET) was conducted with the Priestley-Taylor method. The downscaled dataset for Wisconsin gives maximum and minimum

temperature along with precipitation; therefore any estimations of PET are going to contain much more inherent uncertainty than either temperature or precipitation. That being said, the PET is modeled to increase 60 mm and 100 mm per year based on Special Report on Emissions Scenarios (SRES) emission scenarios B1 and A2 respectively [*Kucharik et al.*, 2010b]. Winter PET has not been shown to rise but spring, summer and fall all show higher PET with the A2 emission scenario generally showing twice as much PET than the B1 scenario.

4. Groundwater Modeling

4.1. Watershed Scale: Cedar Creek Aquifer Model

The surficial aquifer is comprised of glacial deposits ranging in size from clay to gravel and the underlying Silurian dolomite. The aquifer is classified into 8 units, which include, the Horicon, New Berlin, Waubeka Members and undifferentiated sediment of the Holy Hill Formation, the Oak Creek Formation, the Ozaukee Member of the Kewaunee Formation and the bedrock Silurian Dolomite (Figure 4) [*Mickelson and Syverson*, 1997].

Both steady- and transient-state 3-dimensional model was constructed using MODFLOW-NWT in conjunction with Arc GIS [*Niswonger et al.*, 2011]. Nearly all units in the MODFLOW model (hereafter called groundwater flow model) were imported as shapefiles from ESRI GIS software. The areal dimension of groundwater flow model is 32.1 km by 37.6 km where the Cedar Creek Watershed, a sub-basin of the larger Milwaukee River Watershed, is positioned at the center (Figure 7). The distances from

watershed boundary to groundwater model boundary vary from approximately 5 to 15 km. The “farfield” portion from the watershed model is inserted to reduce the boundary effects on the Cedar Creek Watershed.

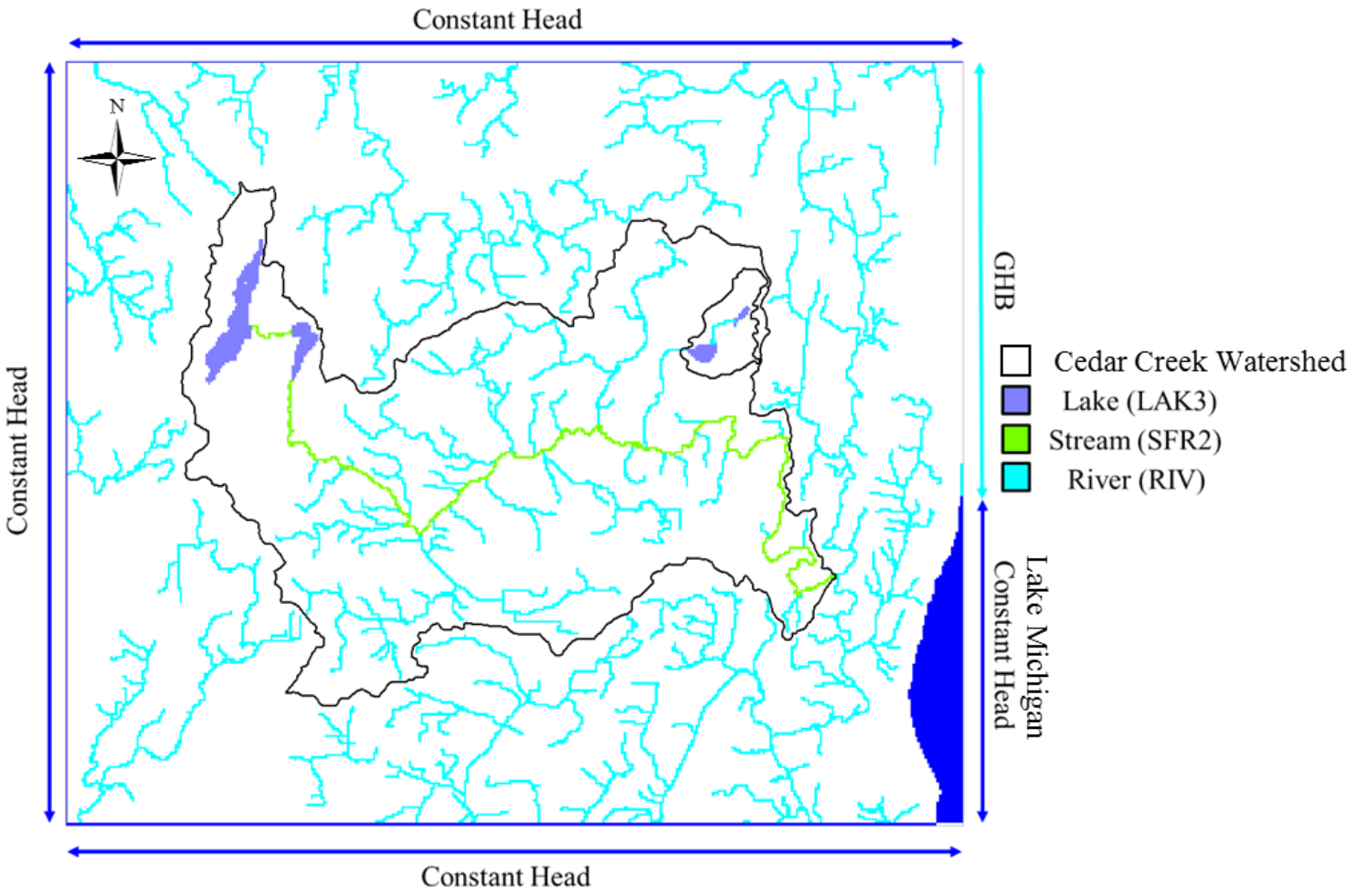

Figure 7. Cedar Creek aquifer model area showing boundary conditions and surface water features.

Four layers representing surficial glacial aquifer with various thickness from 0 to 208 m (1st - 2nd layers), weathered dolomite thickness from 0.12 m to 22.4 m (3rd layer), and the Silurian Dolomite thickness from 127 m to 289 m (4th layer) were included. The layer elevations were determined using the bedrock map as the surface of layer 3, with the overlying glacial deposits divided into two layers of equal thickness, and the base of the model set at 0 m. The bedrock elevation map shown in Figure 8 was created by the Wisconsin Geological and Natural History Survey (WGNHS) for the Southeastern Wisconsin Regional Planning Commission (SEWRPC) by interpolating the depth to bedrock from Well Construction Reports (WCRs) [*SEWRPC*, 2012]. Total dimension of groundwater model is 32.1 km by 37.6 km (321 rows by 376 columns) discretized with uniform areal spacing of 100 m × 100 m and variable thickness.

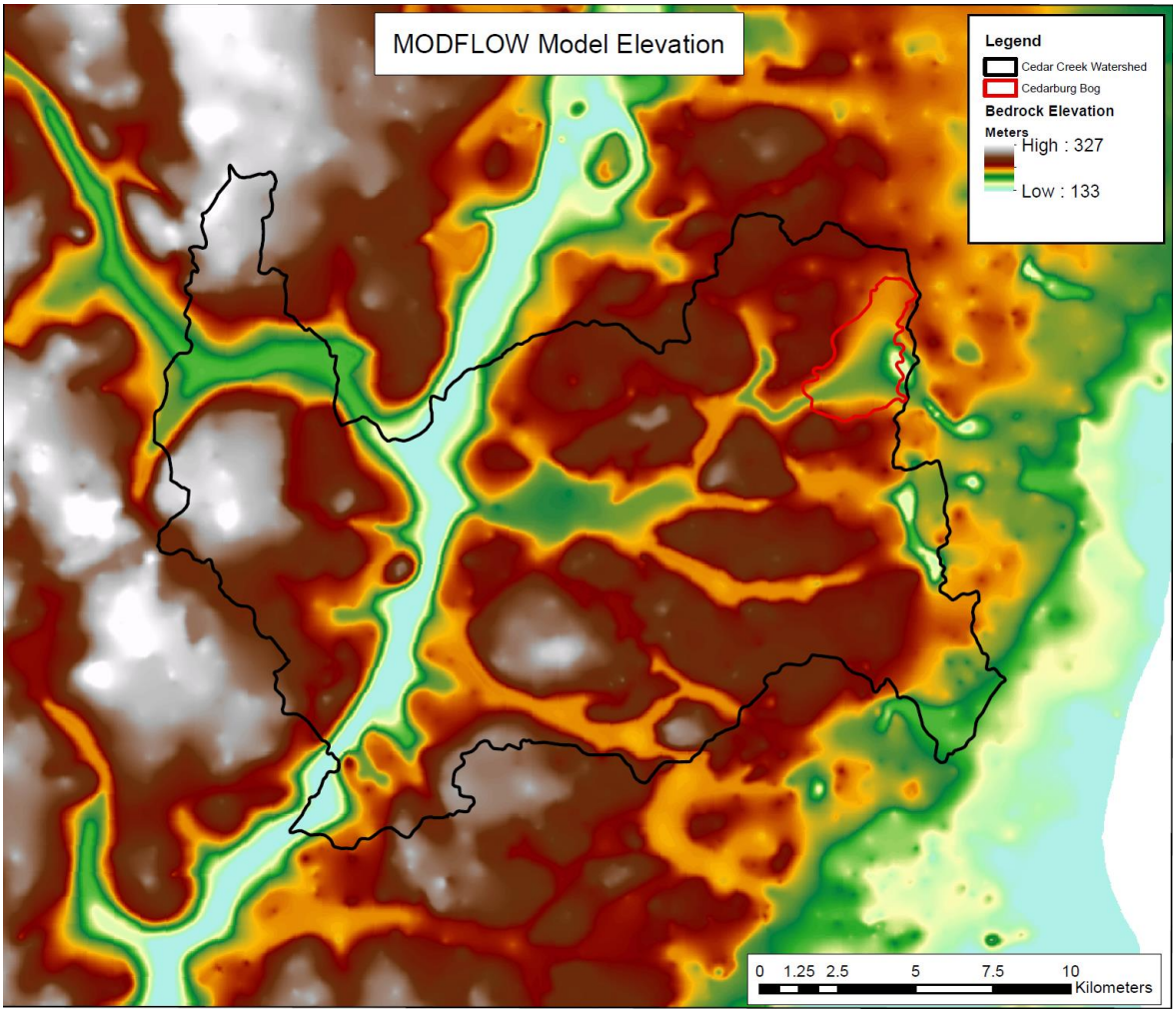

Figure 8. Bedrock Elevation of groundwater flow model, which represents the top of layer 3 in the MODFLOW model

The north, west and south sides of groundwater flow model are bounded by constant head boundary where the assigned groundwater level mimics surface topography. Based on analyses of selected well log reports adjacent to the boundaries, the groundwater levels were set at 10 m below the land surface. The north side of the eastern boundary is assigned as General Head Boundary (GHB) which simulates Lake Michigan, and is approximately 7.5 km away from the GHB in the northernmost cells. The distance between the groundwater model boundary and Lake Michigan and the hydraulic

conductivity of the aquifer were assigned in the GHB cells to calculate the water budget. The south side of east boundary representing Lake Michigan stage is assigned as constant head cells. The lake stage used was the 100-year average Lake Michigan stage (Figure 9). Finally, the bottom of the Silurian Dolomite (4th layer) is bounded by a confining unit known as the Maquoketa shale, which is represented in the model by a zero flux (or no-flow) boundary.

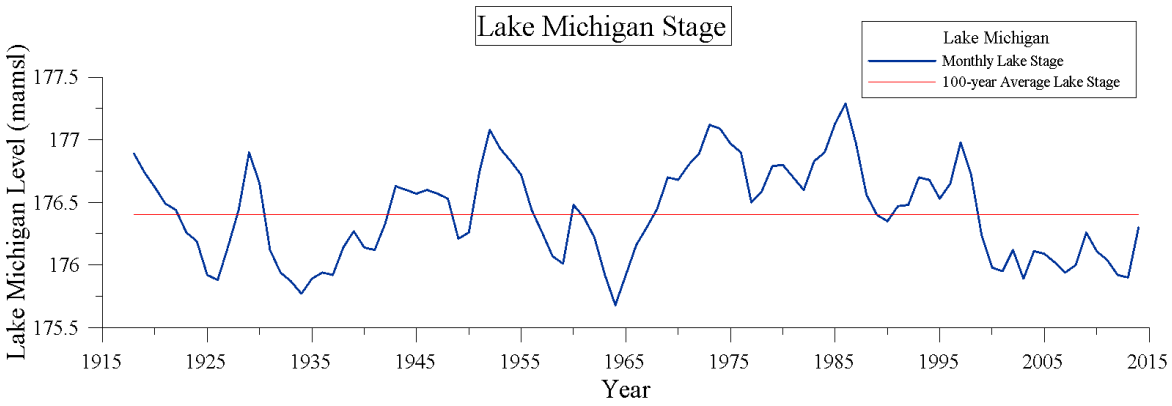

Figure 9. Lake Michigan stage data showing monthly average stage (blue) and long term average (red) for the past 100 years.

4.1.1. Surface Water

There are a total of 43 lakes within the model area with only 2 of them, excluding Lake Michigan, being larger than 1 km^2 (e.g., Big Cedar, Little Cedar). Specific to the Cedar Creek watershed, a total of 14 lakes exist. Among them, the largest four lakes were only assigned in the groundwater flow model (Figure 7). Long Lake is the smallest modeled lake at 0.16 km^2, Mud Lake is 0.6 km^2, Little Cedar Lake is 1.05 km^2, and the largest lake, Big Cedar, is 3.8 km^2.

The main trunk of Cedar Creek is the largest stream body in the watershed. It has a drainage area of 310 km^2 and a mean annual flow of 5.5 m^3/s (National Water Information System, USGS; http://waterdata.usgs.gov/nwis/). The creek originates in Big Cedar Lake in the northwest of the watershed and flows into Little Cedar Lake (Figure 2). At the geographic middle of the watershed, the creek continues through the center of Jackson Marsh and continues flow east and south until its confluence with the Milwaukee River near the basin outlet where Cedarburg and Grafton are located. The discharge of Cedar Creek measured at the USGS gauging station upstream from the City of Cedarburg is shown in Figure 10. The highest discharge rates occur in the spring due to snowmelt and spring rains. The blue bars separating the different years of discharge indicate the time period when the creek was completely frozen, and thus, no discharge could be measured.

In addition to the Cedar Creek, which was simulated using the Stream-Flow Routing 2 package (SFR2), there are over 250 additional tributaries and streams simulated in the model. These streams and rivers are simulated differently from the main trunk of Cedar Creek. The first order streams are simulated similarly as they are all assigned the same depth and width of 0.33 m and 1 m respectively. The second order streams again are simulated similarly, with a depth of 0.66 m and increased width of 2 m. Finally all third order streams are assigned a depth of 1 m and a width of 3 m. This simplified input for the rivers allowed for a more stable model. Furthermore, the lack of data for these small tributaries and rivers did not allow for a more complex and accurate simulation of the rivers. The exception to this is the Milwaukee River, which is the largest river in Southeastern Wisconsin, and is the main river of the larger watershed,

which encompasses the model area (Milwaukee River Basin). The Milwaukee River was simulated with a depth of 1 m and a width of 10 m. All the rivers in the model area had the bottom elevation designated from the digital elevation model and the depth of the river was added to the elevation from the DEM to find the stage in each cell.

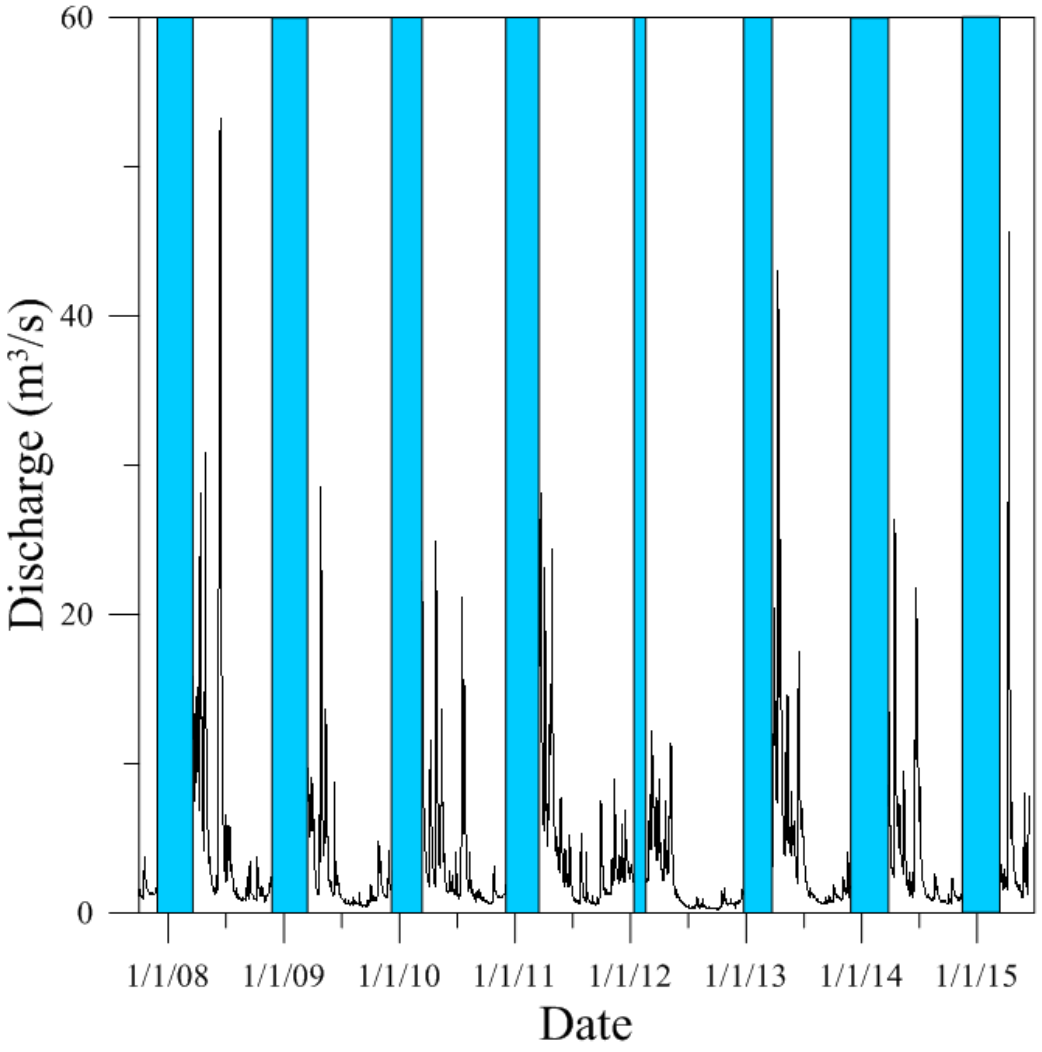

Figure 10. Stream discharge of Cedar Creek from 10/1/2007 through 5/10/2015 monitored at a 15-minute interval retrieved from the National Water Information System of the USGS. (http://waterdata.usgs.gov/usa/nwis/uv?04086500). Vertical blue bars indicate periods of ice on the river in which no discharge measurements were recorded

4.1.2. Soil-Water Balance Recharge Modeling

The Soil Water Balance (SWB) model calculates recharge using readily available GIS datasets in tandem with tabular climate data, precipitation and temperature. The SWB code uses a modified Thornthwaite-Mather method to calculate SWB components at a daily frequency with recharge output for daily, monthly or annual intervals. The use of the SWB is easy and efficient, and has been used successfully in numerous projects [*Dripps and Bradbury*, 2007; 2010]. The design of the SWB model is for use at a regional scale as opposed to site specific modeling and is generally more reliable when averaged over months or even years.

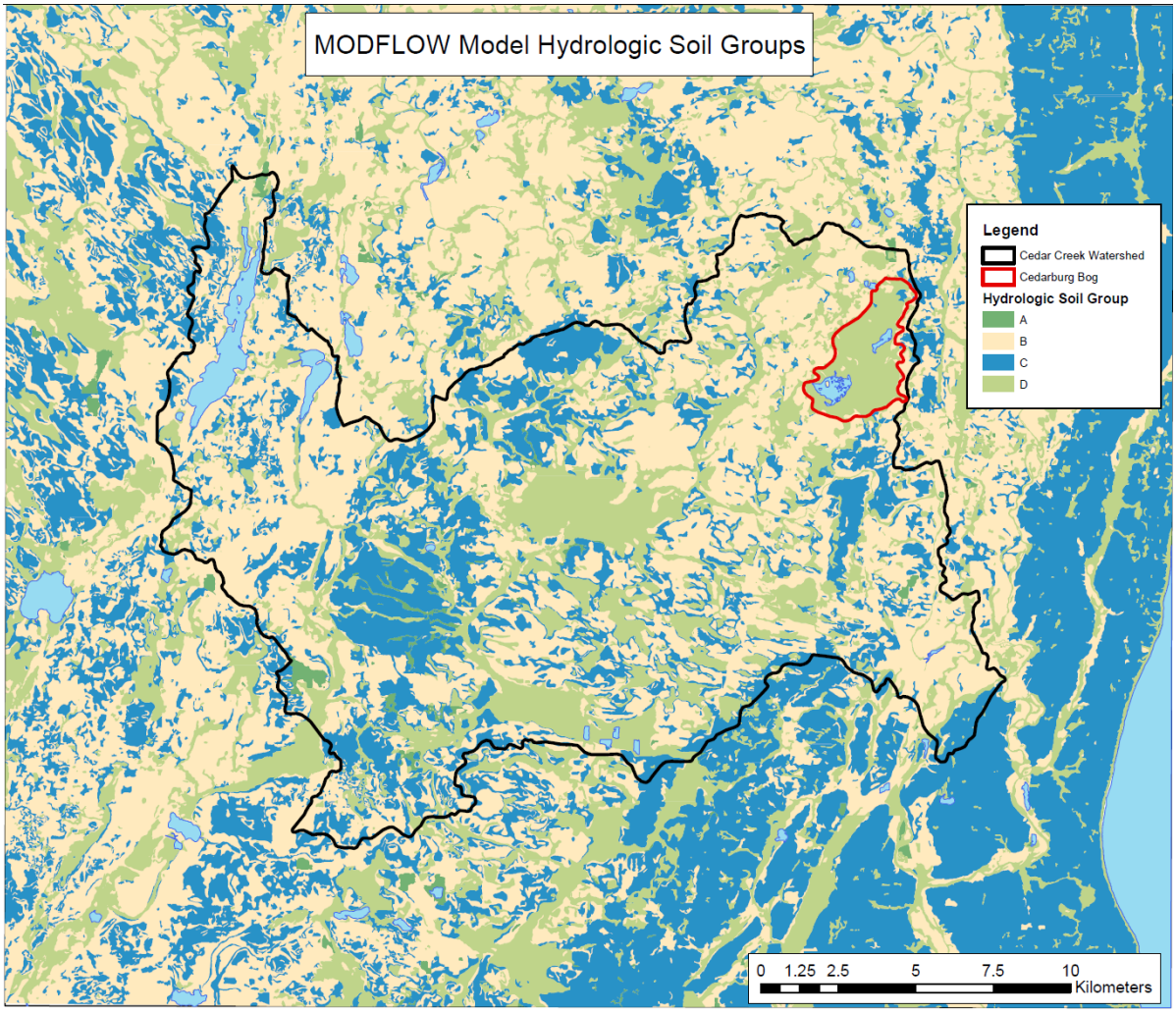

Figure 11. Hydrologic Soil Groups for input to the SWB code, classifications represent infiltration rates with A being highest at >0.75 cm/hour, B from 0.38 to 0.75 cm/hour, C from 0.125 to 0.38 cm/hour and D being lowest <0.125 cm/hour (Retrieved from the National Resources Conservation Service (NRCS) Web Soil Survey)

The inputs into the SWB model are available online from numerous sources and can be manipulated and preprocessed in ArcMap. There are four gridded input datasets in addition to the tabular climate data which are summarized: (1) D-8 Flow Direction (DEM, Figure 2), (2) Land Cover (Figure 4), (3) Available-Water-Capacity (AWC) and (4) Hydrologic Soil Groups (Figure 11). The D-8 flow direction raster is generated from the Digital Elevation Model (DEM) of the study area and has 8 integers each representing

flow direction of the cell, e.g. flow to the east is a 1, flow to the south is a 4, flow to the west is a 16 and flow to the north is 64. The flow direction for each cell is determined by differences in elevation between two adjacent cells. Land cover in addition to available water capacity of the soil are used to calculate surface runoff in addition to the maximum holding capacity for soil water. Finally, hydrologic soil groups are generated from the Natural Resources Conservation Service soil surveys in which each soil series is given a rank of infiltration rate from A, highest, to D, lowest. Each raster must contain the same grid dimensions designed in the groundwater flow model (x and y spacing as well as coordinates) and can be exported from ArcMap as an ASCII grid file which is then listed in the control file as an .asc extension. The tabular daily climate data is the other input and must contain both precipitation and temperature (min, max, mean) but can also contain wind speed, relative humidity, and possible percent sunshine.

Recharge is calculated using a modified Thornthwaite-Mather soil-water balance method, which is based on the difference between the sources and sinks of soil moisture (Eq. 1) [*Thornthwaite and Mather*, 1957].

$$Recharge = (precip + snowmelt + surface\ inflow) - (interception + surface\ outflow + ET) - \Delta soil\ moisture \quad (Eq.\ 1)$$

Here, *Precip* is calculated from daily climate input and because precipitation can fall as either rain or snow a distinction must be made between the two. This distinction is as follows “Precipitation that falls on a day when the mean temperature minus one-third the difference between the daily high and low temperatures is less than or equal to the

freezing point of water is considered to fall as snow"[*Westenbroek et al.*, 2010]. *Snowmelt* is based on temperature index and the maximum and minimum temperatures of the day and the SWB code assumes that 1.5 mm of snowmelt per day per average degree Celsius that the daily maximum temperature is above the freezing point. *Inflow* is based on the flow-direction raster and is calculated from the surface runoff routed to the next downslope cell. *Interception* is essentially the lower threshold of precipitation which must be exceeded for any recharge to reach the groundwater table. *Outflow* is the runoff calculated that leaves the watershed without becoming recharge. The final sink *evapotranspiration* is calculated from Thornthwaite-Mather method [*Thornthwaite and Mather,* 1957].

During the winter months and times in which the ground is completely frozen, therefore preventing infiltration, the SWB code uses a Continuous Frozen Ground Index (CFGI) which is calculated based on daily air temperatures. Two values are specified by the user, above which the ground is considered completely frozen, and below which the ground is considered completely thawed. Between these values the runoff conditions change from normal to allow for lesser recharge. The values used for simulation of recharge for the Cedar Creek watershed are the default values in SWB based on literature review. The upper limit of CFGI is 83 above which the ground is considered "frozen" and the lower limit of CFGI is 55 below which the ground is considered "unfrozen".

4.1.2.1. Recharge

In order to determine a yearly mean recharge for calibration of the steady-state model, the SWB code was run with climate data during 15 years from January 2000 to December 2014. The climate data was obtained from National Oceanic and Atmospheric Administration (NOAA), specifically from the Germantown Weather Station (nearest station with complete climate data for study period). The yearly mean recharge map was calculated from the yearly SWB outputs of the 15 years and input into the steady-state groundwater flow model (Figure 12).

The recharge in the transient groundwater flow model was based on the monthly recharge calculated from the climate data at the University of Wisconsin- Milwaukee Field Station (UWMFS) for the years of 2010-2014 (Table 4). A total of 16 stress periods with each one representing a 3-month season were identified. In detail, the SWB code was run to generate spatially mapped recharge using the monthly climate data during December 2010 through November 2014. The recharge generated from the SWB code was then used to create an average seasonal recharge value for each of the 16 stress periods in the groundwater flow model.

Recharge is the only input parameter that was varied in the transient flow model; inputs associated with stream flow and lakes were held constant throughout both the steady-state and transient flow models. The change in recharge between the steady-state and transient model highlights the sensitivity of groundwater in this area to variations in recharge.

In order to apply recharge to the MODFLOW groundwater flow model, the output from the SWB code were imported into ESRI ArcMap and converted into rasters. These

rasters were then sampled (values extracted) on the same scale as the MODFLOW model, that is 100 m by 100 m cell size, and imported into Surfer (Golden Software Inc.) and a recharge map was interpolated. This Surfer file could then be directly imported in Groundwater Vistas MODFLOW model. The map produces unique recharge values for each cell.

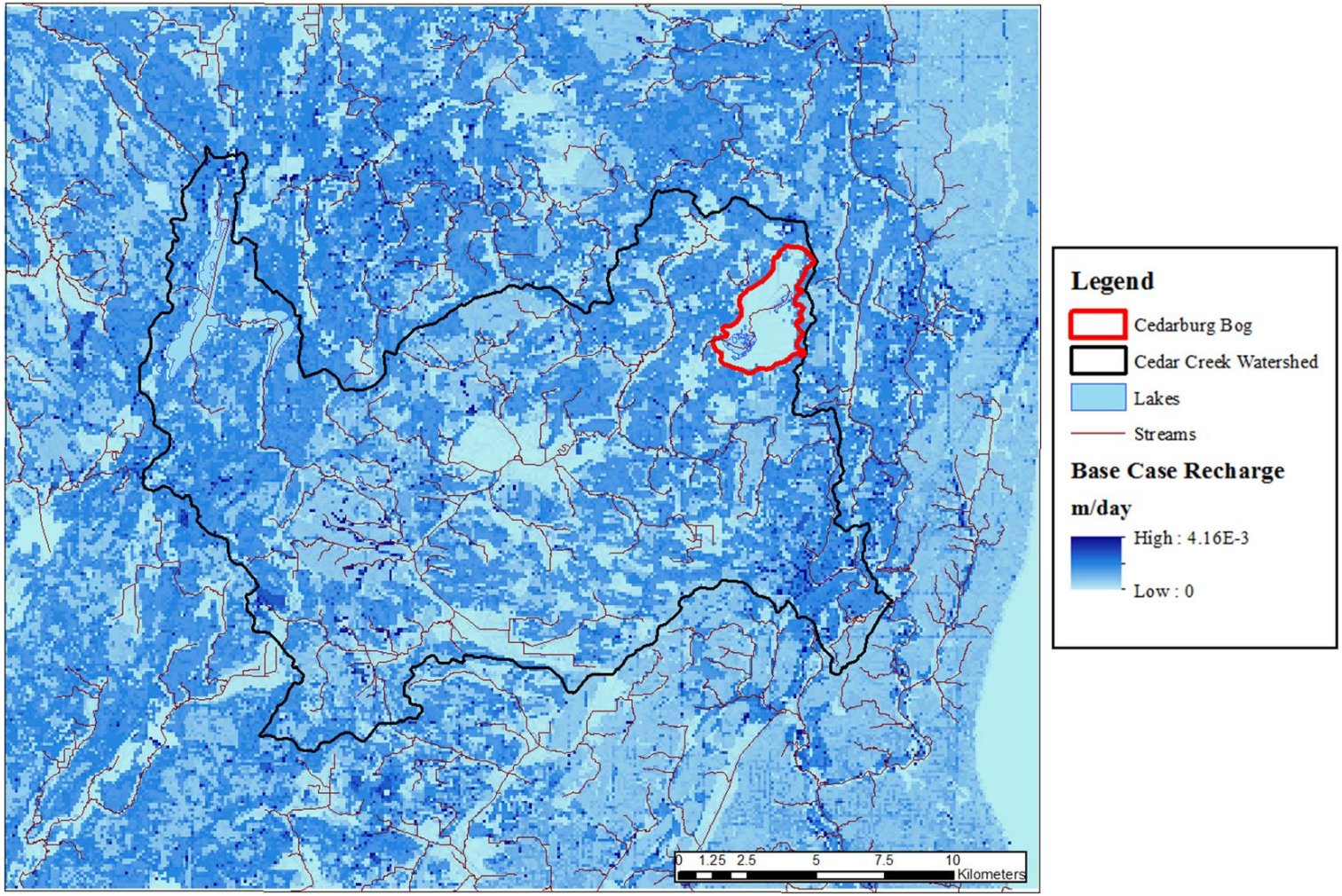

Figure 12. Spatial Distribution of Recharge, input to the Steady-State Base Case simulation. Mean recharge output from the SWB code for 2000-2014 in m^3/day. Average recharge rate across the model area is 5.27×10^{-4} m/day (7.57 in/year).

Table 4. Mean output of Soil Water Balance Code across the Cedar Creek Watershed using 2000-2014 climate data from the UWMFS. Runoff is classified as surface flow plus the overland flow contribution to surface waters. Evapotranspiration is classified as water removed from the system through evaporation from soil and surface waters plus water extracted and released from plants. Recharge is the water the reaches the water table through percolation through the vadose zone. Monthly values shown are in mm/month.

Month	Precipitation (mm/month)	Temperature (°C)	Runoff (mm/month)	ET (mm/month)	Recharge (mm/month)
January	35.0	-6.9	3	0	16
February	37.2	-5.8	2	0	18
March	49.0	0.6	6	5	50
April	102.9	7.3	10	32	40
May	115.4	13.2	8	73	25
June	110.9	18.7	7	98	13
July	87.8	21.5	4	97	4
August	86.8	20.6	4	81	3
September	80.1	16.2	4	53	3
October	64.4	9.6	3	32	4
November	48.1	3.0	4	11	8
December	51.3	-4.4	1	1	10

4.1.2.2. Evapotranspiration

Evapotranspiration (ET) is a crucial parameter when modeling groundwater flow, especially in Southeastern Wisconsin where the highest precipitation falls during the hottest and most important part of the year for agriculture. The SWB Code calculates both the *potential evapotranspiration* (PET) and *actual evapotranspiration* (AET) during each climate year, and is applied directly to recharge, therefore no need to input into the groundwater flow model. As shown in Table 4, evapotranspiration does not occur in the winter months (0 mm/month for December, January and February) and is very low during the colder spring and fall months (15.57 mm/month for April and 4.27 mm/month for November). During the late spring and summer, the evapotranspiration increases greatly

due to the higher temperatures, water availability for ET and the production of crops and growth of other plants through the growing season (104.57, 99.09, and 80.16 mm/month for June, July and August, respectively). This trend is seen in all years that were simulated in SWB and because the AET is already included in the recharge calculations for each month it is unnecessary to include an ET map in the MODFLOW model.

4.1.3. Hydrogeologic Parameters

A total of 18 zones were characterized to designate the hydraulic parameters within the model (Table 5). These zones are areas with the same property value, and therefore all cells are grouped together for hydraulic conductivity and storage parameters such as porosity, specific yield and specific storage. Each glacial unit is represented by two zones (1st Layer and 2nd Layer are different zones) due to the thickness of the glacial deposits and the vertical heterogeneity in these glacial deposits. This division of zones allows for a better representation of the glacial deposits due to the changes of hydraulic parameters with depth.

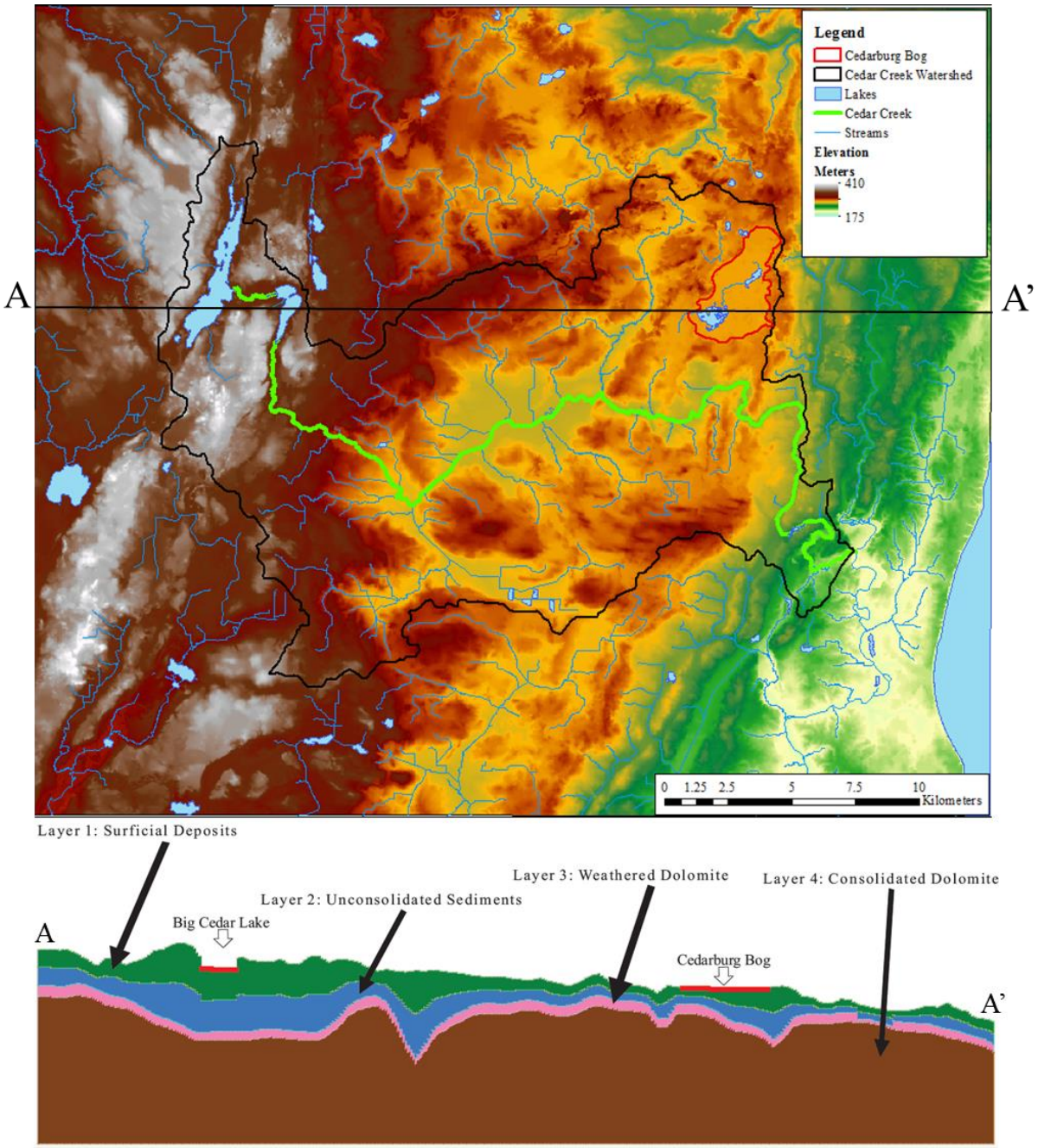

Figure 13. Stratigraphy of the MODFLOW model along cross-section that passes through both lakes and the Cedarburg Bog

Table 5. Initial values for hydraulic conductivity adopted from *Mickelson and Syverson, [1988]* and were upscaled from the field reported value to a model acceptable value. And Kz is tied to Kx at an anisotropy ratio of 0.10 through all PEST iterations. All conductivities are in m/day. Subscript 2 represents the second layer glacial units.

Zone Number	Layer Number	Unit Name	K_x=K_y initial[a]	K_z initial[b]	PEST Range	K_x=K_y PEST	K_z PEST
1	1	Post Glacial sediment	10	1	2-200	3.3	0.33
2	1	Waubeka Member	1	0.1	0.0864-10	1.06	0.106
3	1	Peat & Muck	0.5	0.05	0.2-5	2.9	0.29
4	1	Ozaukee Member	0.25	0.025	0.0864-1	13.6	1.36
5	1	Oak Creek	0.5	0.05	0.0864-2	0.24	0.024
6	1	New Berlin	0.5	0.05	0.0864-15	1.64	0.164
7	1	Horicon	5	0.5	0.0864-15	3.03	0.303
8	1	Undiff Holy Hill	10	1	0.0864-25	0.1	0.01
9	2	Waubeka Member$_2$	1	0.1	0.0864-10	1.56	0.156
10	2	Ozaukee Member$_2$	0.25	0.025	0.0864-15	6.2	0.62
11	2	Oak Creek$_2$	0.5	0.05	0.0864-2	0.33	0.033
12	2	New Berlin$_2$	0.5	0.05	0.0864-15	0.125	0.0125
13	2	Horicon$_2$	5	0.5	0.0864-15	0.2	0.02
14	2	Undiff Holy Hill$_2$	10	1	0.0864-15	0.455	0.0455
15	3	Weathered Dolomite	20	2	20-200	27	2.7
16	4	West Dolomite	2	0.2	0.5-50	0.1	0.01
17	4	Central Dolomite	2	0.2	0.5-50	1.25	0.125
18	4	East Dolomite	2	0.2	0.5-50	2.1	0.21

4.1.3.1. Hydraulic Conductivity

The hydraulic conductivities of the surficial aquifer rely heavily on the type of the glacial deposit in that area. An in depth literature review revealed the range of hydraulic conductivities for surficial sediments in the model area of 10^{-8}-10^{-4} m/s ($8.64x10^{-4}$-8.64 m/day) [*Syverson*, 1988]. Domenico and Schwartz [1990] reported glacial sediment hydraulic conductivities ranging from $8.64x10^{-8}$ to1 m/day, which is a large range encompassing many types of sediment from coarse sands to fine silts and clays. Due to the large range reported by Domenico and Schwartz [1990], a good estimate for the initial values of each glacial unit was hard to determine, therefore the values reported

Mickelson and Syverson [1997] were used as initial parameters (Table 5). These values are more representative of the local glacial deposits whereas the large range of values are representative of all glacial deposits regardless of their location (Figure 4). Due to the disparity between field scale hydraulic conductivity measurements and the model scale hydraulic conductivities representative of large areas, the hydraulic conductivity values were adjusted based on *Rovey and Cherkauer* [1995] and *Schulze-Makuch et al.* [1999]. As stated in *Schulze-Makuch et al.* [1999], "In heterogeneous porous media, hydraulic conductivity increases by half an order of magnitude with each order of magnitude increase in scale of measurement." As slugs test in general have radius of influence of 1-2 m and digital models 20-60 km, the increase in scale of measurement is 4-5 orders of magnitude therefore the scale increase of the hydraulic conductivities should be approximately 2-3 orders of magnitude [*Rovey and Cherkauer,* 1995].

Within the model area, there are 18 groups or zones of hydraulic conductivity, 14 for surficial deposits (glacial and post glacial) and 4 for the Silurian dolomite bedrock (Table 5). There are 4 distinct units of the bedrock within the model area, weathered, Lake Church, Racine/Waukesha and Mayville formations (Figure 13). Each formation has a unique value for hydraulic conductivity with the weathered dolomite being the highest and the Racine/Waukesha Formation being the lowest around one order of magnitude less than the Mayville and two orders less than the weathered unit and the Lake Church Formation [*Rovey and Cherkauer*, 1995].

4.1.3.2. Porosity and Storage

Within the MODFLOW model, the zones specified for hydraulic conductivities are the same zones used for storage parameters; porosity, specific storage and specific yield. A uniform value of 0.2 for porosity was assigned to each zone as an initial value. In terms of specific storage and specific yield, these values are only used in the transient simulation. All the glacial sediments that are represented by the first two layers of the model have the same storage parameters, 1.87×10^{-5} m^{-1} and 15%, for specific storage and specific yield, respectively. The weathered dolomite, 3rd layer, has the same specific storage as the glacial sediments, 1.87×10^{-5} m^{-1}, and a specific yield of 20%. Finally, the bulk dolomite, 4th layer, has a specific storage of 8.53×10^{-7} m^{-1} and a specific yield of 0.5% [*Domenico and Mifflin*, 1965; *Heath*, 1983; *Lohman*, 1972; *Morris and Johnson*, 1967].

4.1.4. Boundary Conditions

Model boundary conditions are an important part of every groundwater flow model as they dictate the movement of water in and out of the model area. Within MODFLOW, there are three types of boundary conditions; specified head, specified flux and head-dependent flux boundaries. Constant head boundaries are a type of specified head boundary in which a user specified head in a cell supplies or removes water from adjacent cells depending on the relationship between individual heads. The recharge package and the well package are both specified flux boundaries in that there is a user defined injection or extraction of water from the model by either recharge to the water table or pumping or injection from a well. The rest of the boundary conditions used in the

Cedar Creek Watershed groundwater flow model (Figure 7) are head-dependent flux boundaries. This is due to the fact that the interaction between adjacent cells is dependent upon the relationship between a head specified at the boundary condition (e.g., river stage), the groundwater head in the cell hosting the boundary condition and a conductance term specifying the resistance of the material separating the boundary condition head from the groundwater (e.g., riverbed, general-head, lake, river, and the streamflow-routing packages are all examples of head-dependent flux boundaries [*McDonald and Harbaugh*, 1988]. The evaporation package incorporates elements of a specified flux boundary condition (the maximum rate) and a head-dependent condition (the flux out of the groundwater system is dependent on the elevation of the water table).

Implementing the proper boundary conditions in the groundwater flow model is a difficult process due to the differences in the boundary condition types but also the different boundary conditions available in MODFLOW. In terms of the groundwater flow model, the boundary conditions at the edge of the grid were chosen to minimize the edge boundary effects on the Cedar Creek Watershed, whereas the internal boundary conditions were chosen to simulate aquifer-surface water interaction. A total of six different boundary types were implemented in the groundwater flow model; constant head, general head, lake, stream flow routing, and river. These different boundary condition cells are further explained in the following sections.

4.1.4.1. Surface Waters

Due to the large scale of the model area, only 4 large lakes are simulated within the watershed area. In addition to the lakes, all streams and rivers found in the National Hydrography Dataset are represented in the model area (Figure 7). Within the watershed itself, the main trunk of Cedar Creek is simulated using the Stream-Flow-Routing 2 package (SFR2) and all other streams and tributaries were simulated using the River package (RIV). Outside of the watershed, all rivers were simulated using the RIV package due to sheer volume of river cells and the instability that arises from using the SFR2 package. All four lakes in the model (excluding Lake Michigan) are simulated using the Lake package (LAK).

The SFR2 package was chosen to simulate the stream-aquifer interaction between Cedar Creek and the underlying aquifer due to its ability to simulate unsaturated zone flow between the surface water features and the water table below and because of the connection to thee LAK package boundary cells [*Niswonger and Prudic*, 2005]. In addition to the ability to simulate unsaturated zone flow, the SFR2 package, like the previous STR and SFR1 packages, has the ability to simulate flow through consecutive stream cells under the assumption of uniform flow with the inflow being equal to the outflow minus sources and sinks (routing of channel flow). This also allows for the simulation of flow from lakes into stream reaches which is important for Cedar Creek as it emanates from Big Cedar Lake, flows through Little Cedar Lake and eventually out the southern end into the main trunk of Cedar Creek. Also, the SFR2 package can simulate the potential drying of stream cells in addition to calculation of stream stage in the cells. Two stream segments are simulated in the model, segment one connects Big Cedar Lake

to Little Cedar Lake and segment two flows from the base of Little Cedar Lake to the outlet of the watershed at the City of Cedarburg. Both segments have a streambed thickness of 0.33 m and a calibrated hydraulic conductivity of 0.1 m/day. The SFR2 package also requires the input of the slope of the channel bottom. The slope of the streambed was calculated using the digital elevation model in GIS and imported into the MODFLOW model. The base of the river channel was also defined by the values from the digital elevation model along the stream channel and the stage of the river is 3 m higher than the elevation of the streambed. The final input for the SFR2 package is the width of the stream channel. As very sparse data is recorded for the width of Cedar Creek, the width was designated as 5 m at the start of segment one to 30 m at the outlet of the stream, with linearly interpolated width along the channel.

The RIV package is a head dependent flux package that involves a user specified riverbed bottom threshold which limits the flow from the river channel into the aquifer as a function of the gradient between the specified river stage and the riverbed bottom [*Harbaugh et al.*, 2000]. Similarly to the SFR2 package the RIV package requires a streambed thickness and hydraulic conductivity. There are 10 "reaches" simulated where each reach is representative of a group of rivers. Ten different reaches were implemented: reach 1 are first order streams in connection with Cedar Creek, reach 2 are first order streams not connected to Cedar Creek, reach 3 are second order streams, reach 4 are third order streams, reach 5 are first order streams outside of the watershed area, reach 6 are second order outside of the watershed, reach 7 are third order outside of the watershed reach 8 is the Milwaukee River, and reach 9 and 10 is the stream in the bog and the outlet stream of Mud Lake respectively. Each different reach has a calibrated hydraulic

conductivity of the riverbed in addition to a thickness of riverbed. All stream reaches have a riverbed thickness of 0.33 m and hydraulic conductivities in order: 2.5, 0.65, 1.65, 0.5, 0.9, 1.1, 3.3, 0.02, 0.5, and 0.5 m/day. The bottom of the riverbed is set at the elevation along the river channel from the digital elevation model in GIS.

Finally, the LAK3 package, another head-dependent flux boundary calculates not only the exchange of the lake with the surrounding groundwater, but also the water budget of the lake itself as a function of the precipitation to and evaporation from its surface, any pumping from the lake, any overland flow to the lake and the groundwater inflows and outflows. This water budget in combination with the specified lake bathymetry determines the lake level under steady state or transient conditions [*Merritt and Konikow*, 2000]. The four lakes simulated in the watershed were given a specified initial stage in addition to a minimum and maximum lake stage for the upper and lower bounds of the calculated lake stage from the LAK3 package. For Big Cedar Lake the initial lake stage was specified at 315 m while the minimum and maximum were specified at 290 m and 325 m, respectively. Little Cedar Lake was given an initial stage of 310 m with and minimum of 290 m and a maximum of 320 m. Finally the two lakes in the bog, Mud Lake and Long Lake, were simulated with an initial stage of 264 and a minimum and maximum of 259 m and 274 m, respectively. The lake bottom thickness for all lakes was set at 0.33 m and each have a hydraulic conductivity that was determined during calibration. The two lakes in the west of the model, Big and Little Cedar, have a lakebed hydraulic conductivity of 0.33 m/day and the lakes in the bog, Mud and Long Lake, have a hydraulic conductivity of 0.04 m/day.

4.1.4.2. Pumping Wells

As most of the watershed is rural, most of the private wells in the area are used in conjunction with underground septic systems which return most of the extracted water immediately to the water table. For example, *Rayne and Bradbury* [2011] developed a groundwater flow model representing the area around the City of Cedarburg, in which one model scenario involved a well density 15 times greater than the current distribution. Despite the presence of a dense private well network, simulations showed less than one foot of drawdown and less than 5% change in baseflow to the nearby Cedar Creek due to direct return of extracted groundwater through septic systems. Therefore, in this model, the contribution of private wells was not included.

There are 27 high capacity wells inside the watershed, all of which pump at different rates and for different times of the year (Figure 14 and Table 6). These 27 high capacity wells are the only wells represented within the MODFLOW groundwater flow model pumping scenario, but are not included in the steady-state base case scenario which is intended to be representative of pre-development condition in order to simulate groundwater levels and flows without disturbance from anthropogenic input.

Table 6. Maximum pumping rates from the 27 high capacity pumping wells simulated in the watershed. The wells are listed in order from west to east. Their locations are shown in Figure 13. Source of data Personal Communication Robert Smail DNR.

High Capacity Well Number	Maximum Pumping Rate (gal/day)	Maximum Pumping Rate (m^3/day)
1	2.0E+04	76
2	2.0E+04	76
3	2.7E+05	1020
4	2.0E+05	766
5	1.0E+03	3.8
6	1.7E+04	64
7	1.0E+03	3.8
8	6.8E+05	2600
9	2.0E+04	76
10	1.4E+05	530
11	2.3E+05	870
12	4.5E+04	170
13	5.6E+04	210
14	5.0E+05	1910
15	1.5E+04	57
16	6.0E+03	23
17	5.0E+03	19
18	5.0E+03	19
19	4.3E+05	1600
20	2.9E+05	1100
21	1.5E+04	57
22	2.7E+05	1010
23	9.7E+05	3670
24	4.9E+05	1860
25	2.3E+05	870
26	3.6E+05	1365
27	4.3E+05	1640

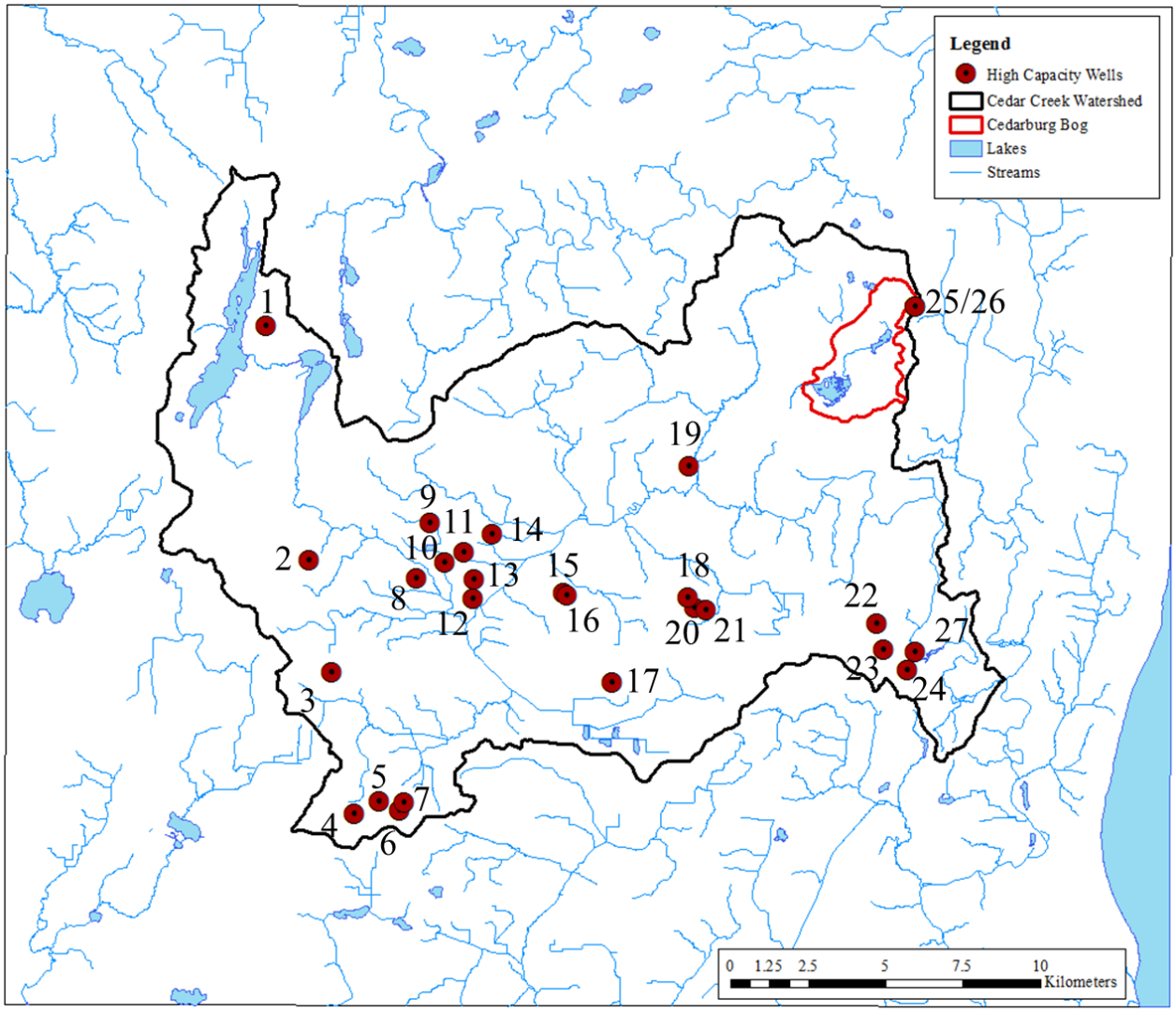

Figure 14. Locations of the 27 High Capacity Pumping Wells located within the Cedar Creek Watershed.

4.1.5. Model Calibration

The Cedar Creek Watershed flow model was calibrated under the steady-state non-pumping scenario using the parameter estimation software, PEST [*Doherty*, 2002; *Doherty and Hunt*, 2010]. A total of 194 wells were used in the calibration of the Cedar Creek flow model with 68% of wells having been drilled in the bedrock (Figure 16). The head targets used were generated from the static water level on each of the 194 well construction reports from the Wisconsin Department of Natural Resources (WDNR) Drinking Water System. The distribution of the wells across the model area is even, with grouping of some calibration targets around Cedarburg, Richfield and Jackson. Also, due to the period of time in which the wells were drilled, approximately 30 years, there is a high margin for error as the static water levels in the wells were likely recorded over different seasons and obviously different years. The PEST estimated parameters and input values are summarized in Table 5.

The hydraulic conductivities of each of the 18 zones were estimated during the calibration, in addition to the storage parameters in the transient simulations. The hydraulic conductivities of the river, stream and lakebeds were also calibrated in the steady-state simulation.

In order to evaluate the accuracy of the model, the calibration statistics were analyzed. The residual mean, calculated by adding all residuals and dividing by the number of residuals, is 0.14 m, the absolute residual mean, calculated by adding the absolute values of all residuals and again dividing by the number of residuals, is 2.01 m. The root-mean-square error or RMS, another statistic for measuring the accuracy of a model, and was 2.69 over a range of residuals from -7.39 m to 9.94 m. The water budget

for the steady-state base case model reveals a percent error of $2.06x10^{-3}$ for a total flux of $2.7x10^{6}$ m^3/day (Figure 15).

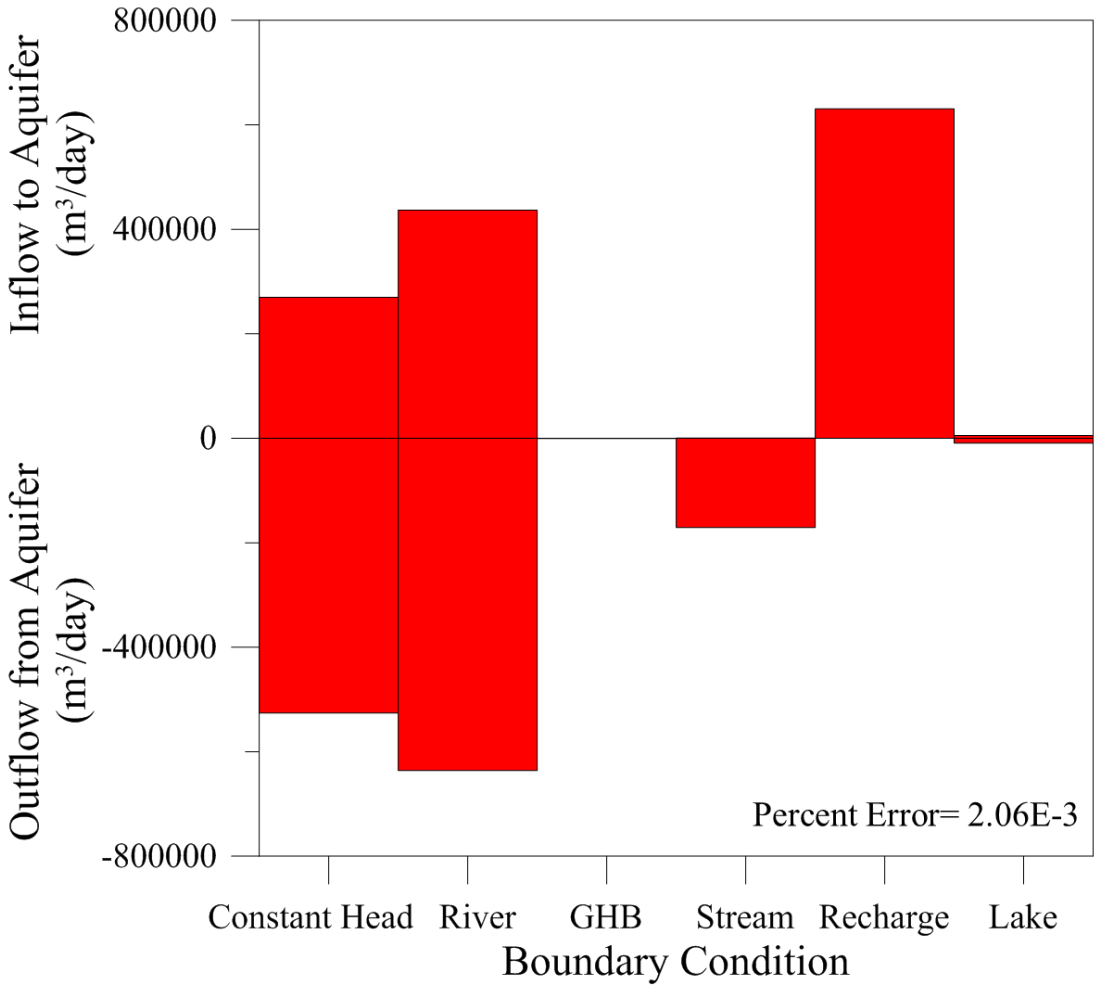

Figure 15. Steady-State Base Case full model water budget. General Head Boundary (GHB) does not display flux due to the small water budget values relative to all other boundary condition cells.

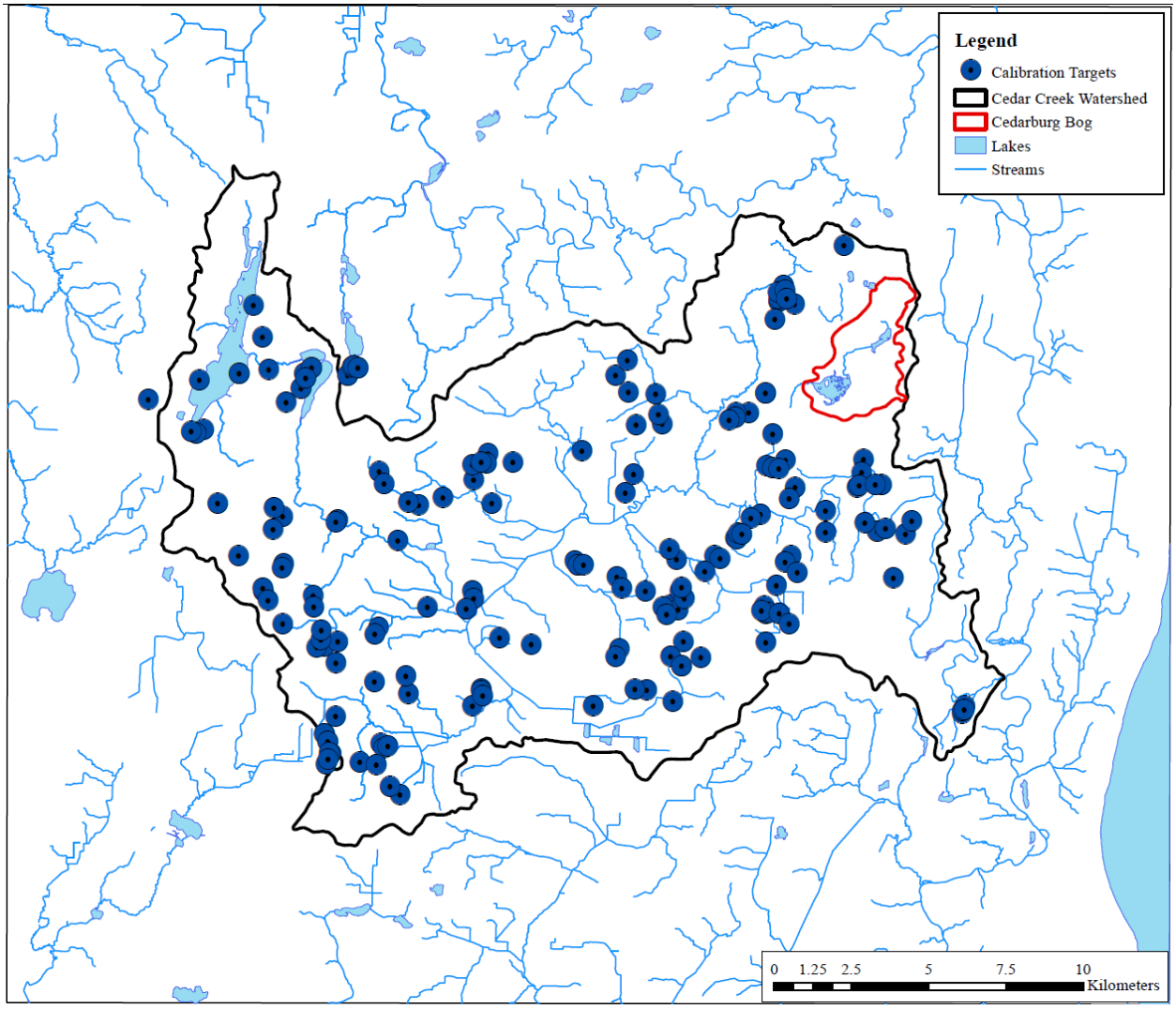

Figure 16. Location of 194 wells used for calibration head targets.

5. Results and Discussion

With the USGS MODFLOW groundwater flow modeling code, a total of 11 different simulations were run, including both steady-state and transient models for past, current, and future projections (Table 7). A total of 10 different steady-state models were run with one being the base case using the 15-year average recharge rate (2000 to 2014), one including high capacity pumping wells, and the rest encompassing the future climate change scenarios. The transient simulation period was chosen in order to encompass both a very low recharge year (high temperature and low precipitation) and a high recharge year (moderate temperatures and high precipitation) during 2010 to 2014. The year of 2012 falls into the drought category with substantially lower precipitation rates and higher temperatures than the yearly average, while the year of 2013 falls into the category of high recharge (Figures 6 and 15).

The 6 variable climate steady-state simulations were as follows, 4 simulations with variable recharge: 20% increase in recharge with a 3 m lower Lake Michigan stage, 20% increase in recharge with a 1.5 m higher Lake Michigan stage, a 20% decrease in recharge with a 3 m lower Lake Michigan stage, and a 20% decrease in recharge with a 1.5 m higher Lake Michigan stage, and 2 simulations with no change in recharge but variable Lake Michigan stage; 3 m lower and 1.5 m higher lake stage. The changes in Lake Michigan stage was chosen based on the most extreme results from climate projections and simulations from *Angel and Kunkel* [2009].

Scenarios 10 and 11 are different from the previous nine scenarios in that the recharge and lake stage are the same as the steady-state base case scenario but changes

were made for addition sensitivity analyses. Scenario 10 used the drain (DRN) package in place of the river (RIV) package in order to determine the changes in head and water budget at one extreme compared to the RIV package at the other extreme. An issue that arises with the RIV package is the excessive water available for circulation in the headwaters of various rivers. The RIV package can supply water from river cells in which there is no water available to the aquifer, while the DRN package cannot supply any water to the aquifer but can only remove it. Therefore, the DRN package run operates as an extreme opposite to the RIV package steady-state base case scenario. The conditions in the field are most likely going to reflect a situation that lies between the results of the RIV package steady-state base case simulation and scenario 10 with the DRN package due to the nature of the RIV and DRN packages. The RIV package has potential to simulate a supply of water to the aquifer that is non-existent due to some streams and rivers being ephemeral, this is remedied by the use of the DRN package. On the other hand the DRN package also has a potential problem in that some streams that are supplying water to the aquifer in nature may not be able to do so in the simulations due to the elevation of the water table and heads in cells adjacent and beneath the DRN cells. Therefore, the result of Scenario 10 (DRN package) likely underestimates the flux from rivers to the aquifer and Scenario 1 (steady-state base case RIV package) likely overestimates the flux from rivers to the aquifer in nature. The differences between the packages and scenarios are further explained in section 5.5 and section 6.

Scenario 11 was created with a low hydraulic conductivity beneath the Cedarburg Bog in order to simulate the effects of the possible low-K lake sediments though to be present under the bog. The hydraulic conductivity was lowered to 0.025 m/day beneath

the bog to simulate the low transmissivity of clay and other lake bed sediments. This hydraulic conductivity change beneath the bog will affect the flow through the base of the bog possibly mitigating the effects of variable recharge from future climate change on the Cedarburg Bog.

Table 7. Scenarios implemented in the groundwater flow model

Scenarios	Model Type	Recharge	High Capacity Wells	Lake Michigan Stage
1 (Base Case)	Steady-State	15-year average (2000-2014)	No	100-year average (176 m)
2	Steady-State	15-year average (2000-2014)	Yes	100-year average (176 m)
3	Transient	Seasonal averages (2010-2014)	No	100-year average (176 m)
4	Steady-State	15-year average (2000-2014)	No	3.0 m lower than average
5	Steady-State	15-year average (2000-2014)	No	1.5 m higher than average
6	Steady-State	20% decrease from average	No	3.0 m lower than average
7	Steady-State	20% decrease from average	No	1.5 m higher than average
8	Steady-State	20% increase from average	No	3.0 m lower than average
9	Steady-State	20% increase from average	No	1.5 m higher than average
10	Steady-State DRN Package	15-year average (2000-2014)	No	100-year average (176 m)
11	Steady-State Low K Bog	15-year average (2000-2014)	No	100-year average (176 m)

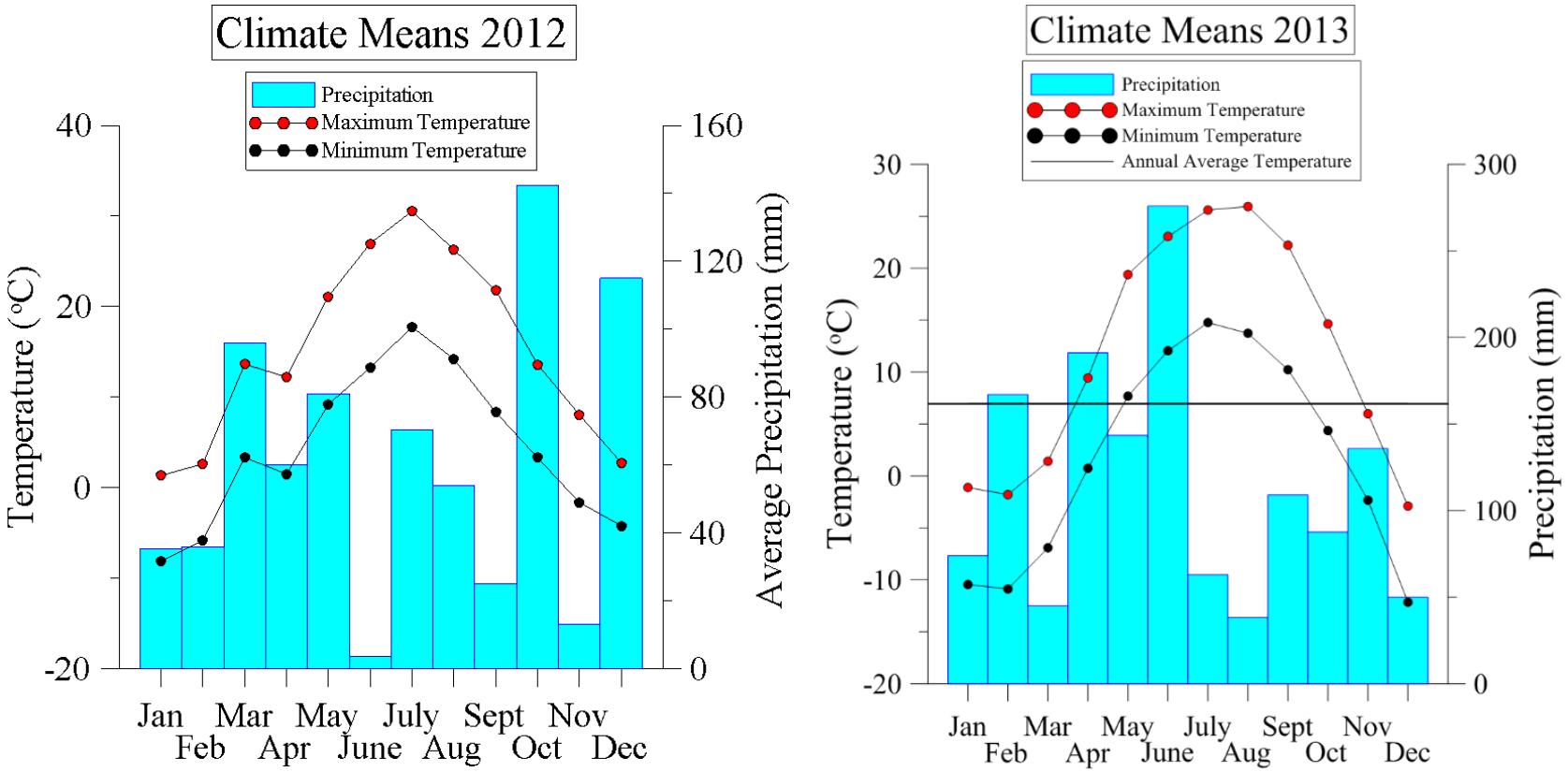

Figure 17. Monthly means of temperature and precipitation of the "drought" year of 2012 (total precipitation 732 mm) showing very low precipitation in June and high temperatures through the summer, and following "wet" year 2013 (total precipitation 1380 mm) with high precipitation in June and lower temperatures in the summer. Weather data is from the UWM Feld Station.

5.1 Base Case (Scenario 1): Steady-State Non-Pumping

The steady-state groundwater flow model was simulated using annual average recharge from the 15-year period from 2000-2014. The non-pumping model is used as the base case scenario in order to delineate the groundwater level without disturbance from anthropogenic stress. Figure 18 shows the head distribution throughout the groundwater flow model area. The highest heads (above 310 m) are found within the undifferentiated sediment of the Holy Hill Formation which lies between the two lakes in the northwestern portion of the watershed. This high water table is likely due to the topography in this watershed where the highest elevations are also in the northwest portion. The high water table can also be attributed to the two lakes located in the region of the watershed. Big Cedar Lake has been simulated as a groundwater source with Little Cedar Lake being a groundwater sink. Overall, groundwater head declines from west (310 m) to east (210 m) with local variations caused by nearby surface water features.

The river cells within the watershed model are relatively balanced in their supply and removal of water from the aquifer. The 1st order rivers and streams are represented as one reach within the model, these river cells supply 59,125 m^3/day to aquifers while both 2nd and 3rd order rivers remove 64,443 m^3/day. A net total 5,317 m^3/day of groundwater discharges to river cells in this watershed. The river cells closer to the stream cells representing Cedar Creek supply more water to the aquifer while river cells farther from the stream remove more water from the aquifer.

The stream cells within the 1st segment connecting Big and Little Cedar lakes remove 427 m^3/day from the aquifer. The 2nd segment from Little Cedar Lake to the outlet of the watershed removes 170,131.9 m^3/day. The whole length of Cedar Creek

stream cells extract water from the aquifer except for a small portion just north of the City of Cedarburg. The cumulative discharge of the Cedar Creek stream cells at the outlet of the watershed is 343,000 m^3/day, which is 8% greater than the average annual Cedar Creek discharge measured at the USGS gauging station in the City of Cedarburg of 316,000 m^3/day.

The water budget of the lake cells show the Big Cedar Lake supplies 862 m^3/day of water to the aquifer while the adjacent Little Cedar Lake removes 5,568 m^3/day from the aquifer. This result shows that Big Cedar Lake is more balanced in the sense that near equal amounts of cells in the lake are removing water and supplying water to the aquifer, conversely a greater area of cells in Little Cedar Lake are removing water from the aquifer. The lakes within the Bog are much smaller than Big and Little Cedar Lakes and combine to supply 170 m^3/day of water to the aquifer.

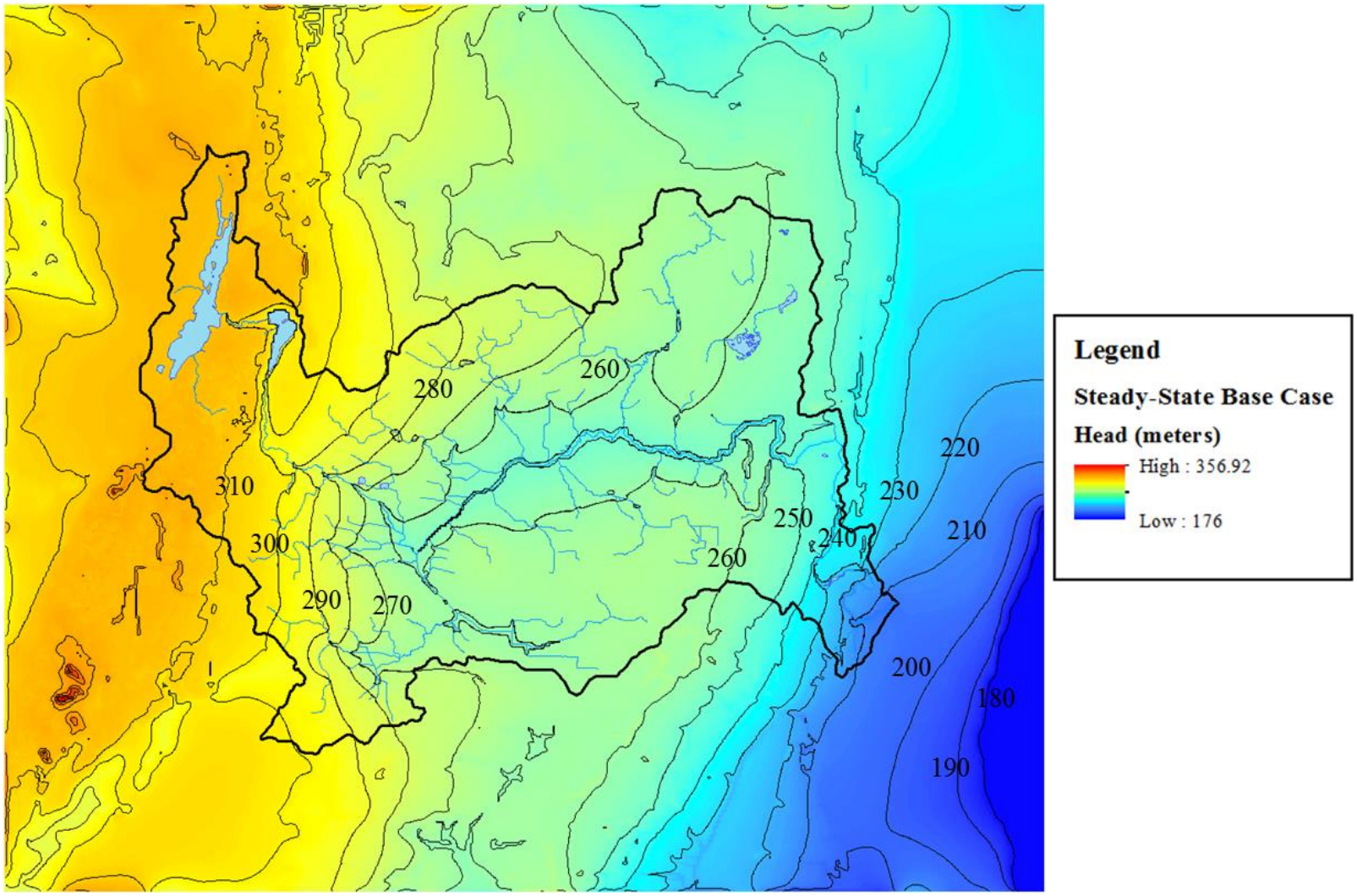

Figure 18. Steady-state groundwater table from 15-year (2000-2014) average recharge non-pumping scenario

5.2 Scenario 2: Steady-State Pumping

Under steady-state pumping conditions with all high capacity wells operating at maximum capacity, small depressions around the pumping wells occur in some locations (Figure 19b). With an analysis of the water budget, the extraction of water from the high-capacity wells causes very little change in the overall head distribution and water budget. The majority of the watershed is unaffected by pumping, as shown in Figures 19b and 20, with less than 1% of cells having a drawdown of greater than 1 m and only 15% of cells having a drawdown greater than 10 cm. The water budget shows that with all wells running at full capacity, they draw less than 2% of the total groundwater discharge from the watershed, 9,656 m^3/day. All other boundary condition cells showed that water budgets change less than 1% from the base case model except rivers and streams, which decrease 2.55% and 1.26% respectively.

These results show that the wells in the watershed are relatively unimportant in terms of both water budget and head distribution, therefore are not required to be active in subsequent simulations. In addition to the small changes in water budget and head distribution, many of these wells are non-municipal high-capacity wells which means they operate for small periods of time throughout the year. Many high-capacity wells supply irrigation for golf courses or water for school districts which are only necessary for small periods of time. This shows that the overall impact of high-capacity wells will be even less than what is shown in the model results.

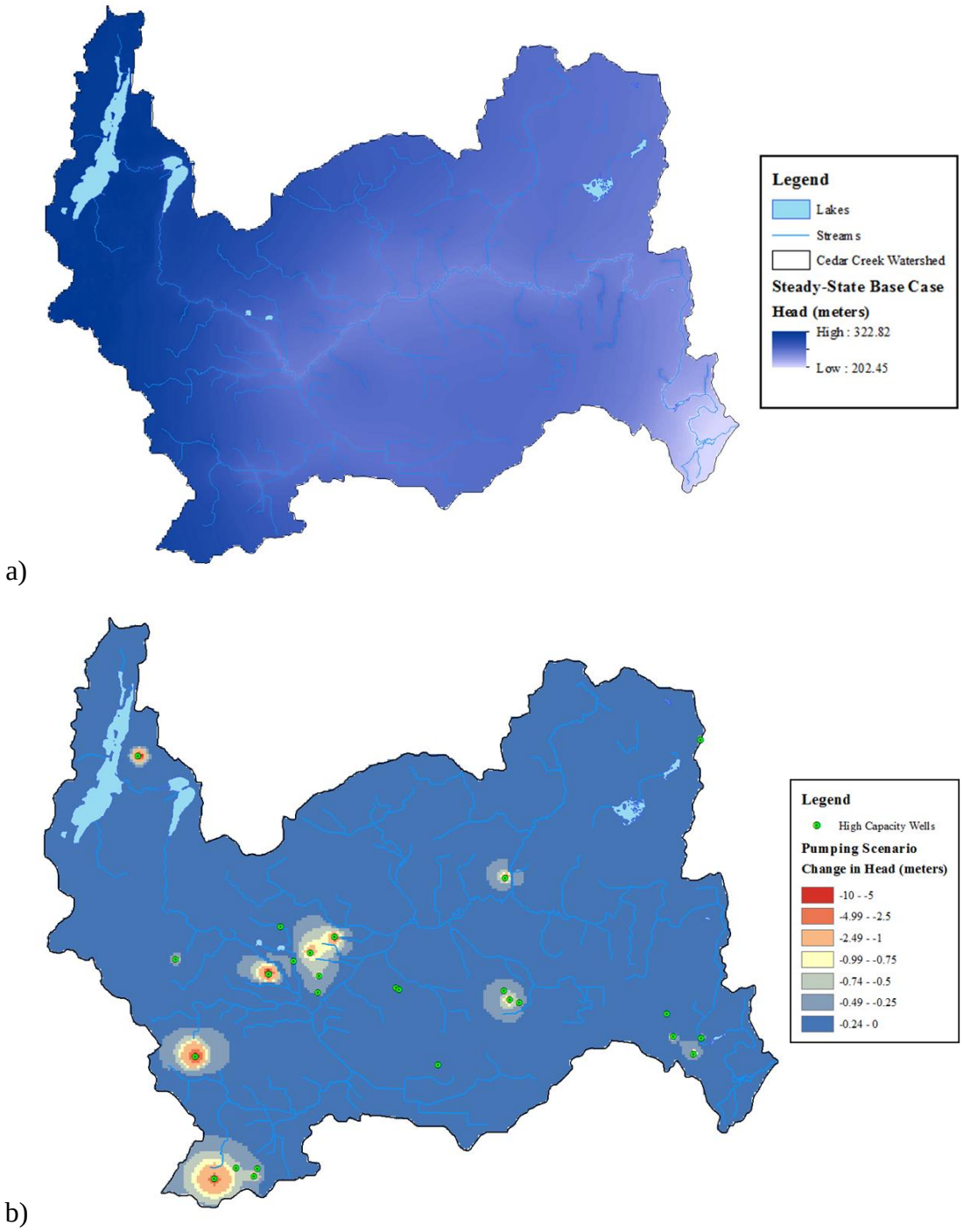

Figure 19. Steady-state head distribution change from the pumping scenario. a) Steady-state base case head distribution within the watershed. b) Steady-state pumping scenario showing cones of depression forming around the high capacity pumping wells

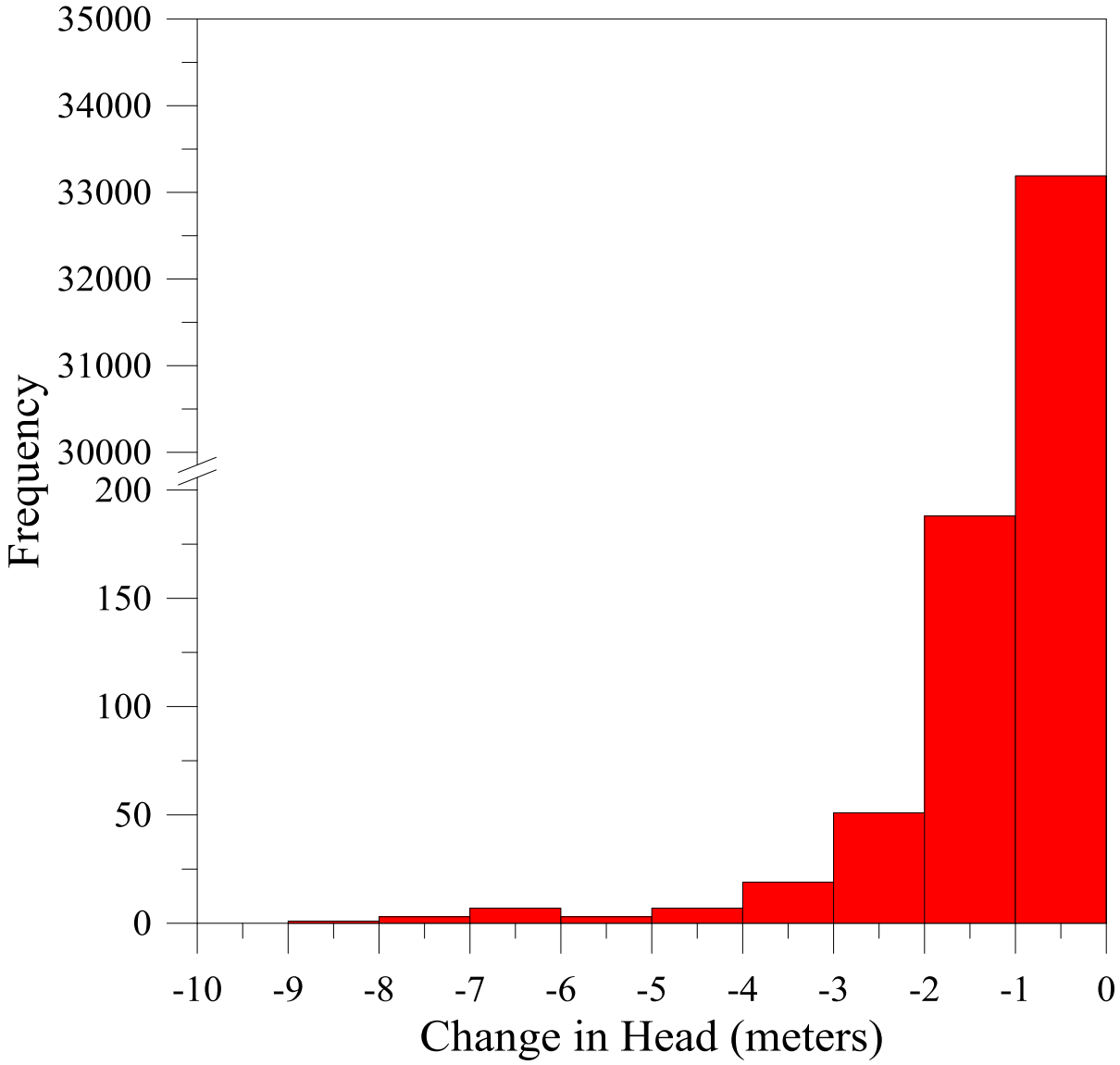

Figure 20. Histogram showing the change in head from the steady-state base case non-pumping scenario and the pumping scenario with all 27 high capacity pumping wells operating a full capacity. Note the break in axis between 200 and 30000 cells. The change from 0 to -1 m represents 99% of the total 33,476 cells.

5.3 Scenario 3: Transient State Non-pumping

The transient MODFLOW groundwater flow model was simulated for four years from 2010-2014 with 16 stress periods, each representing a three month season, December, January, February for winter, March, April, May for spring, June, July, August for summer and September, October, November for fall. Pumping was not simulated due to the small influence on the water budget in the steady-state model (less than 2%) (Figure 20). The boundary conditions for the stream and river cells were held constant throughout the transient simulation, that is to say the stream and river stage were not changed throughout the seasons. The same is true about the lake cells representing Big Cedar, Little Cedar, Mud Lake and Long Lake. The constant head cells in the north, west and south boundaries of the model area were also held constant, but the general head boundary and constant head cells representing Lake Michigan were changed to reflect the lake stages in corresponding stress periods.

The recharge implemented into the transient simulations are developed from daily climate data for the simulation period (2010-2014). The resulting recharge values were then used to calculate monthly mean recharge throughout the watershed, then finally the monthly means were used to calculate three-month mean seasonal recharge representative of the 16 unique stress periods.

Five locations were selected to monitor the response of groundwater heads in the 4-year simulation (Figure 21). One is between Big Cedar and Little Cedar Lakes where the highest groundwater head was observed in the base case scenario. Another three locations were chosen in Jackson Marsh and Cedarburg Bog. Finally, the last location was selected at the outlet of the watershed near the City of Cedarburg. The highest water

table levels in each year of the simulation are the spring stress periods (2^{nd}, 6^{th}, 10^{th}, 14^{th}). The lowest water table values come in the fall stress periods (4^{th}, 8^{th}, 12^{th}, 16^{th}) which indicates a delay in the lowering of the groundwater table after a stress period with very little recharge (summer). Overall, the lowest recharge values occur in the summer stress period of 2012, which falls into severe drought category with substantially lower precipitation rates and higher temperatures than the yearly average in Wisconsin (Figure 17a). The summer of 2012 is denoted as a vertical black line in Figure 21. The lowest water table level in all observation wells is during the following fall stress period of 2012, presumably due to the accumulation of response to low recharge conditions in both summer and fall of 2012. The large recovery of the water table in all locations in the spring of 2013 is due to the enormous increase in recharge in the winter and spring stress periods of 2013 (Figure 17). In general the hydrographs show the typical response of monitoring wells in southeastern Wisconsin, which suggest the transient simulation is operating correctly.

The maximum change of groundwater heads (1.5 m) was simulated at the monitoring location in the City of Cedarburg, located near the outlet of Cedar Creek where it joins the Milwaukee River (Figure 21). In contrast, the lowest head change (0.35 m) seen through the simulation was at the monitoring well in the center of the Cedarburg Bog. This is consistent with data from a piezometer, well 5C, near the stream in the bog, but is more variation than has been recorded at the piezometer in the center of the bog.

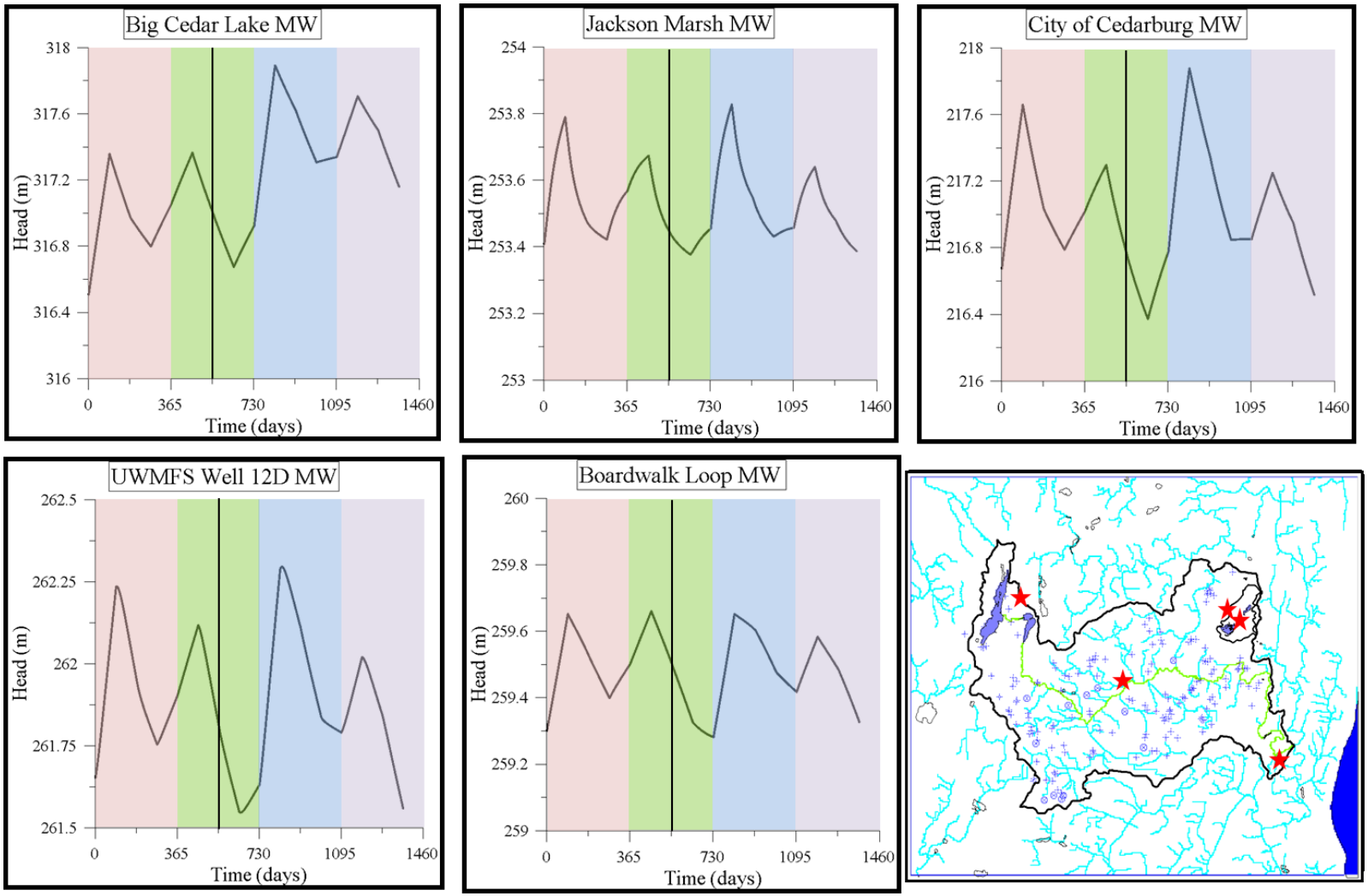

Figure 21. Hydrographs from the transient simulation (2010-2014) with each year represented by a different color column (2010-2011 is red, 2011-2012 is green, 2012-2013 is blue and 2013-2014 is purple). The location of each observation well is shown on the map as a red star. The vertical black line in each hydrograph indicates the summer of 2012 (drought year).

The spatially distributed groundwater table for each stress period in the transient simulation was compared to the steady-state base case non-pumping model in order to determine the differences in water table from steady-state to transient during the dry seasons (summer and fall of 2012 and 2013) (Figure 22). Interestingly, groundwater head in the 2012 fall is lower than the summer stress period even though the fall stress period has a higher recharge rate than the summer stress period. This is most likely due to the fact that the recharge in the 2012 fall is not enough to overcome the low recharge values of summer in addition to the discharge to surface waters, resulting in a lower water table. The fall stress period of 2013 is also lower than the summer stress period but this is more expected due to the fact that this 2013 fall had a lower recharge rate than the summer. When comparing the results from the "drought" stress period in the 2012 summer, to the "wet" stress period in the 2013 summer, it is clear that the drought period water table is much lower than the wet period, but the lowest heads are found in the stress period following the drought, fall 2012 (Figure 22). This result shows that the water table in the fall of 2012 is a cumulative response to the two prior recharge periods, and the water table cannot rise again until inflows from recharge exceed outflows to surface waters which will not occur until the next spring stress period. In the 2012 summer, 9.59% of the cells in the watershed were lowered than the steady-state base case simulation, while the fall of 2012 had 28.25% of the cells were lower than the steady-state base case simulation. In contrast, the summer of 2013 had 1.87% of cells lower than the steady-state base case simulation and the fall of 2013 has 6.86% of the cells lower than the steady-state base case simulation.

The largest decrease in water table throughout the transient simulation occurred in a small portion of high topography in the west central portion of the watershed. The most widespread lowering of the water table occurs in the south central portion of the water table near the southern border of the watershed and also in the north east portion near the Cedarburg Bog.

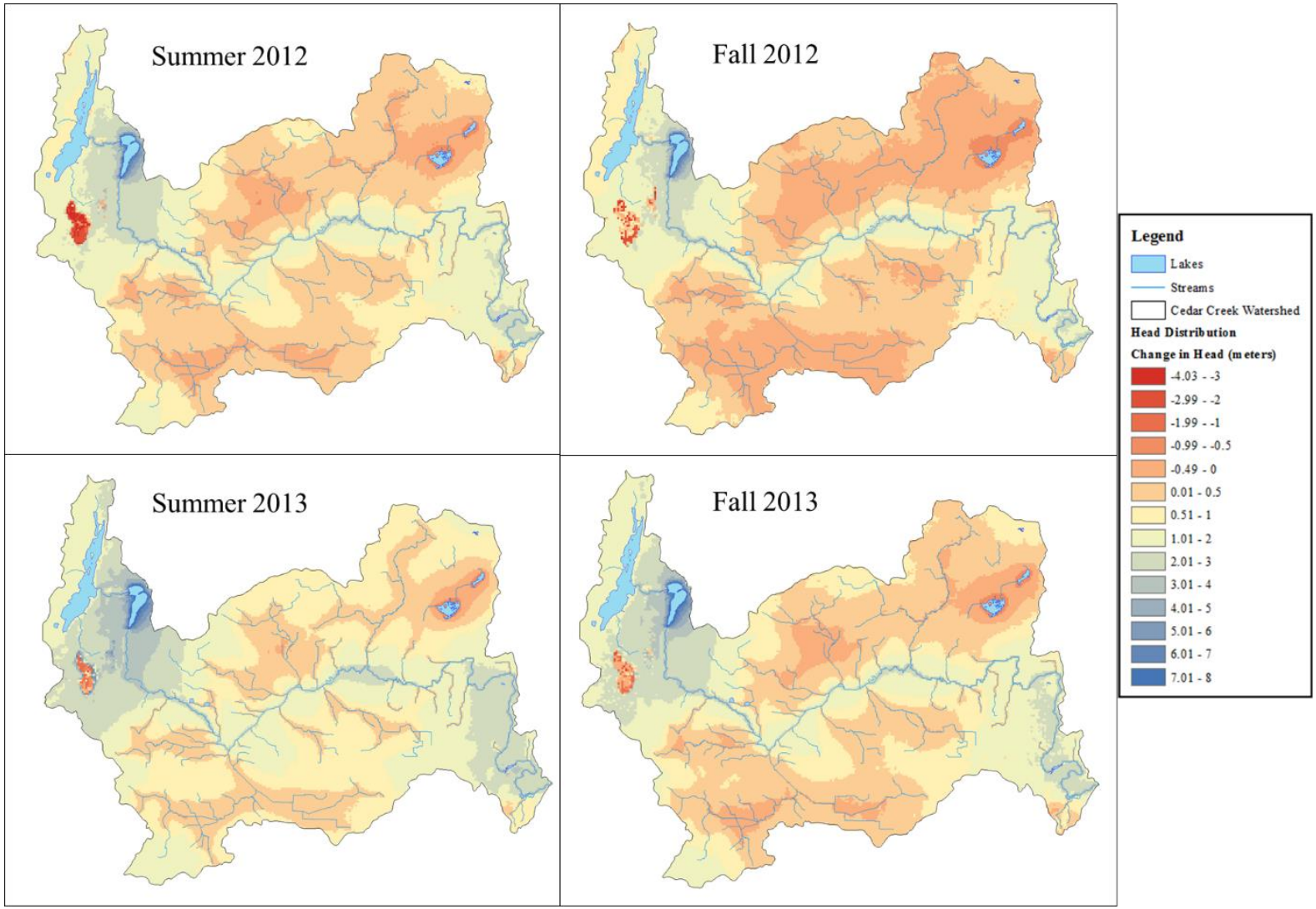

Figure 22. Comparison of steady-state non-pumping model and the transient non-pumping model. Negative values (reds) indicate a drop in the water table when compared to the steady-state base case model, while positive values (blues) indicate an increased water tab table when compared to the steady-state base case model.

5.4. Sensitivity Study on Cedar Creek Watershed

5.4.1. Scenarios 4-9: Future Recharge Simulations

The future recharge climate change scenarios were developed based on a literature review of global climate change and more importantly climate change projections for the Great Lakes Region and State of Wisconsin (Table 7). A strong majority of climate projections indicate a warmer and wetter climate around the Cedar Creek watershed, but there are highly variable changes in both temperature and precipitation through different climate models. In order to determine effects of future climate change on the Cedar Creek watershed, the climate scenarios that were chosen are based on estimates of change in both precipitation and temperature.

The recharge changes simulated in the model, increase and decrease of 20% from the steady-state base case simulation were chosen to find the most extreme response to future climate change. While it is not likely the recharge will increase or decrease a full 20% it is still useful to find the maximum possible changes both up or down in the watershed. In addition to changes in recharge, changes in Lake Michigan stage were also implemented. Similarly to recharge, Lake Michigan stage was altered to the extreme values found in *Angel and Kunkel* [2009], 1.5 m increase in Lake Michigan stage and a 3 m decrease in Lake Michigan stage. Both the constant head cells in the southeast of the model in addition to the general head cells in the northeast of the model, all representative of Lake Michigan, were changed to simulate both the increase and decrease in Lake Michigan stage. Again it is not likely to see a decrease in recharge simultaneously with an increase in Lake Michigan stage and vice versa but these

simulations were also run in order to compare outputs between the variable recharge and variable lake stage scenarios.

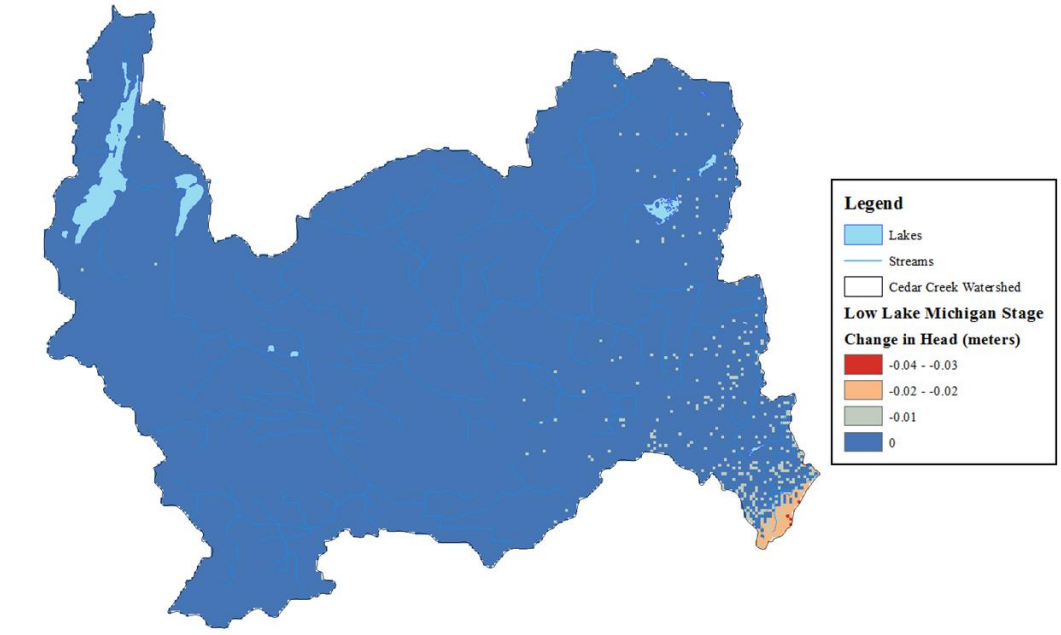

a)

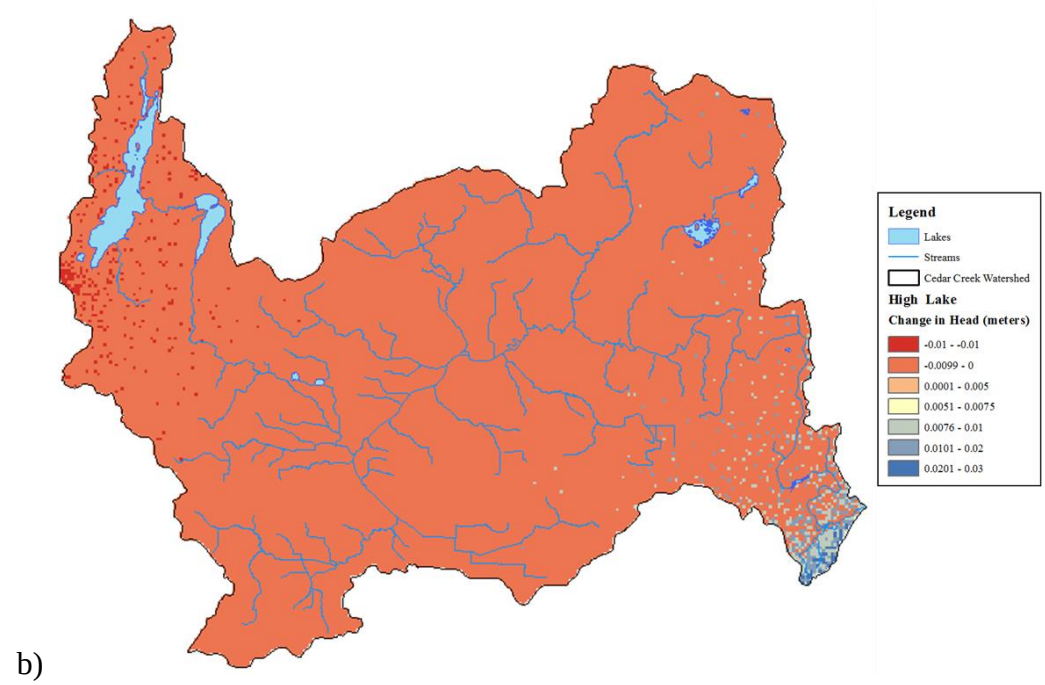

b)

Figure 23. Comparison of heads from variable Lake Michigan stage simulations. a) Steady-State simulation in which the Lake Michigan stage was lowered 3 m (Scenario 4). Where the map is blue there has been no change in head, and the trend towards a more red color indicate greater decreases in the water table. b) Steady-state simulation in which the Lake Michigan stage was raised 1.5 m (Scenario 5). Where the map is orange there has been no change in head, and the trend towards a more red color indicate greater decreases in the water table, while a trend towards a more blue color indicates an increase in water table.

Comparison of the results from the steady-state base case model (Scenario 1) and the models in which only the Lake Michigan stage was altered (Scenarios 4 and 5), it becomes clear that the stage of Lake Michigan has little influence on the water table and water budget within the Cedar Creek watershed. The change in head is less than 5 cm throughout the watershed in both simulations with a large majority having no change (Figure 23). The frequency of head change show that 97.5% of the cells in the watershed have no change in groundwater head in the low Lake Michigan (Figure 24a) and only 2.5% of the cells decreased in head. The high Lake Michigan stage simulation (Scenario 5) shows that 97% of the cells have no change, but unlike the low Lake Michigan stage scenario where all the affected cells are a decrease, 1.2% of the cells have a decrease in head while 1.75% of the cells have an increase in head (Figure 23b and 24b). In terms of the water budget, there is less than a 0.5% change in inflows and outflows from all boundary condition cells within the watershed.

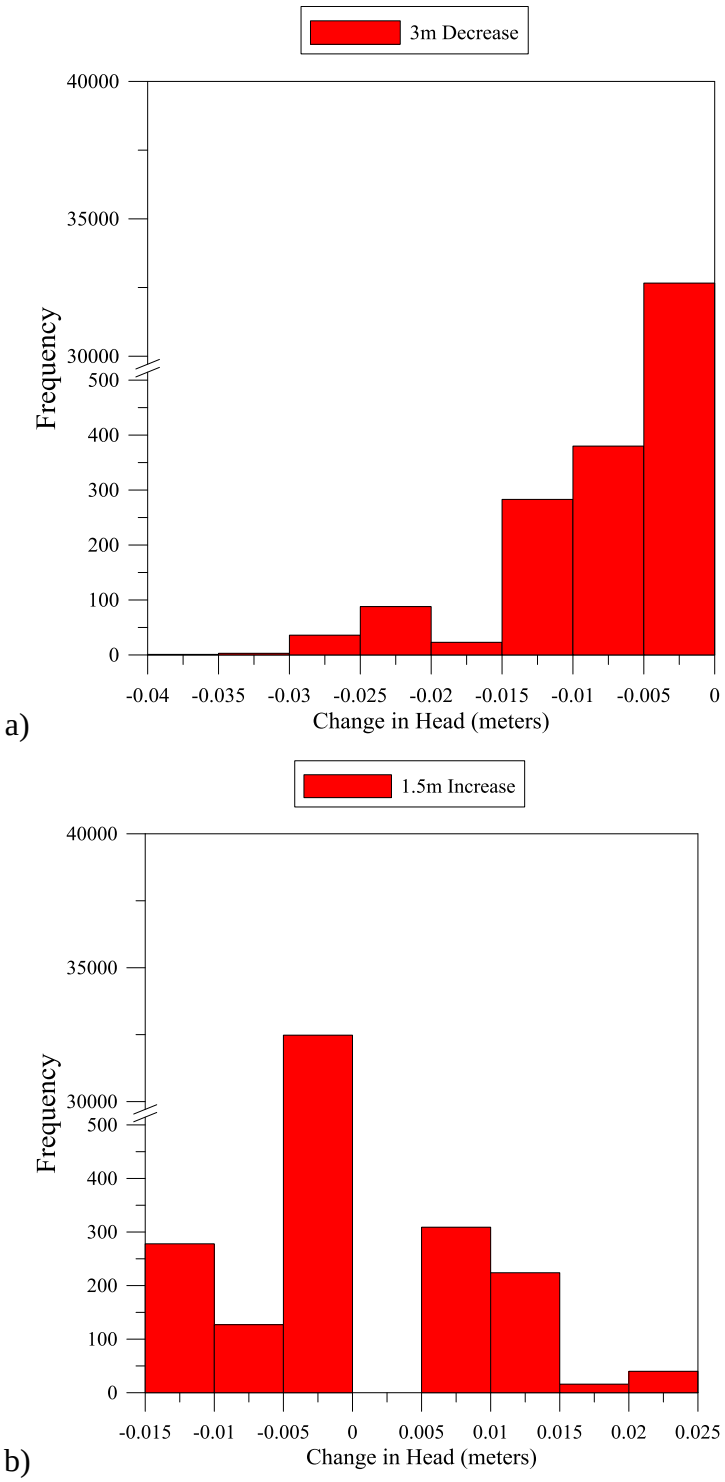

Figure 24. Histograms from variable Lake Michigan stage simulations a) Histogram showing the frequency of head change in the simulation with a 3 m lower Lake Michigan Stage (Scenario 4). Note the break in axis between 500 cells and 30,000 cells. b) Histogram showing the frequency of head change in the simulation with a 1.5m higher Lake Michigan Stage (Scenario 5). Note the break in axis between 500 cells and 30,000 cells. Again the largest bars shown are representative of 99% of the total 33,476 cells.

Throughout all steady-state simulations, there were no changes in head greater than 4 m and the histogram displaying the frequency of head change in number of cells show a majority of change is less than or equal to ±1 m (Figure 25). The distribution of head change across the watershed shows that the largest change in scenarios 6 through 9 are found near the edges of the watershed. The high topography of the northwest portion has the highest head change (Figures 25&26). The majority of the central area of the watershed has little to no change in head. The distribution of head change between the scenarios 6 and 7 are nearly identical due to the small variations created by the variances in Lake Michigan stage (Figure 25a&b).

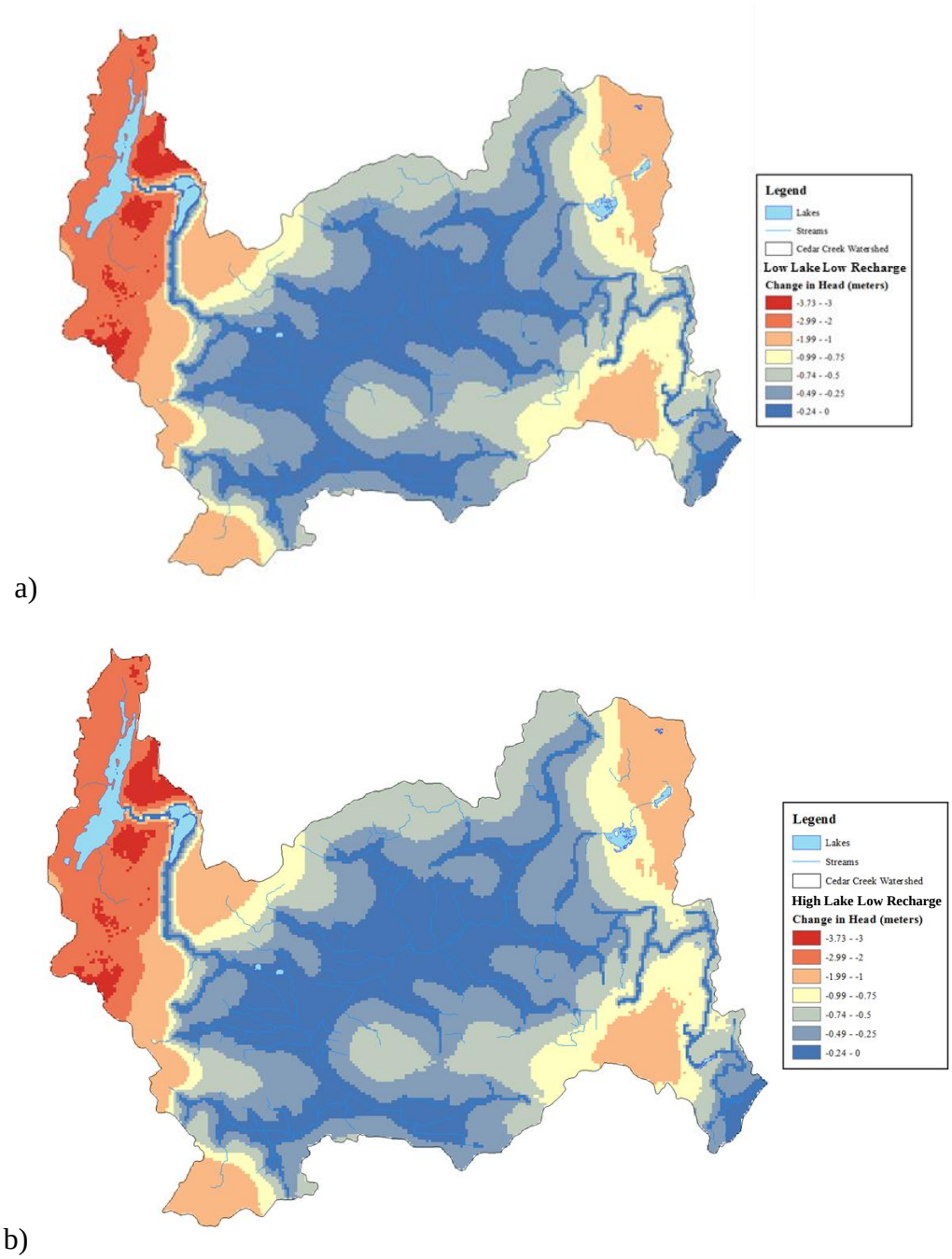

Figure 25. Change in head from base case scenario when recharge is decreased 20% a) Results from a Steady-State simulation in which the Lake Michigan stage was lowered 3 m in addition to a 20% decrease in recharge (Scenario 6). Blue colors indicate a small decrease in the water table where as red colors indicate a larger decrease in water table b) Results from a Steady-State simulation in which the Lake Michigan stage was raised 1.5 m in addition to a 20% decrease in recharge (Scenario 7). Blue colors indicate a small decrease in the water table where as red colors indicate a larger decrease in water table

Similarly, the head change spatial distribution between scenarios 8 and 9 are difficult to distinguish due to small effect of changes in lake stage. The center of the watershed, with the highest density of river cells, has the lowest head change while the areas in the northwest and northeast experience the greatest head change (Figure 26 a&b).

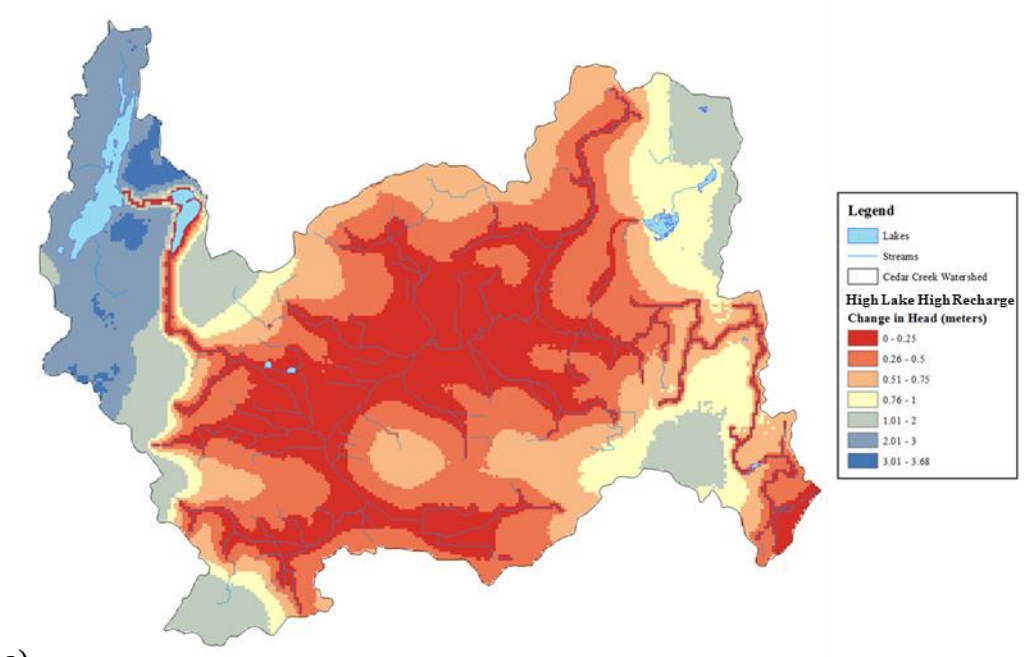

a)

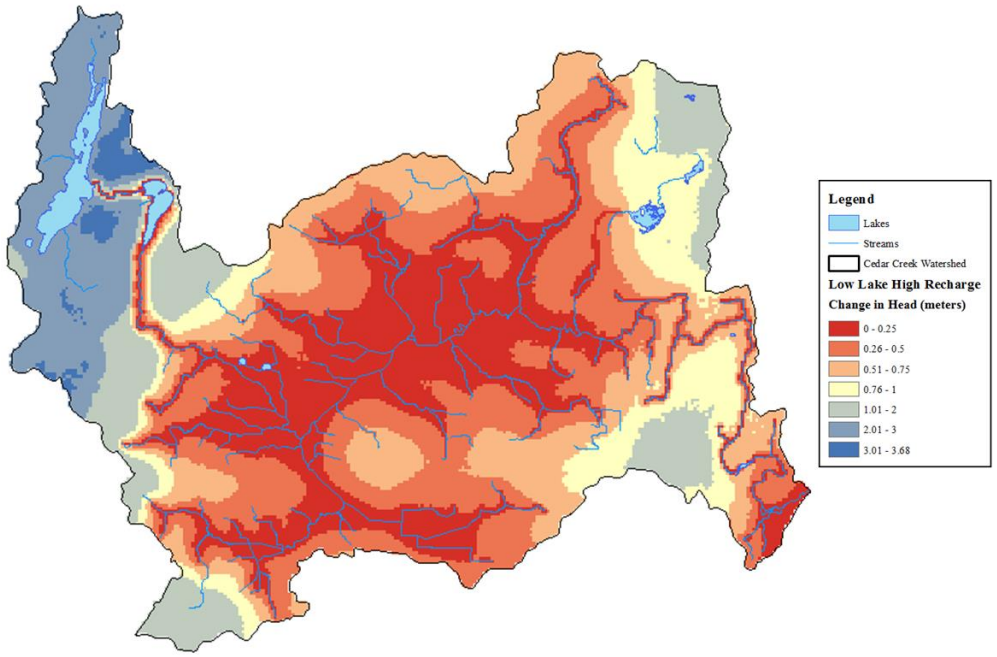

b)

Figure 26. Change in head from base case when recharge increased 20%. a) Results from a Steady-State simulation in which the Lake Michigan stage was raised 1.5 m in addition to a 20% increase in recharge (Scenario 8). Red colors indicate a small increase in the water table where as blue colors indicate a larger increase in water table b) Results from a Steady-State simulation in which the Lake Michigan stage was lowered 3 m in addition to a 20% increase in recharge (Scenario 9). Red colors indicate a small increase in the water table where as blue colors indicate a larger increase in water table

The relationship between different simulations also becomes clear with an analysis of the water budget. The simulations with a 20% decrease in recharge and 20% increase in recharge, scenarios 6, 7 and 8, 9 respectively, are very similar in both the distribution of the water table and the allocation of water in the water budget, regardless of the stage of Lake Michigan. In both the 20% increased and decreased recharge simulations, the difference between the 1.5 m increase and 3 m decrease in lake stage result in less than a 1% difference in overall water flux in the Cedar Creek Watershed. Also, when comparing the increased and decreased recharge simulations (Scenarios 6, 7 vs. Scenarios 8, 9), it becomes clear that the results from the increased recharge are the opposite values as the decreased recharge simulation. For example, the river cells contribute 8% less water to the aquifer in the high recharge scenarios, 8 and 9, while in the low recharge scenarios, 6 and 7, the river cells contribute 8% more water to the aquifer. On the other hand, the river cells remove 10% more water than the steady-state base case scenario in scenarios 8 and 9, while the river cells remove 10% less water from the aquifer in scenarios, 6 and 7.

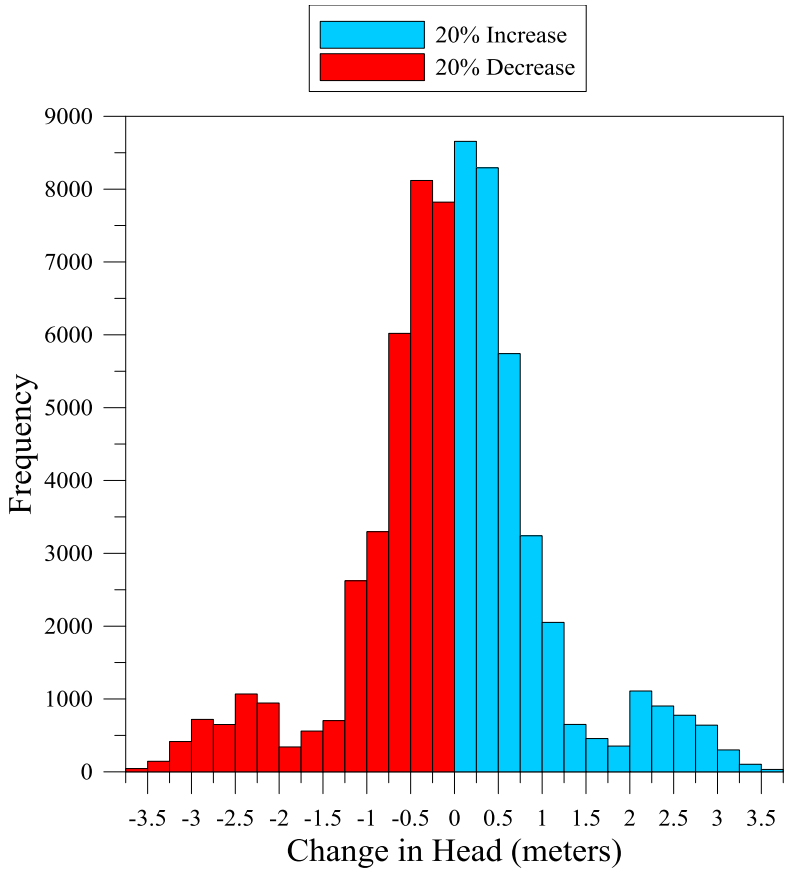

Figure 27. Histogram showing the frequency of head change in both the decreased and increased recharge simulations. The red bars represent simulation 6 in which both recharge and Lake Michigan stage were lowered while the blue bars represent simulation 9 in which both recharge and Lake Michigan stage were increased.

In the water balance for the entire model area, the greatest changes in water budget, excluding recharge, arise in the constant head cells (Figure 28a). The changes seen are correlated to the changes in Lake Michigan stage. The high lake stage scenarios, 5, 7, and 9, show a decreased interaction with the aquifer, both inflows and outflows were decreased, while the low lake stage scenarios, 4, 6, and 8, show higher interaction with the aquifer, both increased inflows and outflows (Figure 28a). The river cells show nearly identical inflows and outflows through the base case scenario and the scenarios in which

only the lake stage was manipulated, scenarios 4 and 5, but the high recharge scenarios, 8 and 9, show a decrease in inflows to the aquifer and an increase in outflows from the aquifer. The opposite is true in the scenarios with a decreased recharge rate, 6 and 7, there is increased inflow to the aquifer and decreased outflow from the aquifer.

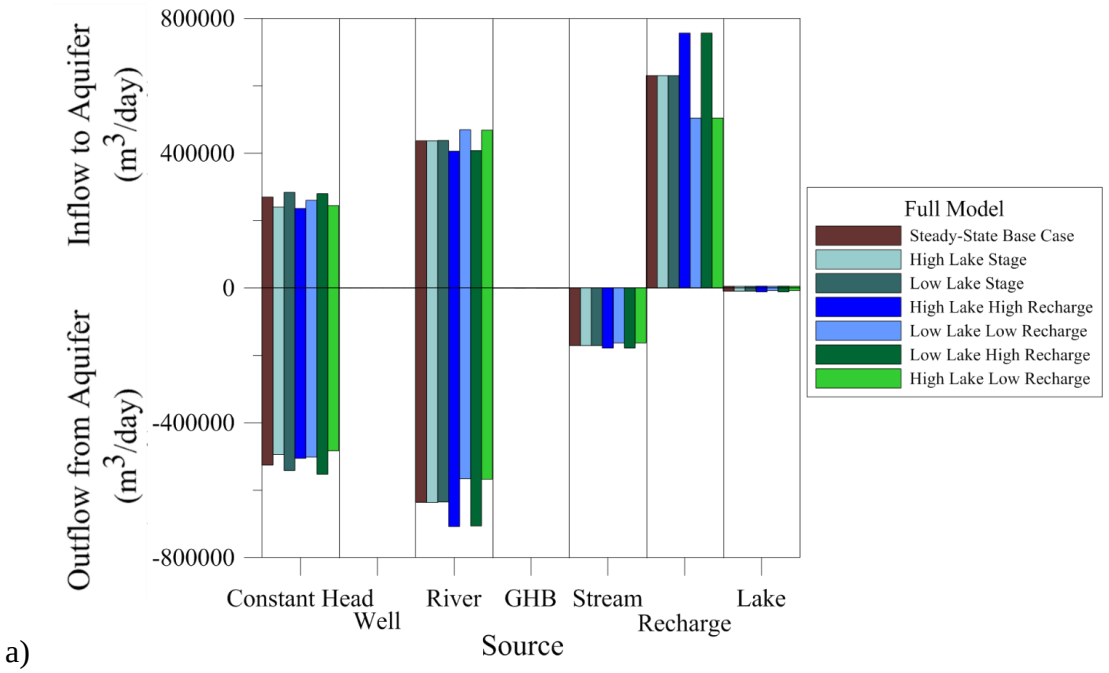

a)

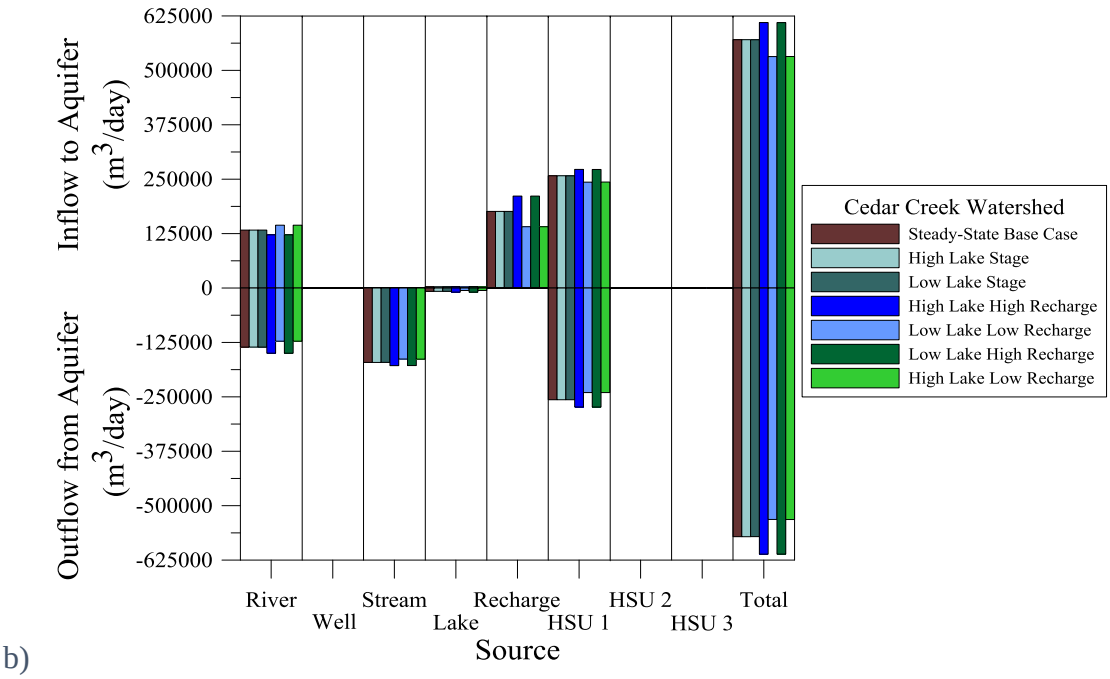

b)

Figure 28. Steady-state water budgets from the full model area and the Cedar Creek watershed a) Water budget from 7 steady-state simulations encompassing the entire groundwater flow model area. b) Water budget from only the Cedar Creek watershed extracted from the MODFLOW model. HSU is short for Hydrostratigraphic Unit which allows from calculation of water budgets for specific regions within the model area. HSU 1 represents the area outside of the watershed, HSU 2 represents the watershed itself, and HSU 3 represents the Cedarburg Bog. Therefore, inflows and outflows from an HSU represents the flux across each boundary between the different HSUs.

When looking at the water budget specifically in the Cedar Creek watershed, it is necessary to investigate the interaction of the boundary cells within the watershed in addition to the flow through the boundaries of the watershed. This is expressed in Figure 28b as flow through Hydrostratigraphic Units (HSUs) 1 and 3. HSU 1 is designated as the model area outside of the Cedar Creek watershed and HSU 3 is designated as the Cedarburg Bog. The flow from HSU 1 into and out of the Cedar Creek watershed is increased in the high recharge scenarios and decreased in the low recharge scenarios (Figure 28b). Flow from HSU 2 (Cedar Creek Watershed) into HSU 3 (the Cedarburg Bog) decreases in all variable recharge scenarios, 6 through 9, but the flow from the bog into the watershed increases by about 6% in the high recharge scenarios, 8 and 9, and decreases by about 2.5% in the low recharge scenarios, 6 and 7. Though this is not possibly to see in Figure 28 due to the relatively low fluxes between the HSUs 2 and 3 when compared to the other boundary conditions. The interaction between the lake cells and the aquifer increase in both inflow and outflow by 12.5% and 25% respectively in scenarios 8 and 9, while in scenarios 6 and 7, the inflows and outflows from the lake cells decrease by 10% and 25.5% respectively.

The interaction between the Cedar Creek stream cells and the aquifer is also very interesting. In all steady-state simulations the stream had almost no input into the aquifer, rather almost every cell is removing water from the aquifer but there is increased outflow from the aquifer to the stream cells during scenarios 8 and 9 and there is decreased flow from the aquifer to the stream cells in scenarios 6 and 7 (Figure 28). The river cells have the largest impact on the aquifer due mostly to the vast quantity of cells in the model. There are significantly more river cells in the model than any other boundary condition

package. In addition, when looking at the distribution of head change between the different recharge scenarios and the base case model it is clear that areas with a larger density of river cells i.e. the center of the model, have the lowest change in water table, in the high recharge and low recharge scenarios. This result is most likely due to the large exchange capacity the river cells have; with changes in recharge the river cells moderate the change in the center of the model.

5.4.2. Scenario 10: Drain Package Replaces River Package

A sensitivity study was conducted on the MODFLOW model to determine the effects of changing surface water boundary conditions from the river (RIV) package to the drain (DRN) package on the MODFLOW model results. The DRN package is used to simulate head-dependent flux boundaries similarly to the RIV package except when the head in the DRN cell falls below the user specified head, the flux from the DRN package cell falls to zero, as opposed to a specified lower bound as is the case in the RIV package. This is used to better simulate headwater tributaries that have not received water from upgradient cells, therefore cannot supply water to the aquifer.

Results described in the following section apply only to the Cedar Creek watershed and not the farfield of the model. When all RIV cells were converted to DRN cells, the mean change in groundwater head is -3.65 m from the steady-state base case scenario. Overall, 1.5% of the watershed show a decrease in head greater than 10 m, 18.3% decrease between 10 m and 5 m, 72.6% decrease between 5 m and 1 m and 7.6% decrease less than 1 m. The maximum change of -17.1 m occurs in the southeast portion of the watershed almost directly south of the Cedarburg Bog (Figure 29). There are also areas of high decrease in the water table around small tributaries of the main trunk of

Cedar Creek. The minimum change in head of 0.01 m occurs along the main trunk of Cedar Creek (simulated with the SFR2 package) and some larger tributaries in the south-central portion of the watershed. This result indicates that there are tributaries simulated by the RIV package in the steady-state base case model which are artificially supplying non-existent water to the aquifer.

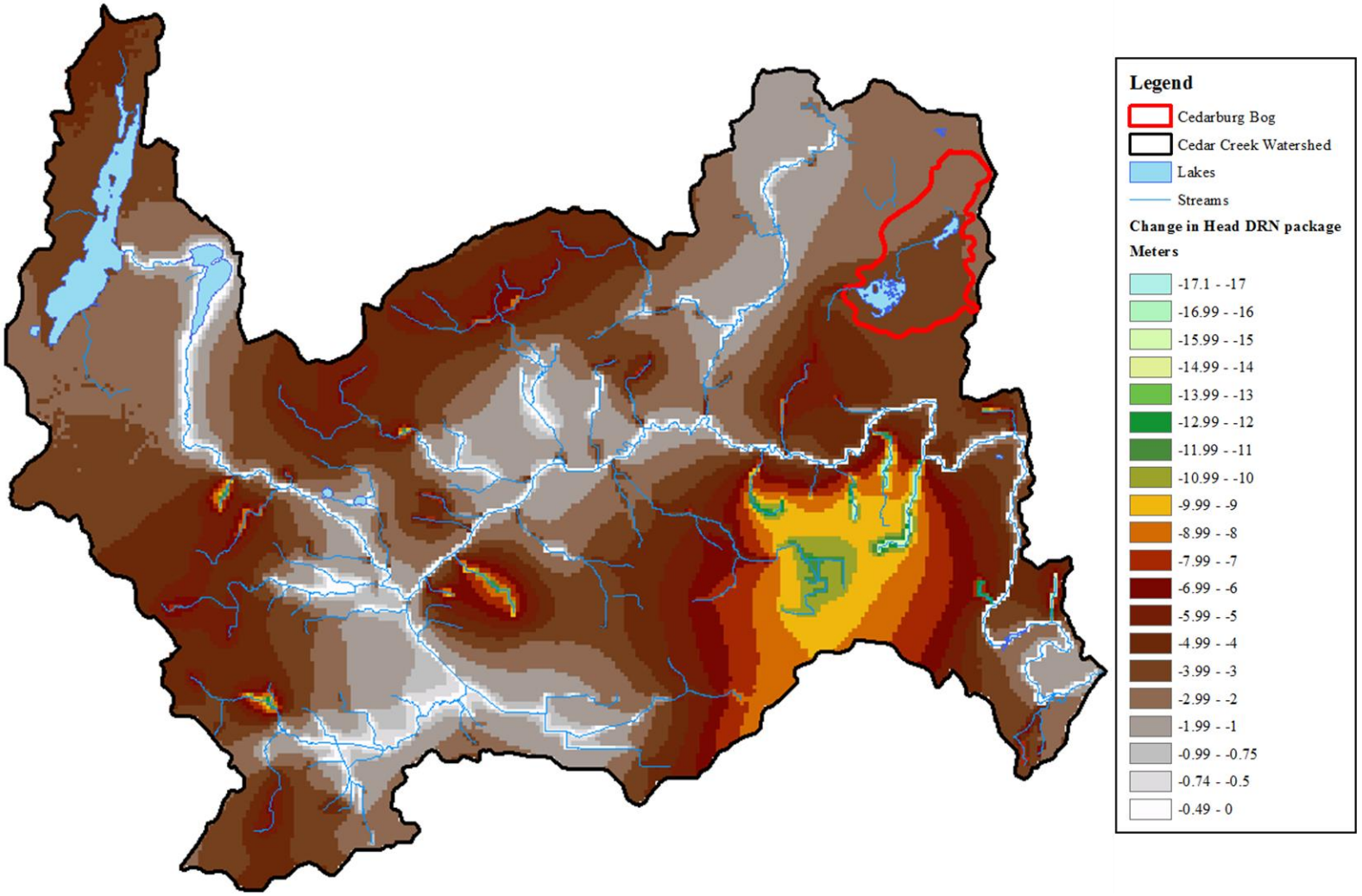

Figure 29. Spatial distribution of head change from Steady-State base case scenario to DRN scenario

The water budget of the DRN sensitivity scenario shows the aquifer is receiving 133,000 m^3/day less water due to the removal of the RIV cells in the watershed, which is partially countered by a 54% decrease in flow from the aquifer to the drain cells, 73,000 m^3/day. The stream interaction with the aquifer also makes up some discrepancy after the removal of river cells by extracting 40% less water from the aquifer, 68,000 m^3/day, and supplying 3 times more water to the aquifer, 900 m^3/day. The lake cells also supply 6% more water to the aquifer and remove 38% less water from the aquifer, but this change only accounts from about 3,000 m^3/day of water to the aquifer. Overall, the total flux into the aquifer decreases 42.8% and the total flux out of the aquifer also decreases by 43.1%. This model also maintains mass balance with less than 1% error in total flux.

While the DRN package scenario has a lower water table and significantly lower input to the aquifer from the rivers in the watershed, it is likely that the natural system will lean more towards the RIV package simulations as climate change is expected to create a warmer and wetter climate in the future. The increased water available to the aquifer may allow for higher than average streamflow values which will allow for more interaction between the rivers and the aquifer.

5.5. Groundwater Resource Management at the Cedarburg Bog

The primary concern that accompanies climate change and the effect it has on wetlands, is the amount of carbon stored and the emissions of stored carbon into the atmosphere in a warmer future. In the area around Cedarburg Bog the concern isn't so much carbon emissions, due to its relative small size, as it is environmental tourism, ecology and recreation. This bog is very important for different species of migratory birds

and other animals, and destruction of this habitat could have devastating effects on the fauna that inhabit the bog year-round and those that use it as a breeding location. The greatest effect climate change will have on the Bog locality arises from the raising or lowering of the water table within the peatland. The accumulation rate of peat relies heavily on water table elevation, and with water table levels above, at, or below the peat surface the accumulation occurs [*Parish et al.*, 2008]. With a lowering of the water table, as suggested in the decreased recharge scenarios, a larger amount of peat would be exposed to the air and subsequent aerobic decay would destroy peat area in addition to increasing carbon emissions from the wetland. This would have a negative effect on the current flora of the bog as decreased habitat space and changes in the functionality as a wetland habitat would reduce chances for flora to continue to thrive in the area.

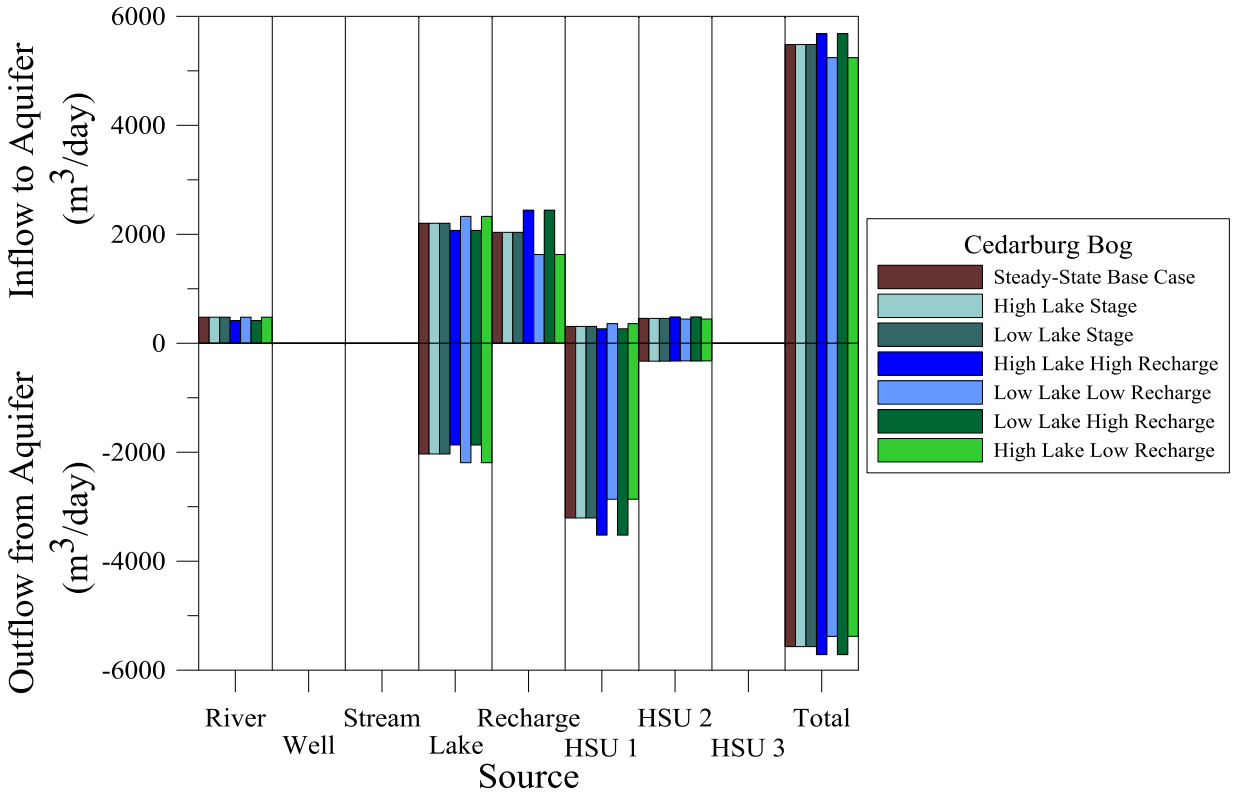

Figure 30. Water budget from only the Cedarburg Bog extracted from the MODFLOW model. HSU 1, HSU 2, and HSU 3 represent the same areas as described in the previous figure.

Results from the MODFLOW model in the area of the Cedarburg Bog show the highest head is 263 m in the southwestern portion near the outlet stream of Mud Lake. This result indicates that the outlet stream of Mud Lake is acting as a source of water for the model mediating the change in head in the southwest portion of the bog. This is possibly a distortion caused by the use of the RIV package because the outlet stream is ephemeral and cannot supply water to the underlying aquifer year round. The head declines steadily from the western edge of the bog to the eastern edge where the lowest head is located almost directly east of the highest head at 254 m (Figure 31). Scenario 1 produces interesting results in the water budget of the two lakes in the bog, Long Lake

and Mud Lake. Long Lake in the north of the bog exclusively supplies water to the aquifer at a rate of 1740 m^3/day which indicates that the northern portion of the bog, at least around Long Lake is acting to recharge the water table. On the other hand, Mud Lake has both inflows to the aquifer and outflows from the aquifer to the lake but the former is much less than the latter. Mud Lake supplies 530 m^3/day to the aquifer while removing 1980 m^3/day from the aquifer for a total flux of 1450 m^3/day from the aquifer to the lake. This result indicates that the southern portion of the bog, around Mud Lake and the outlet stream, is acting as a discharge zone for the underlying aquifer.

Results from the variable Lake Michigan stage scenarios 4 and 5 show very little change within the bog (Figure 32 a&b). The highest change seen is 1 cm which is well within the uncertainty of the model. Therefore essentially no change can be reported. HSU 1 and HSU 3 are in contact at the base of layer 1, or the bottom of the bog, and the water budgets for all simulations show significantly more flow from HSU 1 to HSU 3 through the bottom of layer 1 which indicates a possible discharge location for groundwater at the Cedarburg Bog locality (Figure 30). This does not indicate that the entire bog is a discharge zone but it indicates the possibility of the bog being both a recharge and discharge zone for local groundwater. These results make it very difficult to answer the question of whether or not the Cedarburg Bog is a recharge or discharge location for local groundwater.

The climate change scenarios also show that the stage of Lake Michigan has very little effect on the water table in the Bog, while the changes in recharge rates have a significant effect. Scenarios 8 and 9, in which the recharge was increased 20%, show the highest increase in head (1.14 m) in the north and eastern portions of the Bog, while

change near the outlet stream of Mud Lake is less, a 22 – 50 cm increase(Figure 32 e&f). In the scenarios 6 and 7 with a 20% lower recharge rate, the simulated highest decreases are about 1.19 m in the same portions of the Bog as scenarios 8 and 9. The lowest overall changes are seen near the outlet stream of Mud Lake with a head decrease between 50 and 64 cm (Figure 32 c&d).

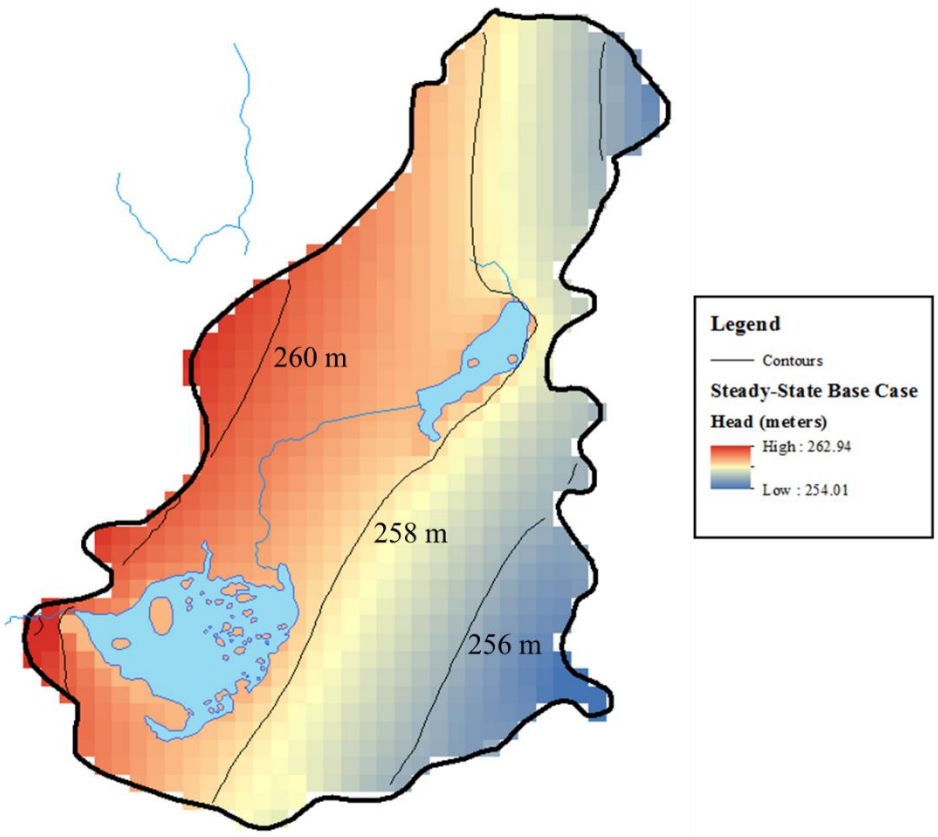

Figure 31. Steady-state base case non-pumping scenario head distribution within the Cedarburg Bog (Scenario 1). Highest head is in southwest portion of the Bog where the outlet stream leaves the Bog and lowest heads are in the southeast portion of the Bog almost directly east of the highest head

The water budget for the Cedarburg Bog reveals that the interaction between the river cells and the aquifer is solely inflows to the aquifer, though the magnitude of inflows varies slightly among the different steady-state simulations. The high recharge scenarios have a decreased flow from the river cells to the aquifer while the low recharge scenarios have no change in the river cells water budget. The lake cells also show diminished interaction between the aquifer and lakes during the high recharge scenarios and increased interactions in the low recharge scenarios (Figure 30).

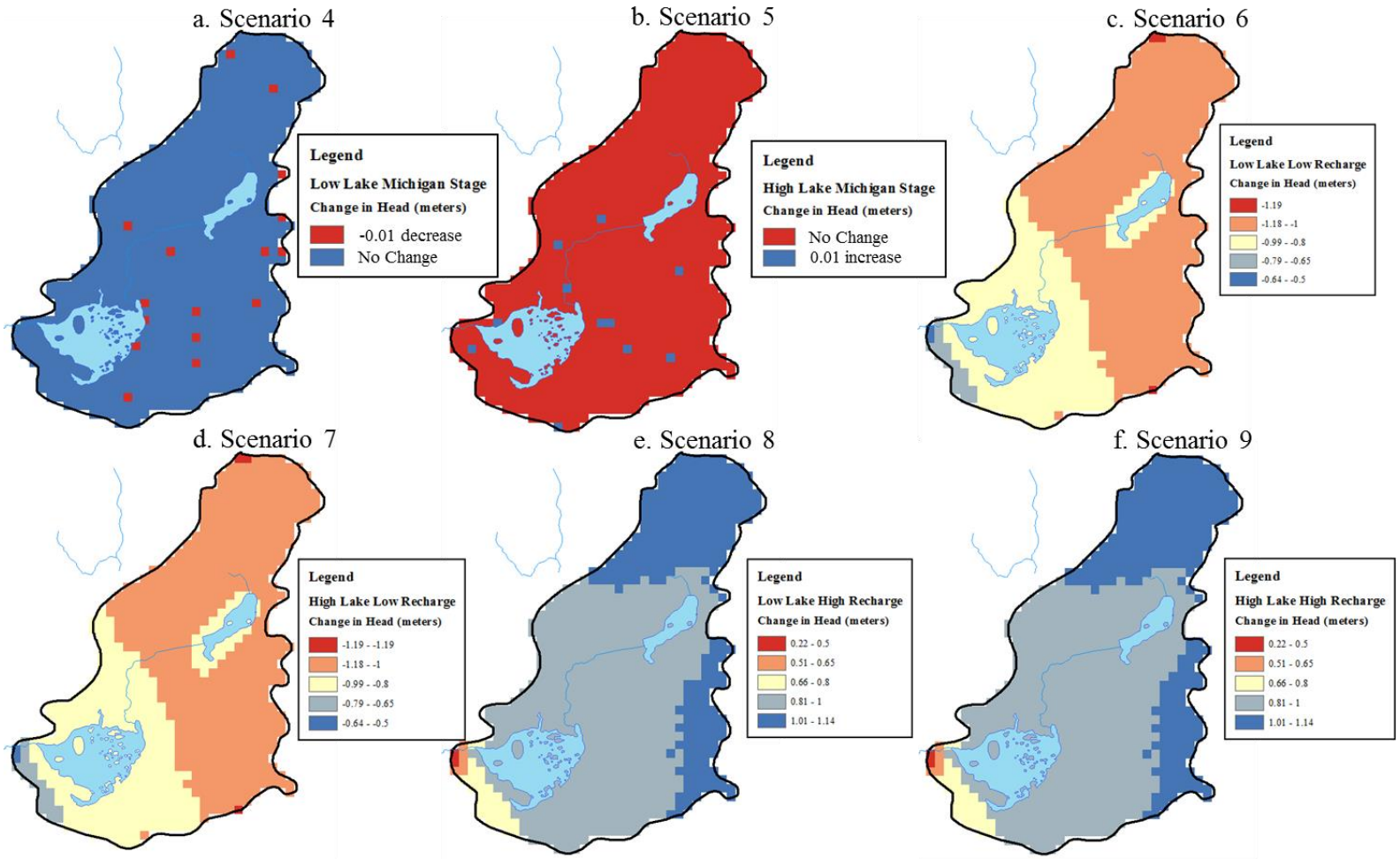

Figure 32. Maps showing the change in head in the Cedarburg Bog throughout 6 climate change steady-state simulations. No difference is seen between maps c and d and e and f respectively due to the low influence of Lake Michigan stage on the watershed. The different colored pixels on maps a and b represent the only cells in the bog that have a change in head.

5.5.1. Scenario 11: Low-K layer beneath the Cedarburg Bog

In addition to the DRN package sensitivity study, another simulation was run, this with a low hydraulic conductivity layer below the Cedarburg Bog, 0.025 m/day, to simulate the low K lakebed sediments that are thought to inhibit vertical flow through the base of the Cedarburg Bog. Again, the results discussed in the following section correspond to only the Cedar Creek Watershed and not the farfield of the MODFLOW model. With the inclusion of the low k unit below the bog, the mean change in groundwater head throughout the watershed was only 0.04 m with 65.6% of cells having no change in head. The maximum change in head, found in the southeast portion of the Cedarburg Bog, was an increase of 2.07 m above the steady-state base case model. This is to be expected as the flow through the bottom of the bog is decreased the head within the bog will increase. In the area adjacent to the bog to the east and north, the head decreased relative to the steady-state base case model, with a maximum decrease of 0.56 m. Throughout the watershed only 1.6% of cells increased in head greater than 1 m and 27.5% of cells increased less than 1 m.

The water budget shows that both river and stream interaction with the aquifer doesn't change but there is a 6.4% increase in flow from the lakes to the aquifer. The lakes in the bog show an overall decreased interaction with the aquifer, with a 69% decrease in flows from the lakes to the aquifer, from about 2,200 m^3/day to 705 m^3/day, and a decrease in flows from the aquifer to the lakes of 74%, from 2,000 m^3/day to 500 m^3/day. The most important change in water budget from the steady-state base case model to the model with a low hydraulic layer under the bog is the interaction between the bog and the watershed, HSU 2, and the underlying layer, HSU 1. There is a 360%

increase in flow from the bog to the watershed (this occurs exclusively in layer 1), so more than 3 times the amount of water is flowing from the bog to the watershed through the lateral boundaries in layer 1. On the other hand, there is a 58% decrease in flow from HSU 2 to the bog through layer 1. The flow from the aquifer to the bog through the base of the bog (from HSU 1 to the bog) decreases by 65% from the steady-state base case scenario, from 3,200 m^3/day to 1,100 m^3/day. The flow from the bog to the aquifer through the base of the bog (the bog to HSU 1) decreases by 97% from the steady-state base case scenario, from 300 m^3/day to 9 m^3/day.

6. Limitations

The primary concern with the Cedar Creek Watershed MODFLOW model is the amount of water supplied to the aquifer from headwater tributaries. The RIV cells which represent the headwater streams for Cedar Creek, supply water to the aquifer which is not possible due to the absence of water from upgradient cells. This influx of water from the headwater river cells into the aquifer is a distortion produced by the use of the RIV package and could be improved with the use of the SFR2 package or the DRN (Drain) package. This modification to the model would produce more reasonable results and may or may not require recalibration of the hydraulic parameters.

In addition to the unrealistic cycling of water in the headwater streams, there was no flux target used to calibrate baseflow on Cedar Creek. The flux target was not included in this model due to the use of SFR2 package only on the main trunk of Cedar Creek. The inclusion of a baseflow flux target on a surface water river is the only way to verify that the recharge and hydraulic conductivity fields are correct. The inclusion of a

baseflow flux target is especially necessary when simulating future climate change and recharge conditions. This can be improved by either using the SFR2 package for all streams and tributaries or by calculating the addition of water to the main trunk from either RIV or DRN cells representing the tributaries. This calculated baseflow from the DRN cells would then be subtracted from the baseflow flux target discharge value, which can then be used in calibration of both recharge and hydraulic conductivity fields. The absence of a flux target in the model leads to an expectation that the recharge and K fields are correlated and it can be difficult to decide which to raise and which to lower in order to achieve the same result.

The variable recharge simulations can also be improved by modifying all other boundary condition cells to reflect the changes in recharge from climate change i.e. increase or decrease river and lake stage to reflect the changes in recharge conditions. In addition the constant head cells which bound the model on the north, west and south sides of the model can be manipulated to simulate the changing water table with future climate conditions. Finally, the thickness of the dolomite (Layers 3 and 4) in the west side of the model is much greater in the model than in the geology of the region. The Maquoketa shale is the first encountered bedrock unit in the west of the model, and though the effective hydraulic conductivities are lower in the west as a result of this thick layer, the model would be improved with the use of the Maquoketa shale as the base of the groundwater flow model.

A limitation inherent with the Soil-Water Balance code is the difficulty of simulating recharge over areas with a water table near the surface or areas with the hydrologic soil type D (least permeable and lowest infiltration rate), i.e. wetlands and The

Cedarburg Bog. The SWB code simulates much lower recharge values over soils which do not drain well and therefore the Cedarburg Bog is presumably being simulated with less recharge than it receives in the natural system. The average recharge calculated in the bog by SWB is $2.3x10^{-4}$ m/day (3.2 in/year) compared to the average recharge calculated for the watershed of $5.3x10^{-4}$ m/day (7.6 in/year). This problem can be addressed by calculating recharge manually outside of the SWB code and implementing the recharge directly to the Bog. This will also change the effect of the variable recharge simulations due to the higher amounts of recharge expected.

7. Conclusions

Due to the high variability in climate change projection, it is difficult to predict with certainty that any outcome of any model with a basis in future projection of climate patterns, especially on a small scale such as the State of Wisconsin, is correct. Nevertheless, the reasonable prediction through groundwater modeling is still important in regulation and management of features in groundwater and surface waters because the modeling have the ability to simulate possible outcomes, extreme events or specific situations involving land use change, urban expansion, large amounts of pumping or divergence and manipulation of water ways.

Based on the results of the steady-state and transient simulations, it is clear that there is a very strong connection between the amount of recharge and the elevation of the water table. The future recharge scenarios have shown that high recharge simulations lead to overall increased water table elevations while lower recharge simulations lead to overall a lower water table.

The simulated effect of an increase or decrease in recharge of 20% on the groundwater table results in 99.9% of cells in the watershed changing head either higher or lower, and approximately 25% of the cells change more than 1 m. A 1-meter decrease in the water table throughout the watershed would have devastating effects on the surface waters especially the rivers and streams due to the high baseflow component in this area. Also with the increase in urban area and changes in land use from forestry or agriculture to developed land, the surface runoff component of the local water budget will increase relative to the baseflow which can lead to warming of surface water features and can be detrimental to aquatic wildlife.

The review of predicted and simulated future climate change indicates that the possibility of higher recharge is more likely than that of lower recharge; therefore it is safe to assume that the results of the simulations with 20% more recharge and higher lake stage are more likely to occur. A 1 m increase in water table within the bog through the end of 2100 could cause the lakes in the bog to increase in both area and depth in addition to expanding the peatland area within the current basin of the Cedarburg Bog.

The consequences that can arise from future climate change can be very different depending on the relationship between temperature and precipitation. If there is sufficient temperature rise to counter the rise in precipitation, recharge will most likely be decreased in the future due to greater evapotranspiration from the water table, soil, surfaces waters and plants. On the other hand if precipitation increases more than temperature, recharge could be increased. Both scenarios have the possibility of forcing the Cedarburg Bog into a new equilibrium state that could possibly return to the normal ecological and biogeochemical functions or it could cause a reduction in peat volume due

to advanced weathering, erosion and aerobic decomposition [*Auterives et al.*, 2011; *Mitsch et al.*, 2013; *Wu*, 2012]. A loss of peatland area in the Cedarburg Bog could be devastating to the ecological diversity found in this locality. Changing water flow and hydrological process that take place in the bog due to recharge changes or groundwater flow patterns could cause a shift in the peat accumulation which leads to a loss of habitat and biodiversity.

References

Allen, D. M., D. C. Mackie, and M. Wei (2004), Groundwater and climate change: a sensitivity analysis for the Grand Forks aquifer, southern British Columbia, Canada, *Hydrogeology Journal*, *12*, 270-290.

Angel, J. R., and K. E. Kunkel (2009), The response of Great Lakes water levels to future climate scenarios with an emphasis on Lake Michigan-Huron, *Journal of Great Lakes Research*, *36*, 51-58.

Auterives, C., L. Aquilina, O. Bour, M. Davranche, and V. Paquereau (2011), Contribution of climatic and anthropogenic effects to the hydric deficit of peatlands, *Hydrological Processes*, *25*, 2890-2906.

Bear, J. (1972), *Dynamics of Fluids in Porous Media*, 757 pp., American Elsevier.

Choi, W., R. Tareghian, J. Choi, and C.-S. Hwang (2013), Geographically heterogeneous temporal ternds of extreme precipitation in Wisconsin, USA during 1950-2006, *International Journal of Climatology*, *34*(9), 2841-2852.

Crowe, K. (2014), Many rural Wisconsin counties lost population since 2010, in *Milwaukee Journal Sentinel*, Milwaukee, WI.

Doherty, J. (2002), PEST: Model-Independent Parameter Estimation, 279 pp.

Doherty, J., and R. J. Hunt (2010), Approaches to Highly Parameterized Inversion: A Guide to Using PEST for Groundwater-Model Calibration, 59 pp.

Domenico, P. A., and M. D. Mifflin (1965), Water from low-permeability sediments and land subsidence, *Water Resources Research*, *1*(4), 563-576.

Domenico, P. A., and F. W. Schwartz (1997), *Physical and Chemical Hydrogeology*, John Wiley & Sons.

Dripps, W. R., and K. R. Bradbury (2007), A simple daily soil-water balance model for estimating the spatial and temporal distribution of groundwater recharge in temperate humid areas, *Hydrogeology Journal*, *15*, 433-444.

Dripps, W. R., and K. R. Bradbury (2010), The spatial and temporal variability of groundwater recharge in a forested basin in northern Wisconsin, *Hydrological Processes*, *24*, 383-392.

Grittinger, T. F. (1970), String Bog in Southern Wisconsin, *Ecology*, *51*(5), 928-930.

Harbaugh, A. W. (2005), MOFLOW-2005, The U.S. Geological Survey Modular Ground-Water Model- The Ground-Water Flow Process: U.S. Geological Survey Techniques and Methods 6-A16, 253 pp.

Harbaugh, A. W., E. R. Banta, M. C. Hill, and M. G. McDonald (2000), MODFLOW-2000, the U.S. Geological Survey modular ground-water model- User guide to modularization concepts and the Ground-Water Flow Process, U.S. Geological Survey, Reston, Virginia.

Heath, R. C. (1983), *Basic Ground-water Hydrology*, 84 pp.

IPCC (2013), *Climate Change 2013: The Physical Science Basis. Contribution of Working Group I to the Fifth Assessment Report of the Intergovernmental Panel on Climate Change*, 1535 pp., Cambridge University Press, Cambridge, United Kingdom and New York, NY, USA, doi:10.1017/CBO9781107415324.

Kucharik, C., S. P. Serbin, S. Vavrus, E. Hopkins, and M. M. Motew (2010a), Patterns of Climate Change Across Wisconsin From 1950 to 2006, *Physical Geography*, *31*(1), 1-28.

Kucharik, C., D. J. Vimont, K. Holman, E. Hopkins, D. Lorenz, M. Notaro, S. Vavrus, and J. Young (2010b), Climate Change in Wisconsin, Wisconsin Initiative on Climate Change Impacts.

Kuhns, R., and J. A. Reinartz (2007), A Natural History of The Cedarburg Bog: Part I - Geology Insights.

Lohman, S. W. (1972), Ground-Water Hydraulics, 70 pp.

McDonald, M. G., and A. W. Harbaugh (1988), *A Modular Three-Dimensional Finite-Difference Ground-Water Flow Model*: U.S. Geological Survey Techniques of Water-Resources Investigations, book 6, chap. A1, 586 pp.

Merritt, M. L., and L. F. Konikow (2000), Documentation of a Computer Program to Simulate Lake-Aquifer Interaction Using the MODFLOW Groundwater Flow Model and the

MOC3D Solute-Transport Model: U.S. Geological Survey Water-Resources Investigations Report 00-4167, 146 pp.

Mickelson, D. M., and K. M. Syverson (1997), Quaternary Geology of Ozaukee and Washington Counties, Wisconsin, *Wisconsin Geological and Natural History Survey*, *Bulletin 91*, 1-56.

Mitsch, W. J., B. Bernal, A. M. Nahlik, U. Mander, L. Zhang, C. J. Anderson, S. E. Jorgensen, and H. Brix (2013), Wetlands, carbon, and climate change, *Landscape Ecology*, *28*, 583-597.

Moore, T. R., and N. T. Roulet (1995), *Methane emissions from Canadian peatlands*.

Moran, J. M., and E. J. Hopkins (2002), *Wisconsin's Weather and Climate*, The University of Wisconsin Press, Madison, Wisconsin.

Morris, D. A., and A. I. Johnson (1967), Summary of hydraulic and physical properties of rock and soil materials, as analyzed by the hydrologic laboratory of the U.S. Geological Survey, 1948-60, : U.S. Geological Survey Water Supply Paper 1839-D, 42 pp.

MRCC (2015), Midwestern Regional Climate Center, edited, Midwestern Reigional Climate Center, Illinois State Water Survey, Prairie Research Institute, University of Illinois at Urbana-Champaign.

Niswonger, R. G., S. Panday, and M. Ibaraki (2011), MODFLOW-NWT, A Newton Formulation for MODFLOW-2005: U.S. Geological Survey Techniques of Water-Resources Investigations, book 6, chap. A37, 44 pp.

Niswonger, R. G., and D. E. Prudic (2005), Documentation of the Streamflow-Routing (SFR2) Package to Include Unsaturated Flow Beneath Streams-A Modification to SFR1: U.S. Geological Survey Techniques of Water-Resources Investigations, book 6, chap. A13, 50 pp.

Parish, F., A. Sirin, D. Charman, H. Joosten, T. Minayeva, M. Silvius, L. Stringer, and (Eds.) (2008), Assessment on Peatlands, Biodiversity and Climate Change: Main Report, Global Environment Centre, Kuala Lumpur and Wetlands International, Wageningen.

Rayne, T. W., and K. R. Bradbury (2011), Evaluating impacts of subdivison density on shallow groundwater in southeastern Wisconsin, USA, *Journal of Environmental Planning and Management*, *54*(5), 559-575.

Reeve, A. S., J. Warzocha, P. H. Glaser, and D. I. Siegel (2001), Regional ground-water flow modeling of the Glacial Lake Agassiz Peatlands, Minnesota, *Journal of Hydrology*, *243*, 91-100.

Reinartz, J. A. (1985), A Guide to the Natural History of the Cedarburg Bog: Part I, *UWM Field Station Bulletin*, *18*(2).

Reinartz, J. A., S. Appel, N. Nadelhoffer, M. White, and K. Korth (2013), Cedarburg Basin Topography, UWM Field Station.

Rovey, C. W., and D. S. Cherkauer (1995), Scale Dependency of Hydraulic Conductivity Measurements, *Ground Water*, *33*(5), 769-780.

Schulze-Makuch, D., D. A. Carlson, D. S. Cherkauer, and P. Malik (1999), Scale Dependency of Hydraulic Conductivity in Heterogeneous Media, *Ground Water*, *37*(6), 904-919.

Serbin, S. P., and C. Kucharik (2009), Spatiotemporal Mapping of Temperature and Precipitation for the Development of a Multidecaldal Climatic Dataset for Wisconsin, *Journal of Applied Meterology and Climatology*, *48*, 742-757.

SEWRPC (2012), A Regional Water Supply Plan for Southeastern Wisconsin: Southeastern Wisconsin Regional Planning Commission Planning Report Number 52, 831 pp.

Smail, R. (2014), Personal Communication.

Syverson, K. M. (1988), The glacial geology of the Kettle Interlobate Moraine region, Washington County, Wisconsin, Master's Thesis, University of Wisconsin- Madison.

Thornthwaite, C. W., and J. R. Mather (1957), Instructions and tables for computing potential evapotranspiration and the water balance., *Climatology*, *10*, 181-311.

Turunen, J., E. Tomppo, K. Tolonen, and A. Reinikainen (2002), Estimating carbon accumulation rates of undrained mires in Finland: Application to boreal and subarctic regions, *The Holocene*, *12*, 69-80.

Veloz, S., J. W. Williams, D. Lorenz, M. Notaro, S. Vavrus, and D. J. Vimont (2011), Identifying climatic analogs for Wisconsin under 21st-century climate-change scenarios, *Climatic Change*, *112*, 1037-1058.

Westenbroek, S. M., V. A. Kelson, W. R. Dripps, R. J. Hunt, and K. R. Bradbury (2010), SWB-A modified Thornthwaite-Mather Soil-Water-Balance code for estimating groundwater recharge: U.S. Geological Survey and Techniques and Methods 6-A31, 60 pp.

WICCI (2011), Wisconsin's Changing Climate: Impacts and Adaptation, Nelson Institute for Environmental Studies, University of Wisconsin-Madison and the Wisconsin Department of Natural Resource, Madison, Wisconsin.

Wu, J. (2012), Response of peatland development and carbon cycling to climate change: a dynamic system modeling approach, *Environmental Earth Science*, *65*, 141-151.